

**Institute of Bioorganic Chemistry**  
**Polish Academy of Sciences in Poznan**  
**Developmental Biology Department**

**Mechanisms and developmental roles of**  
**XRN-2 mediated RNA regulation in**  
*Caenorhabditis elegans*

**Ilkin Aygün Soyalp**

**Supervisor: dr. habil. Takashi Miki, prof. IBCh**

**Auxiliary supervisor: dr. habil. Agata Tyczewska, prof. IBCh PAS**

**Poznan, 2023**

## **FUNDING**

This research was funded by the National Science Centre OPUS 16 grant (2018/31/B/NZ1/03580).

## ACKNOWLEDGMENTS

I am deeply indebted to my supervisor, dr. habil. Takashi Miki, for giving me the opportunity to work on this PhD research project and to become a part of the *C. elegans* world. His mentorship have been invaluable throughout my journey. I am also grateful to my auxiliary supervisor, dr. habil. Agata Tyczewska, for her careful reading of my thesis and her insightful feedback on my writing.

I would like to express my sincere gratitude to Alicja Rzepczak for her support in the lab, and to Katarzyna Solka for her invaluable assistance with administrative work and her support in Polish. I would also like to thank the members of the Laboratory of Animal Model Organisms at the Institute of Bioorganic Chemistry Polish Academy of Sciences (IBCH, PAS) for their help in preparing culture plates and media.

I would like to extend my special thanks to dr. Rajani Kanth Gudipati for his stimulating scientific discussions, which were instrumental in advancing my work.

I am eternally grateful to my family: my mom, dad, and brother, for their endless love and support throughout my PhD journey. I am profoundly grateful to my husband, Levent Soyalp, for his patience, understanding, and unwavering support.

I am truly humbled and honoured by the support of all the people who have made this dissertation possible.

Thank you.

# TABLE OF CONTENTS

ABBREVIATIONS.....	6
ABSTRACT.....	11
STRESZCZENIE.....	14
INTRODUCTION.....	17
1. Ribonucleases (RNases).....	17
2. XRN2: A Key player in RNA degradation.....	18
2.1 The multifaceted roles of XRN2 in ribosomal RNA processing and quality control.....	21
2.2 The roles of XRN2 in transcription termination and mRNA quality control.....	24
2.3 Regulation of other RNA species by XRN2.....	27
3. <i>C. elegans</i> as a model organism.....	27
AIM OF THE STUDY.....	33
MATERIALS.....	34
1. The chemicals and reagents.....	34
2. Bacterial strains and plasmids.....	36
3. Buffers and media.....	38
4. Equipment and software.....	39
5. Consumables.....	41
6. Primers and oligos.....	42
7. Plasmids.....	47
8. <i>C. elegans</i> strains.....	49
METHODS.....	51
1. <i>C. elegans</i> care and handling.....	51
1.1 <i>C. elegans</i> cultivation and maintenance.....	51
1.2 Synchronization of <i>C. elegans</i> populations through the bleaching procedure.....	52
1.3 Cryopreservation and thawing of <i>C. elegans</i> strains for long-term storage.....	52
2. <i>C. elegans</i> strains observations and profiling.....	53
2.1 Microscopy.....	53
2.2 Phenotypic characterization of <i>C. elegans</i> strains.....	53
2.3 Temperature shifting assay.....	54
2.4 Glycerol incubation.....	54

2.5 Synthetic lethality screen .....	54
3. Designing and preparing <i>C. elegans</i> strains .....	55
3.1 Creating <i>C. elegans</i> transgenic lines .....	55
3.1.1 Genomic DNA isolation .....	56
3.1.2 MultiSite Gateway Cloning .....	56
3.1.2.1 Insert preparation .....	58
3.1.2.2 Entry and destination vector design .....	60
3.1.3 Transgene integration .....	63
3.1.3.1 Pre and post processes of microinjection .....	63
3.1.3.2 <i>C. elegans</i> microinjection .....	65
3.2 Generating double mutant strain via crossing .....	66
4. Bacterial transformation .....	66
5. Colony PCR .....	67
6. Plasmid isolation .....	67
6.1 The protocol for QIAprep® miniprep Kit .....	67
6.2 The protocol for PureLink™ Quick Plasmid Miniprep Kit .....	68
7. Purification methods .....	69
7.1 PCR purification .....	69
7.2 Gel extraction method .....	69
8. Gene expression level analysis .....	70
8.1 Worm lysis .....	70
8.2 Single worm PCR for genotyping .....	70
8.3 RNA interference (RNAi) assay .....	71
8.4 RNA isolation from <i>C. elegans</i> .....	72
8.5 Complementary DNA (cDNA) synthesis .....	73
8.6 Real-time quantitative PCR (qPCR) .....	74
9. Brood Size assay .....	75
10. Embryonic Survival Assay .....	76
11. Statistics .....	76
RESULTS AND DISCUSSIONS .....	77
1. Developmental significances of XRN-2 .....	77
1.1 Screening suppressors of <i>xrn-2</i> sterility .....	78

1.1.1	Creating germline-specific <i>xrn-2</i> conditional mutants .....	80
1.1.2	Phenotypic characterization of <i>xrn-2ts<sup>germ</sup></i> .....	81
1.1.3	The genes <i>dpy-10</i> , <i>osr-1</i> , <i>ptr-6</i> , and <i>C34C12.2</i> were identified as genetic suppressors of <i>xrn-2ts<sup>germ</sup></i> .....	83
1.1.4	DPY-10, OSR-1, and PTR-6 regulate the accumulation of glycerol .....	86
1.1.5	The depletion of <i>dpy-10</i> , <i>osr-1</i> , or <i>ptr-6</i> did not alleviate the larval arrest phenotype observed in <i>xrn-2ts</i> animals.....	89
1.1.6	The primary localization of C34C12.2 is within the nucleolus of germ cells.....	92
1.1.7	The depletion of NRDE-2 led to the restoration of fertility in <i>xrn-2ts<sup>germ</sup></i> animals .....	94
1.2	Identifying potential synthetic lethality partners of <i>xrn-2</i> .....	96
1.2.2	PUF-9 is expressed in both germline and soma during development .....	100
1.2.5	<i>puf-3</i> and <i>puf-8</i> were identified as synthetic lethality partners of <i>puf-9</i> .....	106
1.2.6	<i>puf-9</i> and <i>xrn-2</i> share same or parallel functions in germline development .....	110
2.	Mechanisms of mRNA degradation by XRN-2 .....	112
2.1	XRN-2 ensures the integrity of gene expression by transcription termination.....	113
2.2	XRN-2 repressed expression of <i>ceh-99</i> by causing premature transcription termination of RNAPII.....	115
2.3	Upstream region of <i>ceh-99</i> is responsible for regulation by XRN-2 .....	117
2.4	The crucial elements for XRN-2-mediated regulation are identified within the <i>ceh-99</i> promoter region.....	118
2.5	Alternative transcription start sites have been identified in the <i>ceh-99</i> gene.....	121
CONCLUSIONS .....		127
LIST OF FIGURES .....		129
LIST OF TABLES .....		131
REFERENCES .....		133

## **ABBREVIATIONS**

**%**: Percentage

**°C**: Degrees Celsius

**3'ETS**: 3' External transcribed spacer

**5'ETS**: 5' External transcribed spacer

**ACT-1**: Actin-1

**AMP**: Ampicillin

**Amp<sup>R</sup>**: Ampicillin resistance

**ANOVA**: Analysis of variance

**bp**: Base pairs

***C. elegans***: *Caenorhabditis elegans*

**C34C12.2**: An uncharacterized gene.

**CA**: California, U.S.

**CDKN2AIP**: Cyclin-dependent kinase inhibitor 2a interacting protein

**cDNA**: Complementary DNA

**CGC**: *Caenorhabditis* genetics center

**ChIP-seq**: Chromatin immunoprecipitation sequencing

**CRISPR/Cas9**: Clustered regularly interspaced short palindromic repeats/CRISPR-associated protein 9

**Ct**: Cycle threshold

**ddH<sub>2</sub>O**: Double-distilled water

**DH5 $\alpha$** : A strain of *Escherichia coli*

**DIC**: Differential interference contrast

**DMSO**: Dimethyl sulfoxide

**DNA**: Deoxyribonucleic Acid

**DOM-3:** Downstream of tyrosine kinase 3

**DOM3Z:** DOM3 Zinc-finger protein

**DPY-10:** Dumpy protein-10

**dsrm:** Double-stranded RNA-binding motif

**DXO:** Decapping exoribonuclease

**EDTA:** Ethylenediaminetetraacetic acid

**EGFP:** Enhanced green fluorescent protein

**EMS:** Ethyl methanesulfonate

**FBF:** *fem-3*-binding factor

**GFP:** Green fluorescent protein

**GPDH-1:** Glycerol-3-phosphate dehydrogenase 1

**H<sub>2</sub>O:** Water

**IDT:** Integrated DNA Technologies

**IPTG:** Isopropyl  $\beta$ -D-1-thiogalactopyranoside

**ITS1:** Internal transcribed spacer 1

**ITS2:** Internal transcribed spacer 2

**KAN:** Kanamycin

**kb:** Kilobases

**LAP3:** Leucine aminopeptidase 3

**LB:** Lysogeny Broth

**MA:** Massachusetts, U.S.

**MFE:** Minimum free energy

**miRNA:** MicroRNA

**mM:** Millimolar

**MosSCI:** Mos1-mediated single-copy insertion

**mRNA:** Messenger RNA

**NCBI:** National center for biotechnology information

**NEB:** New England BioLabs

**NGM:** Nematode growth medium

**NJ:** New Jersey, U.S.

**NKRF:** Nuclear factor-kappa b repressing factor

**OP50:** *E. coli* bacterial strain

**OSR-1:** Osmotic stress response protein-1

**PA:** Pennsylvania, U.S.

**PAXT-1:** Partner of XRN-Two-1

**PCR:** Polymerase chain reaction

**poly(A):** Polyadenylation

**PTR-6:** Patched family protein gene

**PUF-3:** Pumilio/FBF family protein 3.

**PUF-8:** Pumilio/FBF family protein 8.

**PUF-9:** Pumilio/FBF family protein 9.

**PUM1/2:** Pumilio 1 and Pumilio 2, human homologs of the Pumilio protein.

**qPCR:** Quantitative polymerase chain reaction

**RAI1:** Rat1-interacting protein

**RBPs:** RNA-binding proteins

**rDNA:** Ribosomal DNA

**RNA:** Ribonucleic acid

**RNAi:** RNA interference

**RNAPI:** RNA polymerase I

**RNAPII:** RNA polymerase II

**RNA-seq:** RNA sequencing

**RNases:** Ribonucleases

**rpm:** Revolutions per minute

**rRNA:** Ribosomal RNA

**RRP6:** Ribosomal RNA processing protein 6

**RT-qPCR:** Reverse transcription quantitative polymerase chain reaction

***S. cerevisiae:*** *Saccharomyces cerevisiae*

**SEM:** Standard error of the mean

**siRNAs:** Small interfering RNAs

**TEC:** Transcription elongation complex

**TERRA:** Telomeric repeat-containing RNA

**TET:** Tetracycline

**Tet<sup>R</sup>:** Tetracycline resistance

**T<sub>m</sub>:** Melting temperature

**TN:** Tennessee, U.S.

**tRNA:** Transfer RNA

**ts:** Temperature-sensitive.

**TSS:** Transcription start site

**U.S.:** United States

**ul:** Microliter

**unc:** Uncoordinated

**UTR:** Untranslated region

**UV:** Ultraviolet

**XRN1:** Exoribonuclease 1

**XRN2:** Exoribonuclease 2

**$\beta$ -globin:** Beta-globin gene

## ABSTRACT

This research offers an in-depth exploration of developmental roles and RNA regulation mechanisms of XRN-2, a 5'-to-3' exoribonuclease primarily found in the nucleus. This enzyme plays multifaceted roles in gene expression and development in the nematode *Caenorhabditis elegans* (*C. elegans*). XRN-2 is involved in degrading and trimming various classes of RNA, significantly affecting processes such as transcription termination and ribosome biogenesis. Although it exhibits broad substrate specificity *in vitro*, XRN-2 selectively targets specific RNA subsets through interactions with other proteins *in vivo*. This research emphasizes that while XRN-2 is indispensable for critical developmental stages in *C. elegans*, the precise molecular pathways through which it operates remain enigmatic due to its widespread expression pattern throughout development.

To gain a deeper understanding of XRN-2's role in animal development, this study details two investigative strategies. The first strategy focused on identifying genetic suppressors linked to XRN-2 during development, with the aim of uncovering the specific role played by XRN-2 in this context. The second approach involved identifying synthetic lethality partners of XRN-2. By finding synthetic lethality partners of XRN-2, the study aimed to uncover the functional interplay between XRN-2 and these partners, thereby providing a more comprehensive understanding of XRN-2's developmental roles within specific molecular pathways.

In the first part of this research, the developmental roles of XRN-2 in the germline of *C. elegans* were explored using a germline-specific conditional mutant (*xrn-2ts<sup>germ</sup>*) of XRN-2, which had been created for the purpose of identifying genetic suppressors of sterility. Four genes, *dpy-10*, *osr-1*, *ptr-6*, and *C34C12.2*, were found to possess loss-of-function alleles, and their roles in suppressing sterility in the mutant were investigated. Among these genes, *dpy-10*, *osr-1*, and *ptr-6* were identified as positive regulators of *gpdh-1*, a crucial enzyme in glycerol production. When these genes were knocked down, elevated *gpdh-1* mRNA levels were observed, and fertility in *C. elegans* was restored. Furthermore, *C34C12.2*, a nuclear protein, found as sharing homology with *S. cerevisiae* Net1, was implicated in the potential regulation of rRNA maturation. Moreover, the restoration of fertility in *xrn-2ts<sup>germ</sup>* animals was observed as a result of the depletion of NRDE-2, which is a component of the nuclear RNAi machinery

and serves as an interacting partner of C34C12.2 in *C. elegans*. These findings suggested the critical role of XRN-2 in germline development, particularly in the context of rRNA maturation.

In the second part of the study, PUF-9 was identified as a synthetic lethality partner of XRN-2 in *C. elegans*. This discovery underscores the crucial role of PUF-9 in the development of this organism. When *puf-9* was knocked down in *xrn-2* temperature sensitive mutant (*xrn-2ts*) animals, the worms exhibited a significant decline in vitality, sluggish behaviour, and exacerbated phenotypes such as blister formation and molting defects. Importantly, PUF-9 was found to be indispensable for germline development. *puf-9* mutant worms displayed reduced brood size and significant germline deficiencies, including abnormal oocyte development, impaired gonad migration, and sterility. Furthermore, *puf-9* exhibited synthetic lethality with *puf-3* and *puf-8*, indicating a potential genetic interaction between these proteins. Knockdown of either *puf-3* or *puf-8* in *puf-9* mutant animals resulted in significant germline developmental abnormalities, further highlighting the pivotal role of PUF-9 in this critical biological process. In addition to this, the observation of a diminished brood size in the *xrn-2;puf-9* double mutant, in contrast to the effects seen in each single mutant, implies a shared functionality between PUF-9 and XRN-2 in the regulation of *C. elegans* germline development.

Finally, the specific mRNA targets regulated by XRN-2 and the mechanisms employed for RNA degradation were sought to be identified. To achieve this, a dataset derived from a comprehensive time-course RNA expression analysis conducted using a temperature-sensitive *xrn-2* mutant was employed. As a result of the inactivation of *xrn-2*, distinct sets of upregulated and downregulated RNAs were observed. It was noted that the majority of upregulated RNAs appeared to be influenced by transcription read-through events originating from their upstream gene counterparts, while the subsets of downregulated RNAs resulted from collisions between RNA polymerase II (RNAPII) molecules. Upon an in-depth examination of the *xrn-2ts* RNA sequencing data, a significant discovery was made concerning a gene designated as *ceh-99*. Interestingly, following *xrn-2* inactivation, an increase in *ceh-99* expression was observed, although this increase could not be attributed to transcription read-through from its upstream gene. This intriguing observation aroused our interest, leading to the selection of *ceh-99* as a prime candidate for uncovering the mechanisms underlying XRN-2-mediated regulation. It was demonstrated that XRN-2 represses the expression of *ceh-99* through premature termination of RNAPII and the selective repression of a *ceh-99* isoform with a longer 5' UTR. Additionally, an insertion of the TC1 autonomous DNA transposon was identified in the first intron region

of the *ceh-99* gene. Furthermore, it was observed that TC1 expression increased following XRN-2 inactivation, and the overexpression of *ceh-99* resulted in an elevated TC1 expression, suggesting that XRN-2 regulates the TC1 expression partially through the *ceh-99* locus.

## STRESZCZENIE

Badania przeprowadzone w ramach niniejszej rozprawy doktorskiej oferują dogłębne zrozumienie funkcji XRN-2, eksorybonukleazy 5'-3', występującej głównie w jądrze komórkowym. Enzym ten odgrywa istotne role w procesie ekspresji genów i rozwoju nicieni *Caenorhabditis elegans* (*C. elegans*). XRN-2 bierze udział w degradacji i cięciu różnych klas RNA, co istotnie wpływa na procesy takie jak terminacja transkrypcji i biogeneza rybosomów. Pomimo szerokiej specyficzności substratowej *in vitro*, na skutek interakcji *in vivo* z różnymi białkami XRN-2 selektywnie oddziałuje z wybranymi cząsteczkami RNA. XRN-2 jest niezbędna podczas krytycznych etapów rozwoju *C. elegans*, jednakże dokładne molekularne mechanizmy jej działania pozostają nieznane ze względu na jej rozległy wzorzec ekspresji w trakcie rozwoju organizmu.

Aby uzyskać głębsze zrozumienie roli XRN-2 w rozwoju nicieni, niniejsza praca szczegółowo opisuje dwie obrane strategie badawcze. Pierwsza strategia koncentrowała się na zidentyfikowaniu genetycznych supresorów powiązanych z XRN-2 w trakcie rozwoju, w celu odkrycia konkretnej roli, jaką w tym kontekście odgrywa XRN-2. Drugie podejście polegało na zidentyfikowaniu partnerów tzw. syntetycznej letalności XRN-2. Badanie to miało na celu odkrycie funkcjonalnej zależności między XRN-2 a jego partnerami, prowadząc do zrozumienia ról XRN-2 w określonych szlakach molekularnych podczas rozwoju nicienia.

Zastosowanie tych dwóch strategii badawczych miało na celu poznanie złożonej sieci molekularnej, w której XRN-2 funkcjonuje w trakcie rozwoju, ze szczególnym uwzględnieniem supresorów i partnerów syntetycznej letalności. Ostatecznym celem było wyjaśnienie funkcji i mechanizmów regulacyjnych XRN-2 w złożonych procesach rozwojowych. Celem badania było lepsze zrozumienie biologii rozwoju, a tym samym dostarczenie cennych informacji na temat wzajemnego oddziaływania genów i szlaków molekularnych podstawowych procesów biologicznych.

W pierwszej części badań zbadano rolę XRN-2 w linii zarodkowej *C. elegans* przy użyciu specyficznego dla linii zarodkowej mutantu warunkowego (*xrn-2<sup>ts<sup>germ</sup></sup>*) XRN-2, który został stworzony w celu identyfikacji genetycznych supresorów bezpłodności. Stwierdzono, że cztery geny, *dpy-10*, *osr-1*, *ptr-6* i C34C12.2 posiadają allele utraty funkcji i zbadano ich rolę w znoszeniu bezpłodności u mutantu. Spośród tych genów zidentyfikowano *dpy-10*, *osr-1* i *ptr-6* jako pozytywne regulatory *gpdh-1*, kluczowego enzymu w procesie produkcji glicerolu. Po

wyciszeniu ekspresji tych genów zaobserwowano podwyższony poziom mRNA *gpdh-1* i przywrócenie płodności u *C. elegans*. Co więcej, zasugerowano, że białko jądrowe C34C12.2, wykazujące homologię z *S. cerevisiae* Net1, odgrywa rolę w regulacji dojrzewania rRNA. Ponadto zaobserwowano przywrócenie płodności u nicieni *xrn-2ts<sup>germ</sup>* w wyniku obniżenia poziomu białka NRDE-2, które jest składnikiem maszyny jądrowego RNAi i służy jako partner oddziałujący białka C34C12.2 u *C. elegans*. Odkrycie to sugeruje kluczową rolę XRN-2 w rozwoju linii zarodkowej, szczególnie w kontekście dojrzewania rRNA.

W drugiej części badania zidentyfikowano PUF-9 jako partnera syntetycznej letalności XRN-2 u *C. elegans*. Odkrycie to podkreśla kluczową rolę PUF-9 w rozwoju tego organizmu. Kiedy poziom *puf-9* został obniżony u wrażliwego na temperaturę mutantu *xrn-2* w (*xrn-2ts*), nicienie były ospałe, wykazywały znaczny spadek witalności i zaostrzenie fenotypów takich jak tworzenie pęcherzy i wady w okresie linienia. Co ważne, stwierdzono, że PUF-9 jest niezbędny do rozwoju linii zarodkowej. Zmutowane nicienie *puf-9* wykazywały zmniejszoną ilość potomstwa i znaczące defekty linii zarodkowej, w tym nieprawidłowy rozwój oocytów, upośledzoną migrację gonad i bezpłodność. Ponadto *puf-9* wykazywał syntetyczną letalność w stosunku do *puf-3* i *puf-8*, co wskazuje na potencjalną interakcję genetyczną między tymi białkami. Obniżenie poziomu ekspresji *puf-3* lub *puf-8* u zmutowanych nicieni *puf-9* spowodowało znaczące nieprawidłowości w rozwoju linii zarodkowej, co dodatkowo podkreśla kluczową rolę PUF-9 w tym procesie biologicznym. Oprócz tego obserwacja zmniejszonej liczby potomstwa u podwójnego mutantu *xrn-2;puf-9*, w przeciwieństwie do efektów obserwowanych u pojedynczych mutantów tych genów, implikuje wspólną funkcjonalność PUF-9 i XRN-2 w regulacji rozwoju linii zarodkowej *C. elegans*.

Na koniec, podjęto próbę identyfikacji specyficznych docelowych cząsteczek mRNA regulowanych przez XRN-2 i mechanizmów degradacji RNA. Aby to osiągnąć, wykorzystano dane uzyskane z kompleksowej analizy ekspresji RNA w czasie, przeprowadzonej u wrażliwego na temperaturę mutantu *xrn-2*. Wyodrębniono dwa zbiory cząsteczek RNA, u których zaobserwowano zwiększone i obniżone poziomy ekspresji w wyniku inaktywacji *xrn-2*. Zauważono, że na większość genów o podwyższonym poziomie ekspresji wpływały zdarzenia typu *read-through* z genów znajdujących się powyżej, podczas gdy obniżony poziom RNA wynikał z zawady przestrzennej pomiędzy cząsteczkami polimerazy RNA 2 (RNAPII). Dogłębna analiza danych z sekwencjonowania RNA mutantu *xrn-2ts* wykazała, że po inaktywacji *xrn-2* zaobserwowano wzrost ekspresji *ceh-99*, chociaż wzrostu tego nie można

było przypisać transkrypcji typu *read-through* z genu znajdującego się powyżej. Ta intrygująca obserwacja wzbudziła nasze zainteresowanie, co doprowadziło do wyboru *ceh-99* jako głównego kandydata do odkrycia mechanizmów leżących u podstaw regulacji za pośrednictwem XRN-2. Wykazano, że rola XRN-2 polega na tłumieniu ekspresji *ceh-99* poprzez przedwczesną terminację RNAPII i selektywną represję izoformy *ceh-99* z dłuższym 5'UTR. Dodatkowo zidentyfikowano insercję autonomicznego transpozonu DNA TC1 w pierwszym regionie intronu genu *ceh-99*. Ponadto zaobserwowano, że poziom ekspresji TC1 wzrósł po inaktywacji *xrn-2*, co wskazuje, że XRN-2 reguluje transpozon TC1, przynajmniej częściowo, poprzez locus *ceh-99*.

# INTRODUCTION

## 1. Ribonucleases (RNases)

RNA regulation is a fundamental process that governs gene expression and plays a crucial role in cellular function and development [Hwang et al., 2016; Christofi and Zaravinos, 2019]. Within this intricate regulatory network, Ribonucleases (RNases), emerge as key players responsible for modulating the stability, processing, and degradation of RNA molecules [Suzuki and Tsukahara, 2014; Trinquier et al., 2020]. The significance of RNases in RNA regulation is multifaceted, with diverse implications for various biological processes [Trinquier et al., 2020].

One primary significance of RNases lies in their ability to control the levels of RNA transcripts within the cell [Arraiano et al., 1988; Cheng and Deutscher, 2005]. By selectively degrading or processing specific RNA molecules, RNases help regulate gene expression and fine-tune the abundance of various RNA species. This dynamic control enables cells to respond rapidly to internal and external stimuli, allowing for precise and timely gene regulation [Zhang et al., 2021]. Moreover, RNases contribute to the maintenance of cellular homeostasis by preventing the accumulation of aberrant or unnecessary RNA molecules that could disrupt cellular functions [Boix et al., 2020; Boo and Kim, 2020].

RNases also participate in the quality control mechanisms that ensure the fidelity and accuracy of RNA molecules. RNases are involved in surveillance systems that identify and eliminate defective or damaged RNA species, safeguarding the integrity of the cellular transcriptome [Houseley and Tollervey, 2009]. This process is particularly vital in preventing the translation of faulty or potentially harmful proteins, thereby preserving cellular functionality and preventing the onset of various diseases.

Furthermore, RNases play critical roles in post-transcriptional processing events, such as RNA splicing, maturation, and decay [Arraiano et al., 2010]. These processes are essential for generating functional RNA molecules from precursor transcripts to shape the final RNA repertoire. RNases contribute to the precise cleavage and removal of specific RNA segments, allowing for the generation of mature RNA molecules with defined sequences and structures. This intricate control of RNA processing ensures the production of functional RNA species

required for diverse cellular functions, including protein synthesis, regulation of signalling pathways, and cellular differentiation.

In addition to their fundamental roles in normal cellular processes, the dysregulation of RNases has been implicated in various human diseases [Sun and Sheng, 2022]. Altered expression or function of RNases can lead to aberrant RNA processing, accumulation of unstable transcripts, or disruption of regulatory networks, ultimately contributing to the development of pathologies such as cancer, neurological disorders, and autoimmune diseases [Rosenberg, 2008; Boulianne and Feldhahn, 2018; Castro et al., 2021]. Understanding the significance of RNA regulation by RNases is therefore essential for unravelling the molecular mechanisms underlying these diseases and for exploring potential therapeutic interventions.

RNases can be categorized as either endoribonucleases or exoribonucleases, each of which encompasses multiple sub-classes. Endoribonucleases cleave RNA internally, playing vital roles in RNA maturation, splicing, and the maintenance of functional tRNA and rRNA. Exoribonucleases degrade RNA from the ends, actively participating in RNA degradation pathways and facilitating the turnover of mRNA, non-coding RNA, and RNA fragments.

While certain RNases may specialize in specific functions, others exhibit a broader range of activities across diverse processes. This is especially evident in the case of XRN2 [Nagarajan et al., 2013; Miki and Großhans, 2013]. Among the exoribonucleases, XRN2 assumes critical functions in RNA degradation, orchestrating turnover dynamics and maintaining RNA homeostasis to ensure accurate gene expression. Collaborative interplay of XRN2 with RNA-binding proteins and regulatory factors further reinforces the precise control of RNA degradation and turnover processes. Since this function of XRN2 has been studied mainly in simple cellular system such as yeast and mammalian cell lines, its significance in intact multicellular organisms remains poorly understood.

## **2. XRN2: A Key player in RNA degradation**

XRN2 is an evolutionary conserved 5'-3' exoribonuclease, originally known as RAT1 (ribonucleic acid trafficking protein 1), which initially identified in the budding yeast *Saccharomyces cerevisiae* (*S. cerevisiae*) as a gene mutated in cells with a poly(A) + RNA

(polyadenylated RNA) nuclear export defect [Amberg et al., 1992]. Through subsequent investigations, orthologous genes were discovered in other eukaryotes [Sugano et al., 1994; Zhang et al., 1999] and referred to as TAP1, HKE1, and DHM1 [Di Segni et al., 1993; Kenna et al., 1993; Shobuie et al., 1995]. Notably, the complementation of an XRN2 null mutation in *Schizosaccharomyces pombe* by mouse Xrn2 demonstrated its widespread conservation throughout evolution [Shobuie et al., 1995]. XRN2 shares homologous regions with the 5'→3' exoribonuclease XRN1 [Amberg et al., 1992; Aldrich et al., 1993; Miki and Großhans, 2013], both exhibiting comparable exonuclease activity *in vitro*. They recognize single-stranded RNA with a 5'-terminal monophosphate and efficiently degrade it to mononucleotides [Kenna et al., 1993; Poole and Stevens, 1995; Stevens and Poole, 1995]. However, XRN2 predominantly localizes in the nucleus [Johnson, 1997], while XRN1 is primarily found in the cytoplasm [Heyer et al., 1995].

XRN2 stands as a cornerstone in the intricate landscape of RNA processing and regulation, orchestrating a symphony of vital functions that shape the cellular RNA dynamics (Figure 1). Among its multifaceted responsibilities, XRN2 plays a central role in trimming and maturing snoRNAs [Petfalski et al., 1998; Chanfreau et al., 1998; Qu et al., 1999], a process critical for the maturation and functionality of these essential RNA molecules. Furthermore, XRN2 is a proficient executor in the degradation of specific tRNAs, miRNAs, and TERRA (Telomeric repeat-containing RNA) [Luke et al., 2008]. This comprehensive RNA degradation profile is instrumental in maintaining the precision of gene expression, ensuring that the cellular machinery operates with accuracy. Beyond its roles in RNA degradation, XRN2 also stands as a sentinel for transcription fidelity, especially in the vicinity of transcription start sites. Its vigilant oversight of these crucial regions plays a pivotal role in safeguarding the integrity of the transcription process, ensuring the faithful and accurate transcription of genetic information. [Wei et al., 2012]. Collectively, these multifaceted roles highlight the indispensable contributions of XRN2 to the dynamic realm of RNA and the overall functionality of the cell. Its ability to shape the landscape of various RNA species, ensuring their precise processing, degradation, and transcription fidelity, underscores XRN2's vital presence in the intricate web of cellular RNA dynamics.

Given XRN2's ability to degrade 5'-monophosphorylated single-stranded RNA indiscriminately without sequence specificity *in vitro* [Stevens and Poole, 1995], its recruitment to specific subcellular compartments or RNA targets through interactions with partner proteins

becomes crucial for exerting cellular functions. In the pursuit of understanding these factors, Miki et al. [2014a] uncovered an XRN-2-binding domain (XTBD) within Partner of XRN-Two-1 (PAXT-1) from *C. elegans*. They found XTBD proteins, NKRF and CDKN2AIP, binding XRN2 in humans. They determined the XTBD-XRN2 complex structure, identifying interface residues essential for bonding [Richter et al., 2016; Aygün et al., 2021]. Over 800 XTBD family proteins exist across 350+ species in metazoans or alveolates [Pfam, n.d.]. Some members, having RNA-binding motifs like dsrm, G-patch, and R3H domains, likely guide XRN2 to targets [Aygün et al., 2020]. Interestingly, yeast lacks XTBD proteins. Instead, Rat1-interacting protein (Rai1) enhances Rat1/XRN2 exoribonuclease activity [Stevens and Poole, 1995; Xiang et al., 2009]. In contrast, *C. elegans* DOM-3 and human DXO/DOM3Z likely don't interact with XRN2 due to absent interface residues [Xiang et al., 2009; Chang et al., 2012]. This implies yeast coordinates Rai1's activities with XRN2, while others use XTBD proteins to enhance XRN2's efficacy.

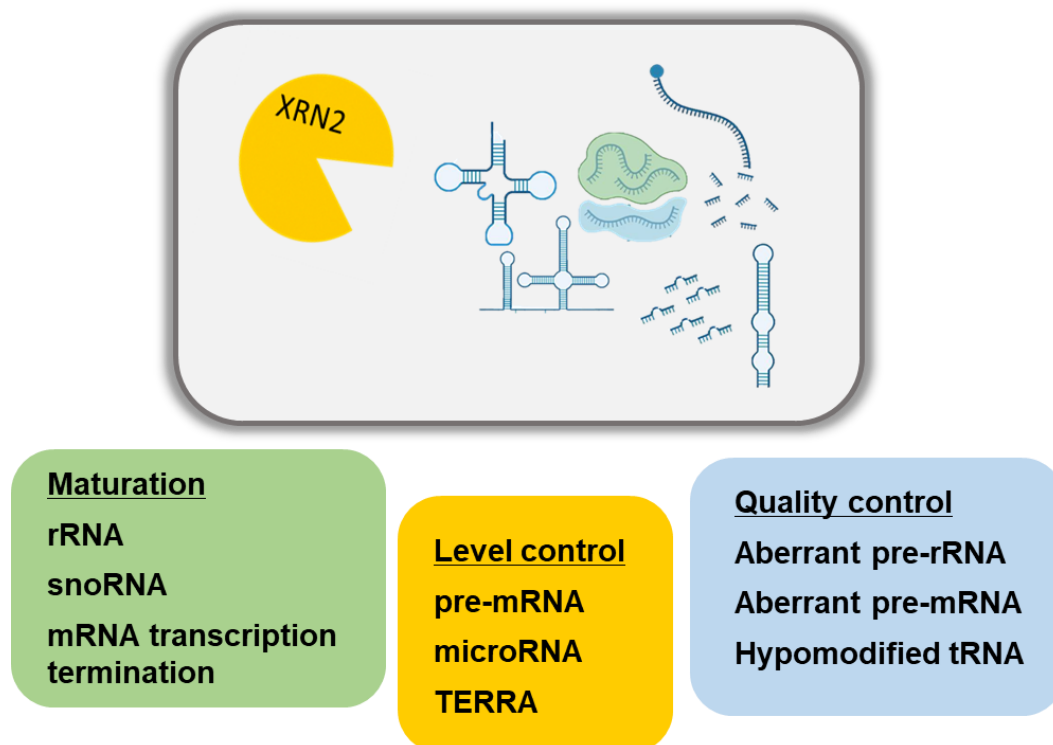


**Figure 1: XRN2 targets different types of RNA for varied purposes.** XRN2 plays a multifaceted role in RNA biology by selectively targeting various RNA species. It is involved in the maturation of rRNA, snoRNA, and mRNA transcription termination. Additionally, XRN2 participates

in level control through its interactions with pre-mRNA, microRNA, and TERRA. Furthermore, it contributes to quality control mechanisms by recognizing and degrading aberrant pre-rRNA, aberrant pre-mRNA, and hypomodified tRNA molecules.

## **2.1 The multifaceted roles of XRN2 in ribosomal RNA processing and quality control**

Ribosomes, intricate molecular machines responsible for protein synthesis, undergo a complex assembly pathway within cells [Kressler et al., 2010]. In eukaryotes, the ribosome's primary structural components consist of the 18S rRNA in the small subunit and the 5.8S/25S rRNAs (or 5.8S/28S rRNAs in higher eukaryotes) in the large subunit. These vital ribosomal RNAs are initially transcribed by RNA polymerase I (RNAPI) as a single, extensive precursor molecule, encompassing additional regions known as spacer regions, which are subsequently removed during the maturation process of pre-rRNA. For instance, in mammalian species, the precursor molecule called 47S pre-rRNA contains distinct external (5'ETS, 3'ETS) and internal (ITS1 and ITS2) transcribed spacers [Wang and Pestov, 2011]. The synthesis of functional ribosomal subunits involves a series of endonucleolytic cleavage events within the spacer regions, followed by exonucleolytic trimming to establish the precise 5' and 3' ends of the mature rRNAs [Eichler and Craig, 1994; Venema and Tollervey, 1999].

XRN2 has been reported to have crucial roles in the maturation of 5.8S and 25S/28S rRNAs and the degradation of spacer fragments that are excised during rRNA maturation in various organisms, including yeast, ciliates, plants, and mammals [Amberg et al., 1992; Di Segni et al., 1993; Petfalski et al., 1998; Fang et al., 2005; Zakrzewska et al., 2010; Wang and Pestov, 2011; Couvillion et al., 2012].

The involvement of XRN2 in rRNA processing was initially demonstrated in a temperature-sensitive mutant of *S. cerevisiae* XRN2 [Amberg et al., 1993]. Among the two isoforms of yeast 5.8S rRNA, namely 5.8S(S) and 5.8S(L), the level of the major isoform, 5.8S(S), decreased upon shifting to a restrictive temperature. The involvement of XRN2 in 25S rRNA maturation was also observed in yeast. After endonucleolytic cleavage at the upstream site, XRN2 rapidly trims the extension to generate the 5'-end of 25S rRNA [Fang et al., 2005] (Figure 2A). The exonucleolytic trimming by XRN2 to generate the 5'-ends of 5.8S and 28S rRNAs is likely to be conserved in mammals. Knockdown of XRN2 by RNA interference (RNAi) in mouse LAP3 cells resulted in the accumulation of 5'-extended 5.8S and 28S rRNAs

[Wang and Pestov, 2011]. The 5.8S and 25S/28S rRNAs are major components of the 60S ribosomal subunit, and the efficient maturation of these rRNAs requires specific protein components within the pre-60S particles [Granneman et al., 2021].

Considering the crucial role played by ribosomes in facilitating protein synthesis, it becomes imperative to ensure the vigilance and maintenance of high-quality rRNAs through an intricate surveillance system designed to identify and eliminate defective rRNA species. Intriguingly, in the realm of yeast biology, it has been observed that certain fractions of aberrant precursor rRNAs (pre-rRNAs) undergo polyadenylation as a means of flagging them for subsequent degradation [Kuai et al., 2004; Fang et al., 2005]. While the degradation process primarily hinges on the 3'→5' exoribonuclease complex known as the exosome, emerging evidence indicates the involvement of XRN2, an additional key player (Figure 2B) [Fang et al., 2005].

Notably, upon depleting XRN2, a discernible increase in the accumulation of polyadenylated pre-rRNAs has been observed, particularly in strains lacking the exosome subunit Rrp6. Interestingly, this depletion also leads to a reduction in the diversity of pre-rRNA variants at their 5' ends. It is important to highlight, however, that the deletion of XRN2 alone does not seem to exert any noticeable impact on pre-rRNA dynamics within this particular context.

In contrast, investigations conducted in mammalian cells have shed light on a more pronounced role of XRN2. Employing RNAi techniques to knock down XRN2, researchers have discovered a significant build-up of aberrant precursor rRNA species. This finding underscores the pivotal contribution of XRN2 in upholding the fidelity and quality control of pre-rRNAs within mammalian cells [Wang and Pestov, 2011].

Collectively, these observations emphasize the intricate and indispensable nature of the surveillance mechanisms that safeguard the integrity of rRNAs. The interplay between polyadenylation, exosome-mediated degradation, and the multifaceted involvement of XRN2 not only underscores the significance of quality control in ribosome biogenesis but also highlights the remarkable diversity and complexity of these processes across different organisms. Further exploration in this field promises to deepen our comprehensive

understanding of the molecular machinery governing ribosomal RNA surveillance and its crucial role in maintaining cellular homeostasis.

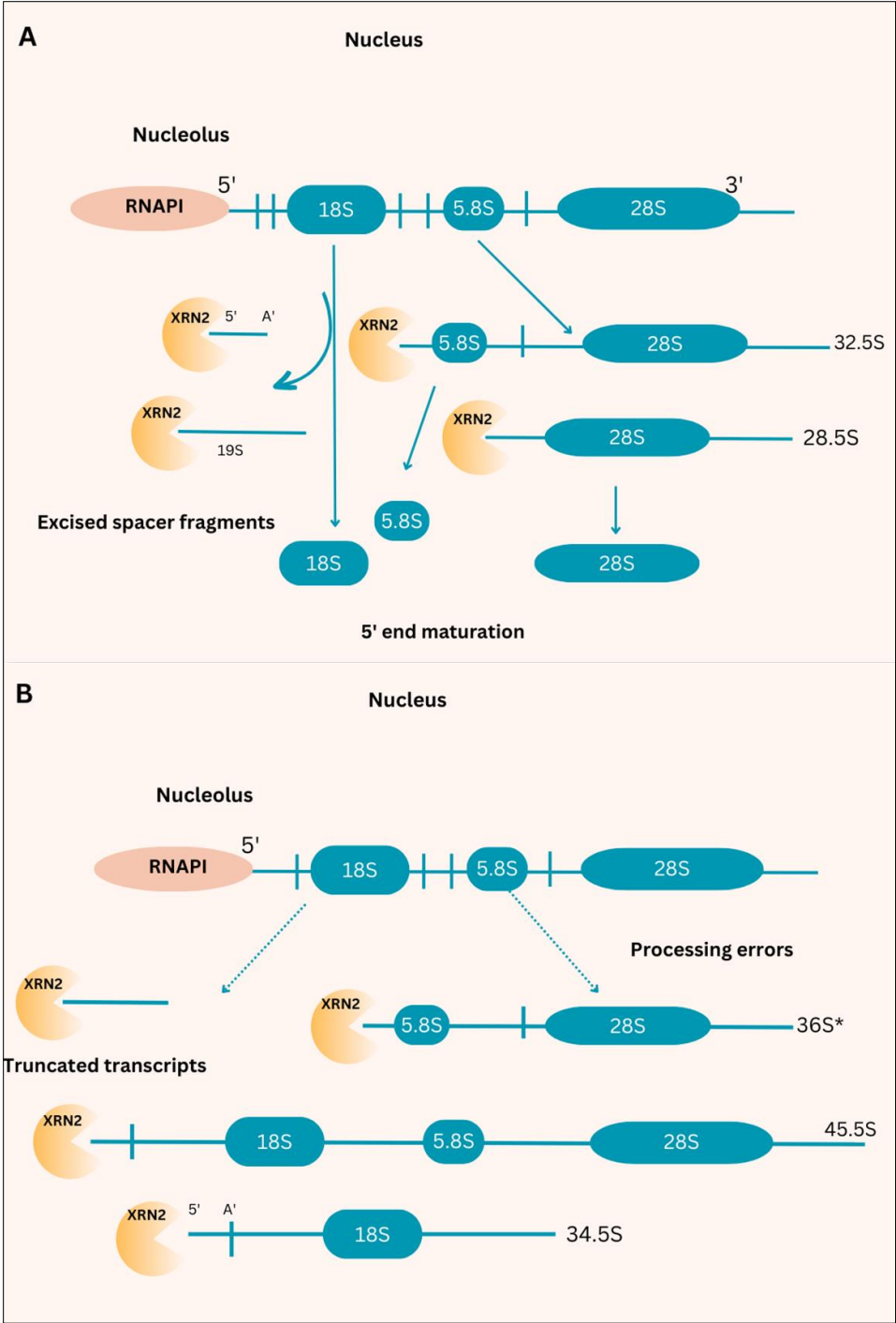


**Figure 2: Processing and quality control mechanisms mediated by XRN2 play crucial roles in mammalian pre-rRNA maturation.** Throughout the maturation process, various 5' ends of pre-rRNA

molecules become substrates for XRN2-mediated modifications. In the case of normal processing (A), XRN2 trims the 5' ends of 32.5S and 28.5S pre-rRNAs, ensuring their proper maturation. Additionally, XRN2 degrades processing byproducts, such as spacer fragments that are excised during the formation of 18S rRNA. These activities of XRN2 contribute to the maintenance of accurate pre-rRNA processing. Furthermore, XRN2 plays a crucial role in correcting errors that may occur during transcription and processing of pre-rRNA. (B) Aberrant species, such as truncated RNAPI transcripts and pre-rRNAs that undergo abnormal cleavage, are targeted by XRN2 for degradation. Examples of such aberrant species include 34.5S, 45.5S, and 36S\* pre-rRNAs. By eliminating these faulty molecules, XRN2 helps maintain the fidelity of pre-rRNA processing and ensures the production of functional ribosomes. Inspired by Wang and Pestov [2011].

## **2.2 The roles of XRN2 in transcription termination and mRNA quality control**

Transcription conducted by RNAPII involves a sequence of three principal phases: initiation, elongation, and termination. Termination of transcription signifies the conclusion of a transcriptional segment through the dismantling of the transcription elongation complex (TEC), leading to the liberation of RNAPII and the transcript from the DNA template [Porrua et al., 2016; Proudfoot et al., 2016]. Termination failure causes transcription read-through, which perturbs expression of downstream genes by interfering with RNAPII pausing at promoters or transcribing the other strands. Two distinct mechanisms have been postulated for the termination of RNAPII-mediated transcription. The "torpedo" model posits that cleavage at the polyadenylation (poly(A)) site severs the pre-mRNA from the TEC, allowing the TEC to persist in generating a nascent transcript downstream (Figure 3) [Kim et al, 2004; West et al., 2004]. On the other hand, the allosteric model proposes that the poly(A) signal or other potential termination signals located in the downstream region prompt the disassembly of the TEC through mechanisms that remain unclear [Kim et al., 2004; Zhang et al., 2015]. It's worth noting that these two models are not mutually exclusive, and efforts have been made to develop comprehensive frameworks that incorporate elements from both models [Luo et al., 2006; Zhang et al., 2015].

The process of transcription termination by RNAPII represents a fascinating and intricate phenomenon, relying on the coordinated actions of numerous protein factors [Richard and Manley, 2009]. Among these factors, the components of the cleavage/polyadenylation machinery take centre stage, as the requirement of an active polyadenylation signal for efficient

termination has been long acknowledged [Richard and Manley, 2009; Proudfoot, 2011]. However, the termination process involves more than just the cleavage/polyadenylation machinery. One key player that has garnered significant attention is XRN2, that plays a crucial role in degrading the nascent RNA downstream from the 3' cleavage site, thereby promoting termination [West et al., 2004; Kim et al, 2006; Skourti-Stathaki et al., 2011]. Recent studies have provided compelling evidence supporting the involvement of XRN2 in the termination of the majority of RNAPII transcripts [Fong et al., 2015].

After RNAPII transcribes a poly(A) signal, specific cleavage factors act to cleave the RNA transcript, resulting in a polyadenylated 5' fragment. However, intriguingly, RNAPII remains bound to the DNA and continues transcription downstream. It has been hypothesized that XRN2 degrades the 3' end of the transcript until it encounters RNAPII, leading to dissociation of RNAPII from the DNA (Figure 3). However, research has revealed that the degradation of the 3' transcript by XRN2 alone is insufficient for proper termination, both in vivo and in vitro [Luo et al., 2006; Dengl and Cramer, 2009]. Astonishingly, while both XRN2 and XRN1 have the capability to degrade the 3' transcript, only XRN2 is indispensable and competent for termination in yeast [Luo et al., 2006]. Further studies demonstrated the cooperative association of XRN2 and the cleavage factor Pcf11 with RNAPII at the poly(A) site, promoting poly(A) site cleavage and subsequent degradation of the downstream transcript [Luo et al., 2006]. It is worth noting that XRN2's involvement in RNAPII transcription termination downstream of poly(A) sites in mammalian cells and *C. elegans* appears to be gene-specific rather than a universal mechanism [Banerjee et al., 2009; Brannan et al., 2012]. Moreover, XRN2 has also been implicated in the termination of pre-rRNA transcription by RNAPI [El Hage et al., 2008; Kawauchi et al., 2008], intergenic primary miRNA (microRNA) transcription by RNAPII [Kawauchi et al., 2008], and premature termination of RNAPII transcription [Brannan et al., 2012; Jimeno et al., 2010; Wagschal et al., 2012]. These findings underscore the diverse roles of XRN2 in transcriptional termination across different RNA types, highlighting its significance in regulating gene expression.

Ensuring the accuracy and fidelity of mRNA processing is of paramount importance to prevent the production of harmful and aberrant proteins within the cell. Thus, the identification and elimination of these erroneous pre-mRNA species become crucial tasks. In the realm of yeast biology, unspliced pre-mRNAs encountering processing errors face swift and efficient degradation from both their 5'- and 3'-ends, primarily through the concerted efforts of XRN2

and the nuclear exosome, respectively [Bousquet-Antonelli et al., 2000]. While the exosome assumes a predominant role in this degradation process, it is noteworthy that environmental conditions can influence the delicate balance at play.

The pivotal role played by XRN2 in maintaining the quality control of pre-mRNAs underscores its indispensable contribution to cellular integrity. By swiftly eliminating defective transcripts, XRN2 acts as a vigilant guardian, preventing the translation of erroneous genetic information into potentially detrimental proteins. In-depth exploration of the intricate interplay between XRN2, the exosome, and the broader regulatory mechanisms governing pre-mRNA quality control promises to unravel the complexity of pathways involved in maintaining the fidelity of gene expression. Such knowledge holds immense potential for the development of therapeutic interventions aimed at mitigating the detrimental consequences of aberrant mRNA processing. As errors in pre-mRNA processing have the potential to give rise to harmful proteins, the elimination of these aberrant species becomes a crucial imperative. Unspliced pre-mRNAs undergo rapid degradation from both their 5'- and 3'-ends, with XRN2 and the nuclear exosome playing significant roles, although the balance may be influenced by environmental conditions [Bousquet-Antonelli et al., 2000]. In human cells, the importance of XRN2 in degrading aberrant pre-mRNA products surpasses that of the exosome. A study revealed that in XRN2-depleted HeLa cells, transcripts derived from  $\beta$ -globin genes lacking proper poly(A) site processing or transcription termination accumulated in chromatin fractions [Davidson et al., 2012]. Additionally, treatment of XRN2-depleted cells with spliceostatin A, a splicing inhibitor, leads to the accumulation of various endogenous pre-mRNAs in chromatin fractions. These findings suggest that XRN2 is involved in co-transcriptional degradation of aberrant pre-mRNAs in human cells. The regulation of mRNA levels is crucial for determining protein amounts and is tightly controlled through turnover at both the pre-mRNA and mRNA stages. Bousquet-Antonelli et al., [2000] demonstrated active degradation of pre-mRNAs in the nucleus by XRN2 and the exosome, with pre-mRNA degradation and splicing competing for mRNA production in *S. cerevisiae*. Furthermore, mRNA degradation has also been observed in the nucleus. Das et al., [2003] used *S. cerevisiae* strains with a nuclear export defect and showed rapid degradation of nuclear-retained mRNAs, a process that is suppressed by depletion of XRN2 or the exosome, although its significance under normal conditions is not yet clear. Similar to the degradation of aberrant pre-mRNAs, the exosome plays major roles in these processes.

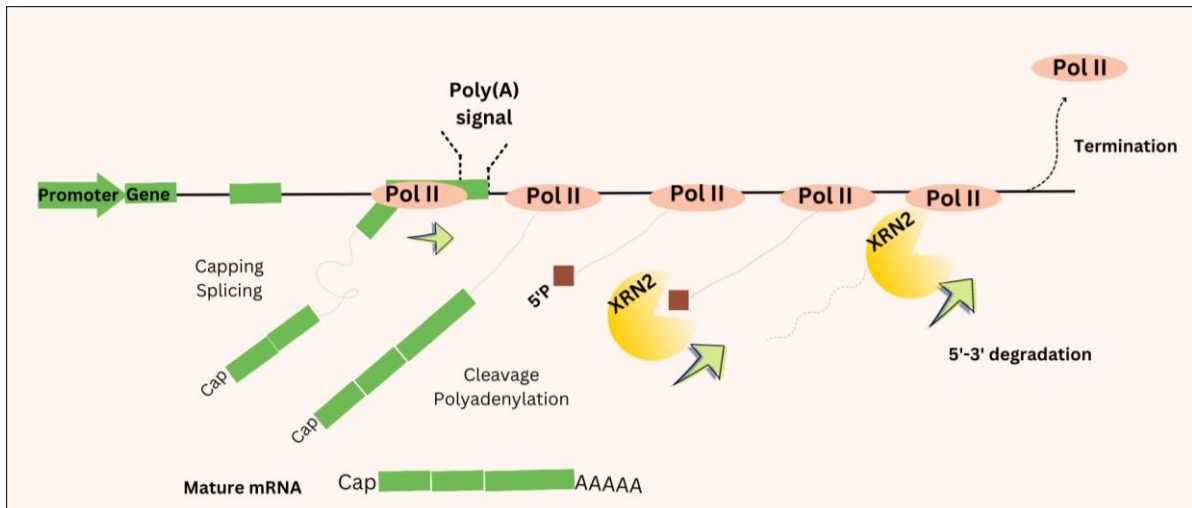


**Figure 3: Schematic representation of XRN2 functions in RNAPII transcription termination.** The torpedo model provides an explanation for the process of transcription termination by RNAPII. According to this model, RNAPII continues transcribing beyond the poly(A) signal. However, cleavage events downstream of the poly(A) signal create a starting point for the exoribonuclease XRN2 to degrade the transcript downstream of the cleavage site. As XRN2 moves along the transcript, it encounters RNAPII and triggers the dissociation of both RNAPII and the upstream transcript from the DNA template. This collision between XRN2 and RNAPII plays a crucial role in the termination of transcription. Inspired by Eaton and West [2018].

### 2.3 Regulation of other RNA species by XRN2

XRN2 is a key player in intricate RNA processing and regulation. It trims and matures snoRNAs [Petfalski et al., 1998; Chanfreau et al., 1998; Qu et al., 1999], degrades specific tRNAs, miRNAs, and TERRA [Luke et al., 2008], maintaining gene expression precision. It ensures transcription fidelity near start sites and degrades non-targeting siRNAs [Wei et al., 2012]. These roles underscore XRN2's vital contributions to RNA dynamics and cellular function.

### 3. *C. elegans* as a model organism

The utilization of *C. elegans* as a model organism presents numerous advantages, rendering it an exceptional option for investigating a wide array of biological processes. This

is especially true when delving into the complex domain of RNA processing and regulation. The remarkable characteristics of *C. elegans*, coupled with the intricate interplay between its biology and the crucial role played by XRN-2 (“XRN-2” is used specifically for *C. elegans*) in RNA-related processes, have significantly contributed to its widespread adoption and have paved the way for revolutionary discoveries.

One of the primary reasons why *C. elegans* stands out as an exceptional model organism is its elegantly simple and precisely defined anatomy. With its precisely 959 somatic cells, each meticulously mapped and characterized [Consortium, 1998], it offers a unique vantage point to comprehensively investigate various developmental processes, including the intricate events of RNA processing, with an unparalleled level of single-cell resolution. This remarkable simplicity, coupled with the ability to observe cellular dynamics in real-time, provides an unparalleled opportunity to investigate the multifaceted roles and functions of XRN-2 in the context of RNA processing.

Additionally, the abbreviated life cycle of *C. elegans* serves as a valuable asset, effectively expediting the pace of scientific advancements. From embryo to adult, the nematode completes its development within a mere three days (Figure 4A). The life cycle of *C. elegans* consists of four larval stages (L1, L2, L3, and L4) before reaching adulthood [Frezal and Felix, 2015]. This rapid lifecycle allows to study multiple generations of *C. elegans* in a relatively short time span, facilitating longitudinal studies and enabling the observation of changes in RNA processing and regulation over successive generations. This temporal dimension provides a unique vantage point to examine the impact of XRN-2 on RNA dynamics and stability across different developmental stages, shedding light on its multifaceted functions throughout the nematode's life cycle.

Reproduction in *C. elegans* predominantly takes place through self-fertilization in hermaphrodites (XX), with the occurrence of outcrossing involving males (XO) being relatively infrequent [Frezal and Felix, 2015]. The germline development in hermaphrodites begins during embryogenesis. At this stage, germ cells, which are the precursors of the germline, are set aside from somatic cells. These germ cells undergo mitotic divisions to increase in number. As the hermaphrodite larva develops, a subset of these germ cells enters meiosis, a specialized type of cell division that results in the formation of haploid gametes. In hermaphrodites, oocytes are the primary product of meiosis, and they undergo further maturation before being fertilized.

Sperm production in hermaphrodites occurs via a separate process known as spermatogenesis. A few germ cells differentiate into sperm, which are stored in the spermatheca until they are needed for fertilization. In males, the germline development in *C. elegans* follows a slightly different trajectory. Male *C. elegans* possess only male-specific reproductive structures and do not produce oocytes. During development, germ cells in males also undergo mitotic divisions, similar to hermaphrodites. However, instead of entering meiosis to produce oocytes, most of the germ cells differentiate into sperm through spermatogenesis (Figure 4B). This process involves a series of cell divisions and morphological changes, ultimately leading to the production of mature sperm. In both hermaphrodites and males, the germline is maintained throughout adulthood. In hermaphrodites, the germline undergoes continuous rounds of oogenesis throughout their reproductive lifespan, allowing them to self-fertilize. In males, the germline continuously produces sperm, which are stored in the seminal vesicle until they are transferred to a mating partner during copulation. The germline in *C. elegans* is highly regulated and controlled by a network of genes and signalling pathways. Numerous studies have uncovered key molecular players involved in germline development, including transcription factors, RBPs, and signalling molecules. Understanding the germline development in *C. elegans* has provided valuable insights into the fundamental processes underlying gametogenesis and reproductive biology [Barton and Kimble, 1990; Morgan et al., 2010].

Another notable feature of *C. elegans* is its exceptional reproductive capacity. Each hermaphroditic worm can generate approximately 300 progeny throughout its lifetime, ensuring an abundant supply of experimental subjects for genetic studies [Hunt, 2017]. This prolific breeding capability facilitates extensive genetic screenings and experiments, rendering the identification and characterization of mutants or genetic variations not only feasible but also highly effective. The availability of extensive mutant libraries and well-established methodologies for generating transgenic animals and performing RNAi further enhances the genetic tractability of *C. elegans*, allowing for precise investigations into the mechanisms by which XRN-2 impacts RNA processing.

The utilization of the complete genome sequence of *C. elegans* provides significant advantages in various research endeavours, enabling in-depth investigations into genetic mechanisms, evolutionary relationships, and the exploration of fundamental biological processes [Leung et al., 2008]. Techniques such as introducing specific mutations, performing

knockdowns or knockouts, and incorporating transgenes provide researchers with a powerful toolkit to decipher the different RNA processing pathways.

Furthermore, while *C. elegans* is a simple organism, it shares numerous conserved biological processes with higher organisms, including humans. Many fundamental aspects of RNA processing and regulation pathways are highly conserved across species. Therefore, studying RNA dynamics and the functions of XRN-2 in *C. elegans* can provide valuable insights into analogous processes in more complex organisms. The knowledge gained from *C. elegans* research can be extrapolated and applied to broader contexts, enhancing our understanding of the roles and significance of XRN-2 in RNA processing and regulation in diverse cellular and physiological systems. Moreover, *C. elegans* offers a valuable advantage to the pharmaceutical industry as its usage is not limited by ethical issues associated with the use of vertebrates [Giunti et al., 2021]. Its simplicity and genetic tractability have paved the way for breakthrough discoveries and advancements in various fields of study. For instance, research conducted using *C. elegans* led to groundbreaking findings in areas such as RNAi and apoptosis [Grishok., 2013; Frezal and Felix, 2015].

In addition, the unique thermoregulation capabilities of *C. elegans* make it an excellent model organism for investigating adaptive mechanisms induced by changes in environmental temperature [Mendenhall et al., 2017]. Cultivated at temperatures ranging from 15 °C to 26 °C, *C. elegans* displays limited survival at temperatures lower than 15 °C or higher than 26 °C [Chen et al., 2019]. This characteristic provides researchers with an opportunity to explore how fluctuations in temperature impact RNA processing and regulation, including the role of XRN-2 in temperature-sensitive pathways.

In conclusion, *C. elegans* stands as a powerful and advantageous model organism for studying various biological processes, with a particular emphasis on RNA processing and regulation. Its elegantly simple anatomy, short lifecycle, genetic tractability, and conservation of key biological processes have provided researchers with invaluable tools and opportunities to unravel the intricate functions of XRN-2 in RNA-related pathways. The profound insights gained from studying *C. elegans* continue to enrich our understanding of complex interplay between RNA processing, XRN-2, and cellular regulation in diverse organisms, ultimately advancing our knowledge of fundamental biological processes.

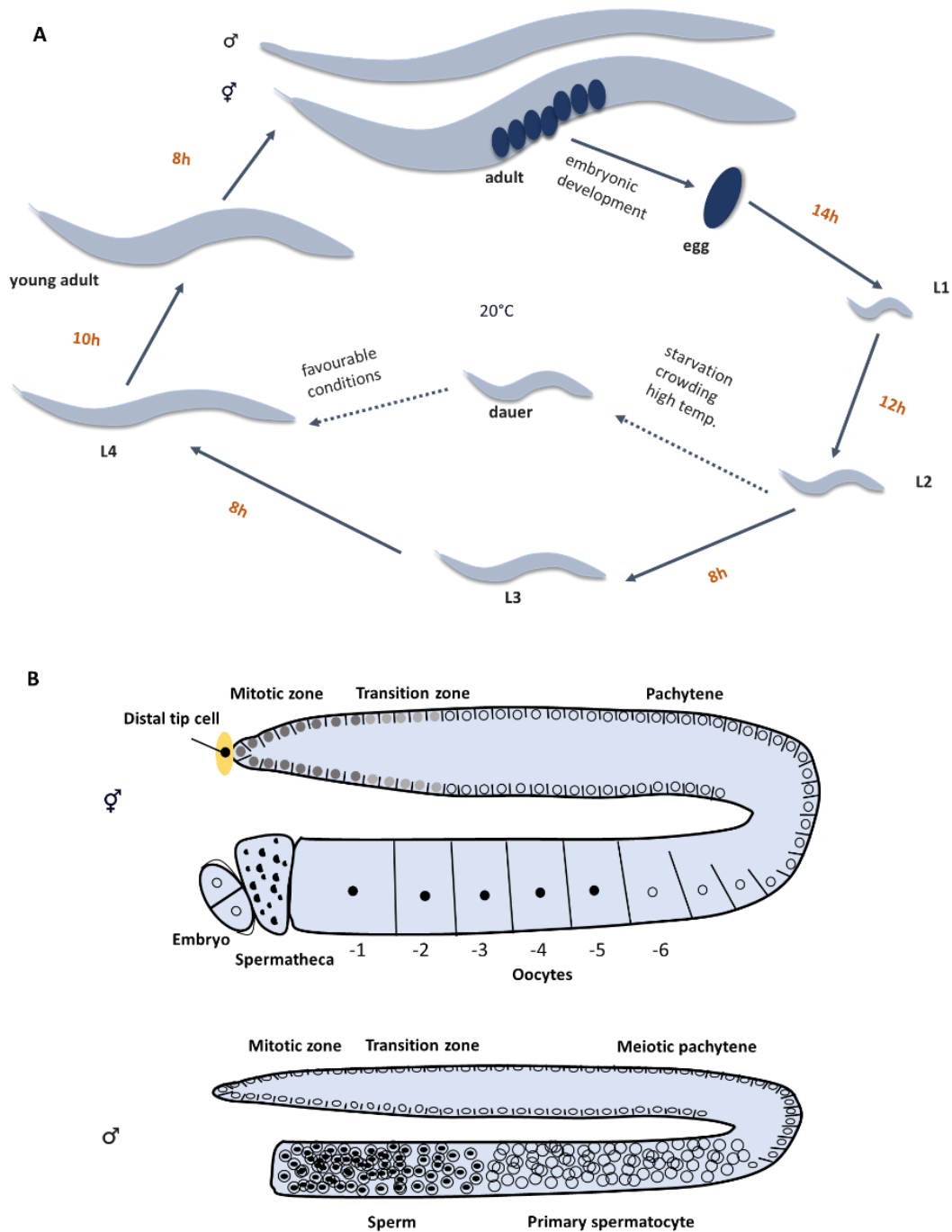


**Figure 4: *C. elegans* life cycle and germline development.** (A) The eggs require approximately 14 hours to hatch, at 20 °C, followed by the completion of the L1 stage within an additional 12 hours. Over the course of their development, the worms go through four cycles before reaching adulthood. In unfavourable conditions, the worm enters the dauer larva stage, a period of suspended feeding where it can survive for months. When conditions improve, it exits this stage, resuming development and maturing into an adult. At this temperature, a majority of the offspring produced are hermaphrodites, while a much smaller proportion develops into males. Adapted from Worm Atlas (Handbook - Introduction, n.d.). (B) In hermaphrodites (upper), primordial germ cells (PGCs) differentiate into

oocytes within the gonad arms, ultimately giving rise to mature oocytes ready for fertilization. Male germline development follows a distinct pathway. Male (lower) PGCs undergo mitotic divisions and subsequently enter meiosis, leading to the generation of spermatocytes within the gonad. These spermatocytes further differentiate into mature sperm cells, which are eventually released into the seminal vesicle. Inspired by Morgan et al., [2010].

## AIM OF THE STUDY

The primary aims of this research encompassed revealing the intricate molecular interactions and regulatory mechanisms that underlie the crucial roles XRN-2 plays in pivotal developmental processes within the *C. elegans* model organism. Among a diverse array of investigative techniques, genetic suppressor screens, the identification of synthetic lethality partners, and in-depth examinations of RNA regulation mechanisms serve as the primary tools for exploration. Systematic genetic suppressor screens were anticipated to unveil specific genetic elements that interact with XRN-2, ultimately influencing fertility outcomes. This systematic approach aimed to reveal the intricate mechanisms by which XRN-2 exerts its developmental effects. Furthermore, the research aimed to uncover potential synthetic lethality partners of XRN-2, shedding light on intricate genetic networks actively shaping the developmental landscape of *C. elegans*. The investigation of these genetic interactions not only provided insight into the interplay between XRN-2 and other genes but also contributed to the broader understanding of the intricate web of gene networks orchestrating development in this model organism. In parallel with the genetic inquiries, the research delved into the regulatory mechanisms of RNA, with a specific focus on how XRN-2 modulates gene expression. This comprehensive exploration of these regulatory pathways aimed to provide profound insights into the intricate details of XRN-2's influence on genetic activity. As this research advances, it was expected to make significant contributions to the field of developmental biology by offering valuable insights into the broader genetic landscape and regulatory mechanisms governing fundamental biological events in the context of *C. elegans*. Ultimately, the research's overarching goal was to enhance our understanding of the complex genetic networks and pathways that orchestrate vital developmental processes in this model organism, thus shedding light on the multifaceted role of XRN-2 within this context.

# MATERIALS

## 1. The chemicals and reagents

**Table 1: Chemicals used in this research**

<b>Name</b>	<b>Company</b>
2-Propanol (Isopropanol)	POCH, Gliwice, Poland
Agar, Bacteriological Grade	BioShop Canada Inc.
Agarose	BioShop Canada Inc.
Calcium chloride dihydrate	BioShop Canada Inc.
Cell Lysis Solution	Qiagen Inc, Valencia, CA, US
Chloroform	POCH, Gliwice, Poland
Cholesterol	Sigma-Aldrich, MA, U.S.
D-(+)-Trehalose, Dihydrate	BioShop Canada Inc.
Dimethyl sulfoxide (DMSO)	BioShop Canada Inc.
Ethanol absolute $\geq 99.8\%$	POCH, Gliwice, Poland
Gelatin	BioShop Canada Inc.
Halocarbon oil 700	Sigma-Aldrich, MA, U.S.
Immersion™ 518F	Zeiss, Oberkochen, Germany
IPTG (isopropyl- $\beta$ -D- tiogalaktopiranozyd)	Blirt, Gdańsk, Poland
LB Broth Lennox	BioShop Canada Inc.
Levamisole hydrochloride, Alkaline phosphatase inhibitor	Abcam, Cambridge, UK
Liquid nitrogen	
Magnesium chloride hexahydrate	BioShop Canada Inc.
Magnesium sulfate anhydrous	BioShop Canada Inc.
Methanol	Chempur, Śląskie, Poland
Nonidet® P-40 Substitute	BioShop Canada Inc.
Peptone, Bacteriological Grade	BioShop Canada Inc.
Pharmacy gasoline Benzinum FP	Amara, Kraków, Poland
Potassium Chloride	BioShop Canada Inc.
Potassium hydroxide Pure P.A	POCH, Gliwice, Poland
Potassium phosphate monobasic	BioShop, Canada Inc, Burlington
Protein Precipitation Solution	Qiagen Inc, Valencia, CA, U.S.
SimplySafe	EURx, Gdańsk, Poland
Sodium chloride	BioShop, Canada Inc, Burlington
Sodium hypochlorite 5 %	Chempur, Śląskie, Poland

Sodium phosphate dibasic	BioShop, Canada Inc, Burlington
SYBR™ Safe DNA Gel Stain	Sigma-Aldrich, MA, U.S.
TAE Buffer, 50X Liquid Concentrate	BioShop, Canada Inc, Burlington
Tris	BioShop, Canada Inc, Burlington
TRIzol	Thermo Fisher Scientific, MA, U.S.
TWEEN® -20, Biotechnology Grade	BioShop, Canada Inc, Burlington
Water, Sterile-filtered, Dnase/Rnase/Protease free	BioShop, Canada Inc, Burlington
Yeast extract	BioShop, Canada Inc, Burlington

**Table 2: Reagents and kits used in the study**

<b>Name</b>	<b>Company</b>
1 kb Plus DNA Ladder	New England BioLabs, MA, U.S.
Cell lysis solution	Qiagen Inc, Valencia, CA, U.S.
Direct-zol RNA MiniPrep Kit	Zymo Research, California, U.S.
DNase I	Zymo Research, California, U.S.
dNTP Mix (10 mM each), 1 ml	Thermo Fisher Scientific, MA, U.S.
Gateway™ BP Clonase™ II Enzyme mix, 20 reactions	Thermo Fisher Scientific, MA, U.S.
Gateway™ LR Clonase™ II Enzyme mix, 20 reactions	Thermo Fisher Scientific, MA, U.S.
GoTaq® G2 Master Mixes, Green, 1000 reactions	Promega, Wisconsin, U.S.
High-Capacity cDNA Reverse Transcription Kit, 200 reactions	Thermo Fisher Scientific, MA, U.S.
Oligo(dT)18 Primer, 120 µl	Thermo Fisher Scientific, MA, U.S.
Platinum II Taq Hot-Start DNA Polymerase, 100 reactions	Thermo Fisher Scientific, MA, U.S.
Platinum™ SuperFi™ DNA Polymerase, 100 units	Thermo Fisher Scientific, MA, U.S.
PowerUp SYBR Green Master Mix, 1 x 5 mL	Thermo Fisher Scientific, MA, U.S.
Proteinase K solution	Thermo Fisher Scientific, MA, U.S.
Proteinase K, Biotechnology Grade	BioShop, Canada Inc, Burlington
PureLink™ Quick Plasmid Miniprep Kits	Thermo Fisher Scientific, MA, U.S.

QIAprep® Miniprep Kit	Qiagen Inc, Valencia, CA, U.S.
QIAquick Gel Extraction Kit	Qiagen Inc, Valencia, CA, U.S.
QIAquick PCR Purification Kit	Qiagen Inc, Valencia, CA, U.S.
RiboLock RNase Inhibitor (40 U/μL)	Thermo Fisher Scientific, MA, U.S.
RNase A	BioShop, Canada Inc, Burlington

**Table 3: Antibiotics used in the research**

Name	Company
Ampicillin, sodium salt	BioShop, Canada Inc, Burlington
Kanamycin Monosulfate	BioShop, Canada Inc, Burlington
Tetracycline HCL	BioShop, Canada Inc, Burlington

**Table 4: Restriction enzymes used in the study**

Name	Buffer	Company
AvaI	rCutSmart	New England BioLabs, MA, U.S.
BglI	NEB r3.1	New England BioLabs, MA, U.S.
HincII	rCutSmart	New England BioLabs, MA, U.S.
HpaI	rCutSmart	New England BioLabs, MA, U.S.
KpnI	rCutSmart	New England BioLabs, MA, U.S.
MboI	rCutSmart	New England BioLabs, MA, U.S.

## 2. Bacterial strains and plasmids

**Table 5: Bacteria strains used in this study**

Name	Description	Source
DH5α	5-alpha Competent <i>E. coli</i>	New England BioLabs, MA, U.S.
OP50	Bacteria <i>Escherichia coli</i>	CGC, US
HT115 (DE3)	Bacteria <i>Escherichia coli</i> contain IPTG-inducible T7 polymerase	Laboratory of Animal Model Organisms library, IBCH, PAS

**Table 6: RNAi clones that used in this research**

Name	Library	Purpose
<i>xrn-2</i>	Ahringer	<i>xrn-2</i> mediated RNA regulation
<i>ama-1</i>	Ahringer	used as a RNAi control
<i>oma-1</i>	Ahringer	<i>puf-9</i> synthetic lethality screen
<i>oma-2</i>	Ahringer	
<i>puf-3</i>	Ahringer	
<i>puf-5</i>	Ahringer	
<i>puf-6</i>	Ahringer	
<i>puf-7</i>	Ahringer	
<i>puf-8</i>	Ahringer	
<i>puf-9</i>	Ahringer	
<i>gld-1</i>	Ahringer	
<i>osr-1</i>	Ahringer	
<i>C34C12.2</i>	Ahringer	
<i>nrde-2</i>	Ahringer	
<i>ptr-6</i>	Ahringer	
<i>dpy-5</i>	Ahringer	

### 3. Buffers and media

**Table 7: Buffers and media used in this research**

Name	Compounds
10x M9 buffer	220 mM KH <sub>2</sub> PO <sub>4</sub> 485 mM Na <sub>2</sub> HPO <sub>4</sub> *2H <sub>2</sub> O 850 mM NaCl 2 mM MgSO <sub>4</sub> *7H <sub>2</sub> O
Trehalose-DMSO worm freezing solution	80 mM Trehalose dihydrate 3.5 % DMSO 1x M9 buffer
Worm bleaching solution	1.5 % Sodium hypochlorite 0.75 mM KOH ddH <sub>2</sub> O
Worm lysis buffer	52 mM KCl 10 mM Tris pH 8.3 2.5 mM MgCl <sub>2</sub> 0.45 % NP40 0.45 % Tween 20 0.05 % Gelatin ddH <sub>2</sub> O
1x TAE buffer	50x TAE buffer, liquid concentrate ddH <sub>2</sub> O
1 % agarose gel	1 % agarose 1x TAE buffer 1000x SimplySafe
3 % agar pads	3 % agarose ddH <sub>2</sub> O
LB medium	20 g/l LB Broth ddH <sub>2</sub> O
LB plates with ampicillin, pH 7.2	0.5 % yeast extract 171 mM NaCl 1 % peptone 1.5 % agar 100 µg/ml ampicillin (added when the solution was cooled down to ~50 °C)

	ddH <sub>2</sub> O
LB plates with kanamycin, pH 7.2	0.5 % yeast extract 171 mM NaCl 1 % peptone 1.5 % agar 25 µg/ml kanamycin (added when the solution was cooled down to ~50 °C) ddH <sub>2</sub> O
NGM plates	2 % agar 0.25 % peptone 0.51 mM NaCl ddH <sub>2</sub> O (cool down the solution to ~50 °C, then add the rest of the compounds) 5 µg/ml cholesterol in ethanol 1 mM CaCl <sub>2</sub> 1 mM MgSO <sub>4</sub> 25 mM potassium phosphate, pH 6.0
RNAi plates	2 % agar 0.25 % peptone 0.51 mM NaCl 5 µg/ml cholesterol in ethanol 1 mM CaCl <sub>2</sub> 1 mM MgSO <sub>4</sub> 25 mM potassium phosphate, pH 6.0 1 mM IPTG 50 µg/ml ampicillin

#### 4. Equipment and software

**Table 8: Equipment used in this research**

Name	Company
Axio Imager.Z2	Zeiss, Oberkochen, Germany

Axio Vert.A1 microscope	Zeiss, Oberkochen, Germany
Azure c600 Imager	Azure biosystems
Centrifuge 5424	Eppendorf, Hamburg, Germany
Centrifuge 5424 R	Eppendorf, Hamburg, Germany
Centrifuge 5804 R	Eppendorf, Hamburg, Germany
Corning® LSE™ Mini Microcentrifuge	Corning, NY, U.S.
Digital incubator INCU-Line®	VWR, PA, U.S.
Horizontal bench-top autoclave DB-65	Systec, Linden, Germany
Horizontal electrophoresis	BTLab Systems, TN, U.S.
InjectMan ®4 micromanipulator	Eppendorf, Hamburg, Germany
Laboratory fume hood	LabDud, Śląskie, Poland
Laboratory incubator with cooling system ILW 115 STD	POL-EKO Aparatura, Poland
Laboratory precise balance PA	OHAUS, NJ, U.S.
Mediaclave 10	Integra, NJ, U.S.
MediaJet vario, with sets for Ø 35 mm, 60 mm, 90 mm Petri plates	Integra, NJ, U.S.
Micro pipettes	HTL
Micromanipulation Systems FemtoJet 4i	Eppendorf, Hamburg, Germany
Micromanipulation Systems TransferMan® 4r	Eppendorf, Hamburg, Germany
Microscope SMZ25, DeltaPix colour camera	Nikon, Tokyo, Japan
Microwave	Amica, Wronki, Poland
NanoDrop OneC Microvolume UV-Vis Spectrophotometer	Thermo Fisher Scientific, MA, U.S.
PC-100 microneedle puller	Narishige, Tokyo, Japan
QuantStudio 3 Real-time PCR systems	Thermo Fisher Scientific, MA, U.S.
Revolver Rotator	Labnet International
SimpliAmp™ Thermal Cycler	Thermo Fisher Scientific, MA, U.S.
Stereoscopic microscope	Nikon, Tokyo, Japan
Stereoscopic microscope	Leica, Wetzlar, Germany
Swiftped Pro Pippetor,	HTL Lab Solution, Warszawa, Poland
Thermomixer C	Eppendorf, Hamburg, Germany
ThermoMixer F1.5	Eppendorf, Hamburg, Germany
Variable Speed 6 Rollers LCD	DLAB Scientific Inc., CA, U.S.
Vortex-Genie 2	Scientific Industry, Inc.

**Table 9: Software used in this research**

<b>Name</b>
ApE (plasmid Editor)
Chromas (viewer for DNA sequencing)
Graph Pad / Prism 8/9 (analyzes and graph creating)
Jalview (DNA/RNA/protein sequence alignment visualization tool)
Microsoft Excel
Microsoft Power Point
Microsoft Word

**Table 10: Online tools utilized in this study**

<b>Name</b>	<b>Link</b>
Add Gene	<a href="http://addgene.org/1654/">http://addgene.org/1654/</a>
Oligo Calculator	<a href="http://biotools.nubic.northwestern.edu/OligoCalc.html">http://biotools.nubic.northwestern.edu/OligoCalc.html</a>
UCSC Genome Browser Gateway	<a href="https://genome-euro.ucsc.edu/">https://genome-euro.ucsc.edu/</a>
Worm Base	<a href="http://wormbase.org">http://wormbase.org</a>
Worm Atlas	<a href="http://wormatlas.org">http://wormatlas.org</a>
RNA fold web server	<a href="http://rna.tbi.univie.ac.at/cgi-bin/RNAWebSuite/RNAfold.cgi">http://rna.tbi.univie.ac.at/cgi-bin/RNAWebSuite/RNAfold.cgi</a>
Worm builder	<a href="https://wormbuilder.org/">https://wormbuilder.org/</a>
String	<a href="https://string-db.org/">https://string-db.org/</a>
Pubmed	<a href="https://pubmed.ncbi.nlm.nih.gov/">https://pubmed.ncbi.nlm.nih.gov/</a>

## 5. Consumables

**Table 11: Consumables used in this research**

<b>Name</b>	<b>Company</b>
0.22 µm pore syringe filter	Bionovo, CA, U.S.
10 ml syringe	BD Discardit II, NJ, U.S.
96 x Well qPCR Plate	Thermo Fisher Scientific, MA, U.S.
Cover Glass 24 x 50 mm	VWR, PA, U.S.
Disposable Glass Pasteur Pipettes 230 mm	VWR, PA, U.S.
Falcon tubes (15-50 ml)	Sarsted, Nümbrecht, Germany
Glass Capillaries	Harvard apparatus, MA, U.S.

Microloader tips	Eppendorf, Hamburg, Germany
Microscope slides	VWR, PA, U.S.
Neptune barrier tips	Gentaur, Kampenhout, Belgium
Neptune tips	Gentaur, Kampenhout, Belgium
Optical adhesive sealing Sheet	Thermo Fisher Scientific, MA, U.S.
Petri plates (60-90mm)	Merck, Millipore, Darmstadt, Germany
Replacement platinum wire	Sigma-Aldrich, MA, U.S.

## 6. Primers and oligos

**Table 12: Primers used in this research**

Primer names	Primer Sequences (5'-3')	Purpose
ceh-99_premir77_fwd1	GCATCTGCCAAACCGCCCGTTT	RT_qPCR
ceh-99_premir77_rev1	TTGGACAGCTATGGCCTGAT	
ceh-99_snoRNA_fwd1	ATACTGATAAGCGAAGGGGT	
ceh-99_snoRNA_rev1	CGAAACGAACAATGGGAGCGG	
ceh-99_miRNA_Pshort_fwd1	TGTTGAATCAGTTATTGGAGT	
ceh-99_miRNA_Pshort_rev1	GTGTACACTTTTCCGCTAAAT	
act_1_qPCR_F	AAATCACCGCTCTTGCCCCATCAA	
act_1_qPCR_R	GCACTTGCGGTGAACGATGGAT	
ceh-99_exon1_2_qPCR_F1	TTCAATATGACTAGGAGAAGGCTCG	
ceh-99_exon1_2_qPCR_R1	AGCTCTCGAGTTACATATTGGTGAG	

ceh-99_exon5_6_7_qPCR_F1	CTGCAGGAGCTGATGCCGATC	
ceh-99_exon5_6_7_qPCR_R1	TTGAACAGTGTGGCTGATTGTTCTC	
egfp_qPCR_F1	GGGAACTACAAGACACGTGC	
egfp_qPCR_R1	TCCATTCTTTTGTGTTGTCTGCCA	
egfp_qPCR_F2	ACTACCTGTTCCATGGGCCAAC	
egfp_qPCR_R2	TTCAAACCTGACTTCAGCACGTGTC	
gpdh_1 qPCR F	GCAATTGTTGGCGGTGGAAACTGG	
gpdh_1 qPCR R	CCTGGTTTCCTGGAATCTCTGCAC	
puf-9_del_fwd_1	GTGATACGTAGTCAGCAGCTC	Strain genotyping
puf-9_del_rev_1	CTCCAGAATACCAATTTCCCG	
puf-9_del_mid_fwd_1	GCGCTGTCATGGTAATTGCAC	
puf-9_del_mid_rev_1	TGATCTTGAGATGGGTGGCC	
puf-9_cgc_fwd_1	GGAAGTCCGAATGGTCCTGTTTCAGG	
puf-9_cgc_mid_fwd_1	CGTGGCCCAGAAGATCCGAATGGT	
puf-9_cgc_rev_1	TCACGGATGTACTTACGCAGGATGTGC	
puf-9_cgc_mid_rev	GAATCTGAAGAGCGTCTAACACTGGC	

puf-9_del_rev	ATTCCGTTCTCATTGTTACGAAT	
puf-9_del_fwd	TCATCGAAACTTATCAAATGACGCAT	
puf-9_del_mid_fwd	AAGTCGGAATCATTTCGGACAATCA	
gfp_mid_fwd	AAGAGTGCCATGCCCCGAAGG	
gfp_end_fwd	TGGCATGGATGAACTATACAAA	
Pceh-99_rev	GGTGATCTAGGAGGTCAAATTAATAT	
ceh-99_nostop_rev	ACAATGCCACATTTCTAAAGTTCGG	
ceh-99_midprimer_rev	TCTTCTATTGTAGAACCAGGCATC	
ceh-99_midprimer_fwd	GTTCTACAATAGAAGAATTAACGCAGG	
ceh-99_seq1_fwd	GAGTCGCTCAACTTCG	Sequencing
ceh-99_seq2_fwd	GGTATGGTAAAATCTGTTG	
ceh-99_seq3_fwd	GAATGGGCTAAACACATCT	
ceh-99_seq4_fwd	TATCCCATGTCAGTTATT	
ceh-99_seq5_fwd	CGATGCCTGGTTCTACA	
ceh-99_seq6_fwd	AGGTCTATACATGACTGTT	
ceh-99_seq7_fwd	GAGCCAAATGAAGAGCCA	

ceh-99_seq8_fwd	TGCCAGAGTCTTCAATTCT	
Pceh-99(0.5kb)_fwd	ACTCATTTTTCAATTTCAACTGAAAGAT	Gateway cloning
Pceh-99(0.5kb)_attB4	GGGGACAACCTTTGTATAGAAAAGTTGAAGTTGA TCCAAAAGGTCATTCCAG	
Pceh-99_5utr_attB1r	GGGGACTGCTTTTTTGTACAAACTTGCAAGTTT GTACAAAAAAGCAGTCCCC	
Pceh-99_5utr_rev	TCTAGTATTTGACAAAAAATAAAGGCG	
Pceh-99(1.5kb)_fwd	AAAGTTGGACAAACATAAGAATTGAG	
Pceh-99(1.5kb)_attB4	GGGGACAACCTTTGTATAGAAAAGTTGAAAGTTG GACAAACATAAGAATTGAG	
ceh-99_attB1_fwd	GGGGACAAGTTTGTACAAAAAAGCAGGCTGAAT GGCACCTTCTTACTCGAGG	
ceh-99_attB2_rev	GGGGACCACTTTGTACAAGAAAGCTGGGTACAA TGCCACATTTCTAAAGTTCGG	
Mos_I L_RecArm fwd	ATCGGTTAGTCATTGCCATCAGAAAATCG	
Mos_I R_RecArm rev	CACTCTGATGAGCGTATCTATCAAGTCC	
pCFJ150 L_RecArm fwd	GTCCTCCTGATTCCATGATGGTAGC	
Mos1_fwd	CAACCTTGACTGTGAACCACCATAG	
Mos1_rev	TCTGCGAGTTGTTTTTGCCTTTGAG	

MosSCI ChrII fwd	CAGAATGTGAACAAGACTCGAGC	
MosSCI ChrII rev	ATCGGGAGGCGAACCTAACTG	
unc_54 3UTR fwd	ATGAGCACGATGCAAGAAAGATCG	
his-58_mid_rev	CGTCAACGATGTATTCTGAACG	
unc-119-3UTR-fwd	ACTCATTTTTCAATTTCAACTGAAAGAT	
M13 F	GTAAAACGACGGCCAG	Plasmid sequencing
M13 R	GTCATAGCTGTTTCCTG	
pL4440 F	AACCTGGCTTATCGAAATTAATAC	

**Table 13: Oligos used in this research**

attB2r-GFP-ceh-99\_3UTR-attb3 (5'-3'):

GGGGACAGCTTTCTTGTACAAAGTGGACATGAGTAAAGGAGAAGAAGCTTTTCACTGGAGTTGTCCCAATTCTT  
GTTGAATTAGATGGTGATGTTAATGGGCACAAATTTTCTGTGAGTGGAGAGGGTGAAGGTGATGCAACATACG  
GAAAACCTTACCCTTAAATTTATTTGCACTACTGGAAAACCTACCTGTTCCATGGGTAAGTTTAAACATATATAT  
ACTAATAACCCTGATTATTTAAATTTTTCAGCCAACACTTGTCACTACTTTCTGTTATGGTGTCAATGCTTC  
TCGAGATACCCAGATCATATGAAACGGCATGACTTTTTCAAGAGTGCCATGCCCGAAGGTTATGTACAGGAAA  
GAACTATATTTTTCAAAGATGACGGGAACACAAGACACGTAAGTTTAAACAGTTCGGTACTAATAACCATA  
CATATTTAAATTTTTCAGGTGCTGAAGTCAAGTTTGAAGGTGATACCCTTGTTAATAGAATCGAGTTAAAAGGT  
ATTGATTTTAAAGAAGATGGAAACATTCTTGGACACAAATTTGGAATACAATAACTCACACAATGTATACA  
TCATGGCAGACAAACAAAAGAATGGAATCAAAGTTGTAAGTTTAAACATGATTTTACTAATAACTAATCTGA  
TTTAAATTTTTCAGAACTTCAAATTAGACACAACATTGAAGATGGAAGCGTTCAACTAGCAGACCATTATCAA  
CAAATACTCCAATTGGCGATGGCCCTGTCTTTTACCAGACAACCATTACCTGTCCACACAATCTGCCCTTT  
CGAAAGATCCCAACGAAAAGAGAGACCACATGGTCCTTCTTGAGTTTGTAAACAGCTGCTGGGATTACACATGG  
CATGGATGAACTATACAAATGATCATTATTTATTCTTTACAATTTACAAATTAGAATGAAACTTTAACGAAAT  
TGAAATATCGGGCTCTTTTCAACTTTATTATACAAAGTTGTCCCC

## 7. Plasmids

**Table 14: Plasmids used in this research**

Name	Insert	Backbone vector	Antibiotics resistance	Application
pDONR P4-P1R	None		Kanamycin	Gateway cloning
pDONR 221	None		Kanamycin	
pDONR P2R-P3	None		Kanamycin	
unc-54 3'UTR-pENTR P2R-P3	unc-54 3'UTR	pDONR P2R-P3	Kanamycin	
FLAG-GFP-TEV-pENTR221	FLAG-GFP-TEV	pDONR 221	Kanamycin	
GFP-H2B-pENTR221	GFP-H2B	pDONR 221	Kanamycin	
PEST-GFP-H2B-pENTR221	PEST-GFP-H2B	pDONR 221	Kanamycin	
Pceh-99(1.5kb)-5utr-pENTR P4-P1r	Pceh-99(1.5kb)-5utr	pENTR P4-P1r	Kanamycin	
ceh-99_pENTR221 (B)	ceh-99	pENTR221	Kanamycin	
ceh-99-woTC1_pENTR221 (S)	ceh-99	pENTR221	Kanamycin	
GFP-ceh-99_3utr_pENTRP2R_P3	GFP-ceh-99-3UTR	pENTR P2R-P3	Kanamycin	
Pceh-99(1.5kb)-5utr-pENTR P4-P1r-ceh-99-pENTR221-GFP-ceh-99-3UTR-PCJ150	Pceh-99(1.5kb)-5utr-pENTR P4-P1r-ceh-99-pENTR221-GFP-ceh-99-3UTR	PCJ150	Ampicillin	
Pceh-99(1.5kb)-5utr-pENTR P4-P1r-ceh-99-woTC1_pENTR221-GFP-ceh-99-3UTR-PCJ150	Pceh-99(1.5kb)-5utr-pENTR P4-P1r-ceh-99-woTC1-pENTR221-GFP-ceh-99-3UTR	PCJ150	Ampicillin	

Pceh-99(1.5kb)-5utr-gfp-his-58-unc-54 3utr-pCFJ150	Pceh-99(1.5kb)-5utr-gfp-his-58-unc-54 3utr	pCFJ150	Ampicillin	
Pceh-99(0.5kb)-5utr-gfp-his-58-unc-54 3utr-pCFJ150	Pceh-99(0.5kb)-5utr-gfp-his-58-unc-54 3utr	pCFJ150	Ampicillin	
Pceh-99(0.5kb)-5utr-pENTR P4-P1r	Pceh-99(0.5kb)-5utr	pENTR P4-P1r	Kanamycin	
Pceh-99(0.5kb)-5utr-pENTR P4-P1r-ceh-99-pENTR221-GFP-ceh-99-3UTR-PCFJ150	Pceh-99(0.5kb)-5utr-pENTR P4-P1r-ceh-99-pENTR221-GFP-ceh-99-3UTR	pCFJ150	Ampicillin	
Pceh-99(0.5kb)-5utr-pENTR P4-P1r-ceh-99-woTC1-pENTR221-GFP-ceh-99-3UTR-PCFJ150	Pceh-99(0.5kb)-5utr-pENTR P4-P1r-ceh-99-woTC1-pENTR221-GFP-ceh-99-3UTR	pCFJ150	Ampicillin	
pCFJ150	None		Ampicillin	
pCFJ601	Peft-3::Mos1 transposase		Ampicillin	
pGH8	Prab-3::mCherry::unc-54UTR		Ampicillin	MosSCI
pCFJ90	Pmyo-2::mCherry:unc-54UTR		Ampicillin	
pCFJ104	Pmyo-3::mCherry::unc-54UTR		Ampicillin	
L4440	None		Ampicillin	

## 8. *C. elegans* strains

**Table 15: *C. elegans* strains used in this research**

Strain ID	Genotype	Notes	Purpose
N2		<i>C. elegans</i> wild isolate	
EG6699	ttTi5605 II; unc-119(ed3) III	chrII MosSCI strain	
HW1660	xrn-2(xe31) II		used in experiments in results and discussion 1.1
HW1682	xrn-2(xe31) II; xeSi217[Pdpy-18::xrn-2(CO)::GFP::his::flag::xrn-2 3'UTR, unc-119(+)] V		
HW1714	xeSi219[Ppes-2.1::xrn-2(CO)::GFP::his::flag::xrn-2 3'UTR, unc-119(+)] I		
HW1715	xeSi219[Ppes-2.1::xrn-2(CO)::GFP::his::flag::xrn-2 3'UTR, unc-119(+)] I; xrn-2(xe31) II; xeSi217[Pdpy-18::xrn-2(CO)::GFP::his::flag::xrn-2 3'UTR, unc-119(+)] V		
TSM19	osr-1(kid1[Q239*]) I; xeSi219[Ppes-2.1::xrn-2(CO)::GFP::his::flag::xrn-2 3'UTR, unc-119(+)] I; xrn-2(xe31) II; xeSi217[Pdpy-18::xrn-2(CO)::GFP::his::flag::xrn-2 3'UTR, unc-119(+)] V		
TSM20	xeSi219[Ppes-2.1::xrn-2(CO)::GFP::his::flag::xrn-2 3'UTR, unc-119(+)] I; xrn-2(xe31) II; C34C12.2(kid2[splicing-affected]) III; xeSi217[Pdpy-18::xrn-2(CO)::GFP::his::flag::xrn-2 3'UTR, unc-119(+)] V		
TSM21	xeSi219[Ppes-2.1::xrn-2(CO)::GFP::his::flag::xrn-2 3'UTR, unc-119(+)] I; ptr-6(kid4[G223E]) II; xrn-2(xe31) II; xeSi217[Pdpy-18::xrn-2(CO)::GFP::his::flag::xrn-2 3'UTR, unc-119(+)] V		
TSM23	xeSi219[Ppes-2.1::xrn-2(CO)::GFP::his::flag::xrn-2 3'UTR, unc-119(+)] I; dpy-10(kid6[G131R])II; xrn-2(xe31) II; xeSi217[Pdpy-18::xrn-2(CO)::GFP::his::flag::xrn-2 3'UTR, unc-119(+)] V		
TSM25	kidSi3[PC34C12.2::flag::gfp::C34C12.2::C34C12.2		

	3'utr] II			
RB1032	osr-1(ok959) I			
TSM55	osr-1(ok959) I; xrn-2(xe31) II			
TSM11	xrn-2(xe31[R182W])		used in experiments in results and discussion 2	
TSM28	EG6699, kidSi6[Pceh-99(0.5kb)::ceh-99 5' utr::gfp::his-58::unc-54 3'utr]II			
TSM29	EG6699, kidSi7[Pceh-99(1.5kb)::ceh-99 5' utr::gfp::his-58::unc-54 3'utr]II			
TSM32	EG6699, kidSi9[Pceh-99(1.5kb)::ceh-99 5' utr::ceh-99::gfp::ceh-99 3'utr]II, clone 1			
TSM43	EG6699, kidSi10[Pceh-99(1.5kb)::ceh-99 5' utr::ceh-99(without TC1)::gfp::ceh-99 3'utr]II			
TSM52	EG6699, kidSi11[Pceh-99(0.5kb)::ceh-99 5' utr::ceh-99::gfp::ceh-99 3'utr]II			
TSM54	EG6699, kidSi12[Pceh-99(0.5kb)::ceh-99 5' utr::ceh-99(without TC1)::gfp::ceh-99 3'utr]II			
MT16311	mir-77(n4286) II			
TSM50	puf-9(ok1136) X 3	3x backcrossed VC894		used in experiments in results and discussion 1.2
TSM51	xrn-2(xe31)I; puf-9(ok1136)X			
PHX2148	puf-9(syb2148[flag::gfp::puf-9]) X			
TSM40	puf-9(tm1520) X			
VC894	puf-9(ok1136) X			

## **METHODS**

### **1. *C. elegans* care and handling**

Proper care of *C. elegans* involves maintaining them in a controlled environment, with access to nutrient-rich agar plates seeded with a specific type of bacteria as a food source. Regular transfers to fresh plates are essential to prevent overpopulation and ensure the health of these tiny nematodes, which reproduce rapidly.

#### **1.1 *C. elegans* cultivation and maintenance**

The experimental model organism employed in this study was *C. elegans*, a nematode species widely utilized in scientific research. All *C. elegans* strains utilized in this investigation were maintained by culturing on Nematode Growth Medium (NGM) plates (Table 7), as described by Brenner [1974]. NGM plates were prepared utilizing the Integra Mediaclave and MediaJet systems. Each NGM agar plate had a diameter of 90 millimetres (mm) or 60 mm, and they were all handled within a sterile laminar flow hood to maintain aseptic conditions. To seed the plates, 1 milliliter (ml) of OP50 *Escherichia coli* (*E. coli*) bacterial culture, serving as the primary food source for the nematodes, was aseptically dispensed into 90 mm plates, and 250 microliters ( $\mu$ l) into 60 mm plates. Following seeding, the plates were left undisturbed to air dry overnight, ensuring uniform distribution of the bacterial culture on the agar surface. Worms were incubated in a temperature-controlled incubators. In order to ensure the long-term preservation and viability of the *C. elegans* strains, the animals were consistently maintained at a temperature of 15 °C. This temperature setting was chosen as it promotes stable growth and reproduction and to maintain a healthy population of nematodes for further experimentation. However, for the specific experimental conditions outlined in this study, the temperature was modulated to either 20 °C, 25 °C, 25,5 °C or 26 °C depending on the requirements of each experimental condition. These higher temperatures were selected to induce certain physiological responses or phenotypic changes in the *C. elegans* strains, allowing to investigate specific aspects of the nematodes' biology under different environmental conditions. For individual worm transfers, worms were picked using a platinum wire worm pick and were then transferred to another plate. To transfer several worms simultaneously, agar from a starved *C. elegans* culture in NGM was chunked onto a new plate containing fresh OP50 bacteria.

## **1.2 Synchronization of *C. elegans* populations through the bleaching procedure**

To synchronize of *C. elegans* by bleaching, adult hermaphrodite worms were collected from a well-established mixed-stage culture using 1x M9 buffer (Table 7) in 15 ml falcon tubes and centrifuged at 1600 g for 1 minute to pellet the worms. The supernatant was then gently decanted, leaving the worm pellet. Eight ml of cold worm bleaching solution (Table 7) was added to the worm pellet, and the mixture was intensively shaken for several minutes (maximum 5 mins), observed under a stereo microscope at 30-second intervals, until the adult worms were dissolved, leaving behind unhatched embryos. Then, the samples were centrifuged at 1,600 g for 1 min, the bleaching solution was decanted, and the egg pellet was washed three times with 10 ml of 1x M9 buffer. The pellet of embryos was then suspended in 10 ml of 1x M9 buffer in a falcon tube which was positioned within a rotating apparatus at 20 °C, and allowed to remain overnight to facilitate hatching. The subsequent day, L1 larvae were counted. To determine the total nematode population within a 10 mL M9 buffer culture, a 10 µL sample was extracted and evenly spread onto an empty NGM plate for counting. The resulting count was subsequently scaled to represent the entire 10 mL volume and same amount of worms was transferred to each plates and maintained at 20 °C for approximately 3 days, facilitating their transition to the one-day-old adult phase.

## **1.3 Cryopreservation and thawing of *C. elegans* strains for long-term storage**

*C. elegans* has the remarkable ability to be cryogenically preserved in liquid nitrogen (-196 °C) for an indefinite period [Brenner, 1974]. Cryopreservation provides a reliable method for maintaining the viability of *C. elegans* strains over extended periods, ensuring their availability for various research applications. To initiate the freezing process, the *C. elegans* strain of interest was cultured and synchronized using the bleaching procedure (section 1.2). The synchronized worms were then placed on NGM plates seeded with *E. coli* OP50 as the food source and cultured under standard conditions. After subjecting the animals (the majority being in the L1/L2 stage) to a starvation period of approximately 2 days, 5 ml of the cold freezing solution (Table 7) per plate was introduced to gather the animals into 2 ml cryogenic tubes. The tubes containing the harvested animals were incubated on ice for 15 minutes to induce a gradual decrease in temperature. Subsequently, the tubes were transferred to a -80 °C freezer for long-term storage. Periodically, one tube containing frozen animals was thawed to assess the recovery ability of the particular strain. Thawing was achieved by removing a

designated tube from the -80 °C freezer and incubating it at room temperature until the ice melted. After the ice had melted, the worm pellet was delicately transferred to a fresh NGM plate seeded with OP50 bacteria using a glass Pasteur pipette equipped with a silicone pipette bulb. The recovered animals were examined for signs of recovery, such as movement and feeding behaviours.

## **2. *C. elegans* strains observations and profiling**

### **2.1 Microscopy**

For the observation and image capture of the worms, two distinct stereo microscopes were used: the M205A stereo microscope (Leica, Solms, Germany) and the SMZ25 stereo microscope (Nikon, Tokyo, Japan). Furthermore, differential interference contrast (DIC) and fluorescent imaging were performed using the Axio Observer Z1 microscope (Carl Zeiss). Both DIC and fluorescent imaging were employed to obtain comprehensive data. To prepare the nematodes for imaging, they were anesthetized in a 10 mM levamisole solution and gently positioned on freshly prepared 3% agar pads (Table 7) on a glass slide. This procedure ensured the immobilization and correct positioning of the specimens for imaging, facilitating the accurate collection of data throughout the experiment.

### **2.2 Phenotypic characterization of *C. elegans* strains**

In the process of observing and phenotypical characterization of *C. elegans* strains through stereo microscopy, synchronization of the worms was achieved by implementing a bleaching procedure (section 1.2) and the synchronized larvae were permitted to reach the desired stage on NGM agar plates containing OP50 bacteria as a food source. During stereo microscopy analysis, phenotypic features of interest, such as body morphology, movement, and developmental rate, were observed and documented, facilitating comparison with the wild-type strain or other control conditions within the experiment. Subsequently, the phenotypic data was analysed to uncover insights into how genetic mutations or experimental treatments impacted the development and behaviour of *C. elegans*.

### **2.3 Temperature shifting assay**

Temperature-shifting experiments were conducted to investigate the developmental role of a specific protein, utilizing temperature-sensitive *C. elegans* mutants. Initially, NGM agar plates containing OP50 *E. coli* as a nutritional source were prepared to facilitate the experiments. The synchronization of temperature-sensitive mutant worms was achieved through a bleaching procedure (section 1.2), resulting in the generation of the same amount of a synchronized larvae. These synchronized larvae were subsequently distributed onto OP50 *E. coli* seeded NGM plates and allowed to progress through their developmental stages, including L1, L2, L3, or L4, within the confines of permissive temperature conditions (e.g., 20 °C). Following this developmental phase, worms were shifted to the restrictive temperature range (e.g., 25-26 °C) at the designated larval stage. This transition aimed to evaluate the protein's significance in the developmental process, enabling a comprehensive examination of its role at precise stages throughout the course of *C. elegans* development.

### **2.4 Glycerol incubation**

Wild-type, *xrn-2ts*, and *xrn-2ts*<sup>germ</sup> animals were synchronized through bleaching and subsequently placed onto NGM plates that had been seeded with OP50 bacteria. The plates were covered with varying glycerol concentrations (2%, 16%, and 64%), and the animals were maintained on the plates at a consistent temperature of 26 °C, commencing at the L1 developmental stage. The incubation period extended for 72 hours. Following this incubation, each animal underwent a comprehensive examination using stereomicroscopy, ensuring that a consistent magnification level was maintained throughout all observations. The primary objective of this examination was to assess developmental alterations and phenotypic responses induced by the diverse glycerol concentrations and temperature conditions.

### **2.5 Synthetic lethality screen**

Synthetic lethality screen via RNAi method (section 8.3) was executed using RNAi feeding clones sourced RNAi libraries (located at the Laboratory of Animal Model Organisms, Institute of Bioorganic Chemistry PAS in Poznań). In this procedure, NGM plates were prepared with the addition of IPTG to activate the expression of RNAi in the bacterial host strains. These plates were then seeded with the RNAi bacteria. For this experiment, *C. elegans*

strains of specific interest underwent synchronization via a gravid hermaphrodite bleaching method (section 1.2). Subsequently, these synchronized worms were transferred to the prepared RNAi plates. The worms were then subjected to incubation at temperatures tailored to the precise experimental design. Throughout the duration of the study, vigilant monitoring of the growth and development of the *C. elegans* was diligently performed. In the event of any observed synthetic lethal interactions between genes or RNAi treatments, these occurrences were scrupulously documented as integral components of the study. This entire process was meticulously repeated three times as biological replicates to ensure the robustness and reliability of the findings.

### **3. Designing and preparing *C. elegans* strains**

In this study, all *C. elegans* strains used were either obtained from an established laboratory collection (located at the Laboratory of Animal Model Organisms, Institute of Bioorganic Chemistry PAS in Poznań) or sourced from suppliers such as CGC (*Caenorhabditis* Genetics Centre, University of Minnesota, Twin Cities, US), and SunyBiotech (Fujian, China), a company recognized for the production of *C. elegans* strains tailored to specific research requirements or obtained from another laboratories. Transgenic strains were generated using the MosSCI technique, and double mutant strains were acquired through strain crossing (Table 15).

#### **3.1 Creating *C. elegans* transgenic lines**

All transgenic lines were created using MosI mediated single copy insertion (MosSCI) method to elucidate the critical regions of *ceh-99* gene that is responsible for XRN-2 mediated regulation (results and discussion section 2.4). This method utilizes Mos1 excision and homologous recombination for precise insertion of transgenes [Frøkjaer-Jensen et al., 2008]. The vectors that were needed for this insertion were created using MultiSite gateway cloning.

### 3.1.1 Genomic DNA isolation

The isolation of genomic DNA, serving as a template, was conducted using N2 Bristol (wild-type) *C. elegans* strain (Table 15), initially gathered from NGM agar plates seeded with OP50 *E. coli* as their source of nutrition. To ensure the elimination of any bacterial impurities and debris, the collected worms underwent several washes with M9 buffer. Following the washes, the worms were subjected to a digestion step. The pellet containing the worms was suspended in 600  $\mu$ l of Cell Lysis Solution supplemented with 20  $\mu$ l of Proteinase K (20 mg/ml). The samples were gently mixed by inverting the tubes and then incubated at 55 °C for approximately 4 hours, with periodic inversions every 30 minutes. After digestion, RNase A was introduced at a final concentration of 40  $\mu$ g/ml. Subsequently, the samples were incubated at 37 °C for 1 hour, followed by a 1-minute ice incubation. Then, 200  $\mu$ l of Protein Precipitation Solution (Qiagen Inc, Valencia, CA, USA) was added to the samples and vortex-mixed for 20 seconds. After a 5-minute cooling period on ice, the samples were centrifuged at 4 °C for 10 minutes at 15,000 g. The supernatant was carefully transferred to new tubes, and this centrifugation and supernatant transfer process was repeated. The remaining pellet was treated with approximately 600  $\mu$ l of ~100% isopropanol, followed by centrifugation at 4 °C for 15 minutes at 15,000 g. After removal of the supernatant, the pellet was washed with 1 ml of 70% ethanol and then centrifuged at 4 °C for 5 minutes at 7,500 g. The supernatant was discarded, and the pellet was left to air-dry. Finally, the dried pellet was re-suspended in 50  $\mu$ l of DNase/RNase-free water, and the concentration of DNA was determined using spectrophotometry.

### 3.1.2 MultiSite Gateway Cloning

To dissecting the *ceh-99* gene, six different constructs were created (Table 16). The Multisite Gateway cloning technique [Gateway Recombination Cloning Technology | Thermo Fisher Scientific - IE, n.d.] was used for efficiently assembling genetic constructs (Table 14). This method (a versatile molecular biology method for efficiently assembling genetic constructs) involves recombining DNA fragments using attB and attP sites, transferring them through BP and LR recombination steps, and assembling a final construct in a destination vector (Figure 5).

**Table 16: Transgenes construct details**

<i>Construct number</i>	<i>Construct design</i>
<i>1</i>	<i>ceh-99 promoter + gfp</i>
<i>2</i>	<i>upstream elements + ceh-99 promoter + gfp</i>
<i>3</i>	<i>upstream elements + ceh-99 promoter + ceh-99 gene body with TC1+ gfp-3' UTR</i>
<i>4</i>	<i>upstream element + ceh-99 promoter + ceh-99 gene body without TC1 + gfp-3' UTR</i>
<i>6</i>	<i>ceh-99 promoter + ceh-99 gene body with TC1 + gfp-3' UTR</i>
<i>6</i>	<i>ceh-99 promoter + ceh-99 gene body without TC1 + gfp-3' UTR</i>

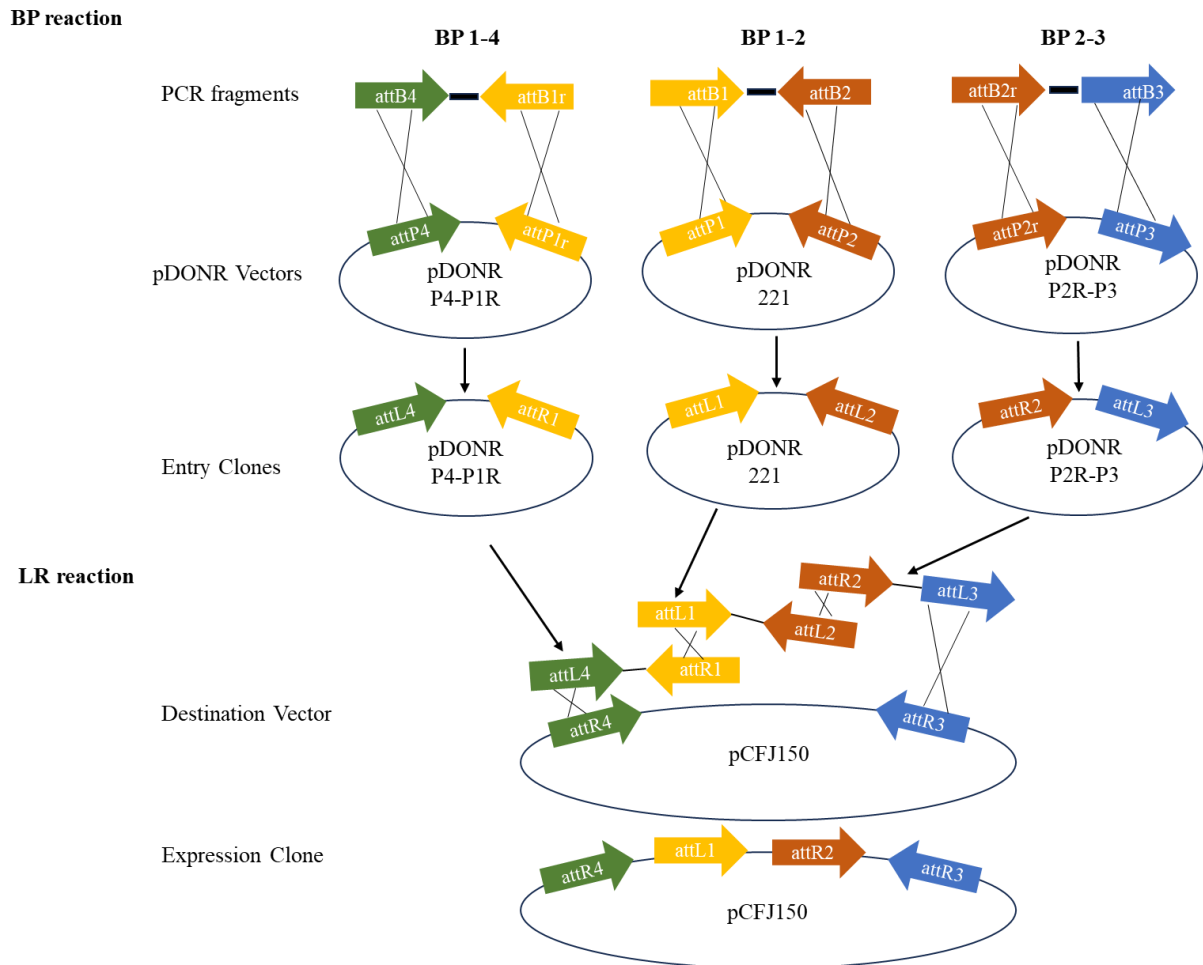


**Figure 5: Schematic representation of example of Gateway MultiSite recombination cloning.** The experimental procedure comprises three main stages. Firstly, primer design is employed for PCR amplification and the introduction of unique attB sites into each component. Subsequently, individual entry clones for each part are generated utilizing specified multisite pDONR vectors. Finally, the recombination process involves combining the three entry clones with a destination vector, facilitated by the Gateway cloning tool.

### 3.1.2.1 Insert preparation

PCR amplifications were carried out using the Invitrogen Platinum II Taq Hot-Start DNA Polymerase Kit (Invitrogen, Carlsbad, CA, USA), targeting specific regions of the *ceh-99* gene (Table 17) with primer sets tailored to those regions (Table 12), and genomic DNA was used as the template for amplification. Reaction mixture (1x) was prepared by combining the following components: 10  $\mu$ l of 5x Platinum II Buffer, 1  $\mu$ l of 10  $\mu$ M forward primer, 1  $\mu$ l of 10  $\mu$ M reverse primer, a sufficient volume of nuclease-free H<sub>2</sub>O to achieve a final volume

of 50 µl, 250 ng of genomic DNA, and finally, 0.4 µl of Platinum II Taq Hot-Start DNA Polymerase. Subsequently, the PCR reaction was conducted (Table 18). Then, the PCR product was analysed on 1 % agarose gel. Following successful PCR, QIAquick gel extraction Kit (Qiagen Inc, Valencia, CA, USA) or QIAquick PCR Purification (Qiagen Inc, Valencia, CA, USA) Kit were used for purification, depending on the final PCR product.

Purified insert of interest flanked with attB sites (GateWay attachment sites) obtained via PCR using previous PCR amplicon as a template. Reaction mixture (1x) was prepared by combining the following components: 10 µl of 5x Platinum II Buffer, 1 µl of 10 µM forward primer, 1 µl of 10 µM reverse primer, a sufficient volume of nuclease-free H<sub>2</sub>O to achieve a final volume of 50 µl, PCR amplicon, and finally, 0.4 µl of Platinum II Taq Hot-Start DNA Polymerase. Subsequently, the PCR reaction was conducted (Table 19). *gfp*-3'UTR flanked with attB sites obtained commercially from IDTDNA (Integrated DNA Technologies | IDT, n.d.) (Table 13).

**Table 17: Cloning inserts obtained via PCR and commercial sources**

<i>ceh-99</i> promoter	PCR product
upstream elements- <i>ceh-99</i> promoter	PCR product
<i>ceh-99</i> gene body with TC1	PCR product
<i>ceh-99</i> gene body without TC1	PCR product
3'UTR- <i>gpf</i>	commercially obtained

**Table 18: PCR conditions for insert preparation**

<i>Temperature [°C]</i>	<i>Time [sec.]</i>	<i>Number of cycles</i>
94	120	1
94	15	
<i>Depends on primers</i>	<i>Depends on primers</i>	30
68	66	
4	∞	1

**Table 19: PCR conditions for attaching “attB” sites to the insert**

<i>Temperature [°C]</i>	<i>Time [sec.]</i>	<i>Number of cycles</i>
94	120	1
94	15	
<i>Depends on primers</i>	<i>Depends on primers</i>	2
68	66	
94	15	27
68	66	
4	∞	

**3.1.2.2 Entry and destination vector design**

The desired insert was cloned in donor vector (Table 14) with BP reaction to generate entry clones. Gateway™ BP Clonase™ II Enzyme mix (Invitrogen, Carlsbad, CA, USA) was used and the supplier protocol was followed for preparing reaction mixture. Reaction mixture was incubated at 25 °C for 1 hour and 1 µl of Proteinase K (provided in the kit) was added to terminate the reaction, and then incubated at 37 °C for 10 min (Table 20). Then, the whole was

product transformed (section 4) and spread on LB plate with Kanamycin (KAN), and incubated at 37 °C for overnight. Bacterial colonies were picked and DNA was amplified via colony PCR using GoTaq® G2 Green Master Mix (Promega, Madison, Wisconsin, USA). Reaction mixture (1x) was prepared by combining the following components: 5 µl of GoTaq® G2 Green Master Mix 2x, 0.3 µl of 10 µM forward primer, 0.3 µl of 10 µM reverse primer, 3.7 µl nuclease-free H<sub>2</sub>O and colonies selected using microvolume pipette tips. Subsequently, the PCR reaction was conducted (Table 21). Selected colonies were cultured with 2ml LB + KAN overnight at 37 °C. Plasmids were isolated using QIAprep Spin Miniprep Kit (Qiagen Inc, Valencia, CA, USA) and then checked via restriction enzyme digestion (Table 4) according to the manufacturers' protocols (Table 22) and the product was analysed by agarose gel electrophoresis (Table 7).

Gateway™ LR Clonase™ II Enzyme mix (Invitrogen, Carlsbad, CA, USA) was used for LR reaction (Table 23) to clone entry vectors into destination vectors (Table 14) to create expression clones. This vector has regions complementary to the genomic target site and the *cb-unc-119* rescue fragment to generate transgenic animals by MosSCI. Then the supplier protocol was followed to prepare reaction mixture, which was incubated at 25 °C for 1 hour, and after that, 1 µl of the Proteinase K solution was added and the mixture was incubated at 37 °C for 10 minutes. Then, 5 µl of the product was transformed and spread on LB plate with Ampicillin (AMP) and incubated at 37 °C overnight. Bacterial colonies were picked and amplified using colony PCR (section 5). Selected colonies were cultured with 2 ml LB+AMP overnight at 37 °C. Plasmids were isolated using QIAprep Spin Miniprep Kit and then checked via restriction enzyme digestion (Table 4) according to the manufacturers' protocols and the product analysed by agarose gel electrophoresis.

**Table 20: Gateway BP reaction (1-4,1-2,2-3)**

<i>Master mix</i>	<i>Amount</i>
<i>Insert DNA</i>	<i>150 ng</i>
<i>Donor vector</i>	<i>150 ng</i>
<i>Qiagen EB</i>	<i>up to 8 <math>\mu</math>l</i>
<i>BP Clonase</i>	<i>2 <math>\mu</math>l</i>
<i>Total</i>	<i>10 <math>\mu</math>l</i>

**Table 21: Colony PCR conditions**

<i>Temperature [<math>^{\circ}</math>C]</i>	<i>Time [sec.]</i>	<i>Number of cycles</i>
<i>94</i>	<i>120</i>	<i>1</i>
<i>94</i>	<i>15</i>	
<i>Depends on primers</i>	<i>Depends on primers</i>	<i>30</i>
<i>72</i>	<i>90</i>	
<i>4</i>	<i><math>\infty</math></i>	

**Table 22: Restriction enzyme digestion**

<i>Master mix</i>	<i>Amount</i>
<i>DNase/RNase-free H<sub>2</sub>O</i>	<i>Up to 10 <math>\mu</math>l</i>
<i>Buffer (depending on the enzyme)</i>	<i>1 <math>\mu</math>l</i>
<i>Restriction enzyme</i>	<i>0.5 <math>\mu</math>l</i>
<i>Plasmid DNA</i>	<i>300 ng</i>
<i>Total</i>	<i>10 <math>\mu</math>l</i>

**Table 23: Gateway LR reaction**

<i>Master mix</i>	<i>Amount</i>
<i>PENTRP4-p1R</i>	<i>30 fmol</i>
<i>PENTR221</i>	<i>30 fmol</i>
<i>PENTRP2R-P3</i>	<i>30 fmol</i>
<i>Destination vector (PCJF150)</i>	<i>2 <math>\mu</math>l</i>
<i>Total</i>	<i>10 <math>\mu</math>l</i>

### 3.1.3 Transgene integration

#### 3.1.3.1 Pre and post processes of microinjection

EG6699 (*unc-119*) MosSCI strain (Table 15) was used for creating the transgenic *C. elegans* lines. EG6699 worms were cultivated on NGM plates seeded with OP50 bacteria as their dietary source, and maintained at a temperature of 20 °C. These mutants exhibit impaired movement. To facilitate ease of preservation and distribution, this strain is accompanied by an additional-chromosomal rescuing array. For the microinjection process, only *unc-119* animals were selected for injection, while non-*unc-119* animals were chosen for long-term maintenance.

Injection mixture prepared with MosSCI plasmids (Table 14, 24) which were; 1) Co-integration of a *cb-unc-119* (+) rescue fragment provides a positive selection marker for identifying extrachromosomal and integrated transgenes (MosSCI plasmid with transgene), 2) Mos1 excision is induced by expression of Mos1 transposase that is achieved in the germline under the *eft-3* promoter (pCFJ601), 3) Fluorescent co-injection markers (mCherry) provides negative selection against the extrachromosomal array thus distinguishing integrations from extrachromosomal arrays (pGH8, pCFJ90, Pcfj104) [Kunkel et al., 2000].

Young adult hermaphrodites were injected with injection mixture (Table 24) via microinjection technique (section 3.1.3.2) and incubated on fresh NMG plates with OP50 bacteria at 20 °C individually. Visual identification of insertions in the F2-F3 offspring of injected animals relied on their demonstration of wild-type movement (*unc-119* rescue), alongside the absence of fluorescent co-injection markers as observed through fluorescent microscopy. A few potential insertion animals were carefully chosen and transferred to fresh OP50 bacteria seeded NGM plates for cultivation. Subsequently, only plates displaying homozygous individuals were singled out for further verification. To confirm the presence of a full-length insertion, the selected worms underwent a two-step genotyping process via single worm PCR (section 8.2). Initially, they were lysed and genotyped via single worm PCR using MosSCI-specific primers (Table 12). Then, a second round of genotyping was performed for confirmation using gene-specific primers.

**Table 24: Injection mixture components**

<i>MosSCI plasmid with transgene</i>	<i>(final 50 ng/μl)</i>
<i>pCFJ601</i>	<i>(final 50 ng/μl)</i>
<i>pGH8</i>	<i>(final 10 ng/μl)</i>
<i>pCFJ90</i>	<i>(final 2.5 ng/μl)</i>
<i>Pcfj104</i>	<i>(final 5 ng/μl)</i>
<i>Qiagen EB</i>	<i>up to 20 μl</i>
<i>Total</i>	<i>20 μl</i>

### **3.1.3.2 *C. elegans* microinjection**

The glass capillaries (Harvard Apparatus, MA, US) were transformed into needles accomplished using the PC-100 microneedle puller (Narishige, Tokyo, Japan). The microinjection process was facilitated by an Axio Vert.A1 microscope (Zeiss, Oberkochen, Germany) equipped with the microinjection set, which included the InjectMan ®4 micromanipulator (Eppendorf, Hamburg, Germany) with dynamic motion control and the programmable FemtoJet ®4i (Eppendorf, Hamburg, Germany) micro diaphragm featuring integrated pressure supply. A needle-loading pipette (Eppendorf, Hamburg, Germany) was filled with 3 µl of injection mix through capillary action. The pipette tip was inserted into the injection needle from the back, and the injection mix was expelled onto the needle's internal filament. Subsequently, a loaded needle was placed into the needle holder and mounted on the manipulator. The needle was positioned in such a way that its tip was centered within the microscope's field of view using the 5X objective. Once positioned, the needle was moved upward using the Z-axis control until it was slightly out of focus. An injection pad consisting of 3% agar was prepared, and a drop of halocarbon oil (Sigma-Aldrich, MA, US) was applied on it. The injection pad was then placed under a dissecting microscope atop a small Petri plate cover. Worms, ranging from one to four, were scooped from a bacteria-free region of an NGM plate using a worm pick and transferred to the oil drop. These worms were meticulously positioned within the oil drop using eyelash too (eyelashes affixed to the micro-pipette tip using nail polish) and gently pressed down onto the pad. The slide, with the worms facing upwards, was transferred to the microscope stage. The first worm to be injected was centered and focused on using the 5X objective. Subsequently, the needle was lowered into close proximity to the dorsal surface of the worm, and the magnification was switched to the 40X objective for precise focus. Before injection, the flow of the needle was verified by moving it into focus and then shifting the stage slightly to move the worm away from the needle, followed by applying pressure to confirm significant flow. The needle was carefully inserted into the worm, and the DNA solution was injected. Injected worms were promptly recovered by adding 3-5 µl of M9 onto the worm. Using eyelashes, the worm was removed from the oil and placed onto a fresh OP50 bacteria-seeded 60 mm plate. To remove excess oil from the worm, 3-5 µl of M9 was dropped onto it. The plates were then incubated at 20 °C, and the worms were observed for indications of microinjection success.

### **3.2 Generating double mutant strain via crossing**

Two distinct strains exhibiting the desired traits were always carefully chosen. Mating plates with NGM agar, featuring a confined area of OP50 bacteria, were prepared. The proximity of worms was facilitated by this limited food supply, thereby enhancing the likelihood of successful mating. Three times more male worms than hermaphrodites were introduced, as an increased number of males improves the mating chances. These worms constituted the P0 generation. The plates were ensured to be maintained at the suitable temperature conducive to *C. elegans* development. On the following day, each hermaphrodite worm was isolated onto new plates, allowing them to lay eggs and progress into the F1 generation. Subsequently, the F1 plates were examined, and those with at least 50% male worms were identified. Ordinarily, male populations in *C. elegans* constitute approximately 1-2% in the wild [A Transparent Window Into Biology: A Primer on *C. elegans*, n.d.], but if successful mating has occurred, the male proportion should be notably elevated. F1 hermaphrodite worms from these plates were selected and isolated, and the F2 generation was genotyped by single worm PCR to confirm the effectiveness of the crossing and for some strains which has point mutation instead of deletion, after the PCR, product confirmed with restriction enzyme digestion which is specific for point mutation.

### **4. Bacterial transformation**

To prepare the transformed bacterial culture, a single vial of NEB® 5-alpha competent (New England BioLabs, MA, US) *E. coli*, a derivative of Dh5 $\alpha$ , was maintained on ice until it reached a liquid state. Plasmid DNA (1 pg-100 ng) was introduced into the thawed bacterial solution and gently mixed. These samples were left on ice for 30 minutes, then subjected to a brief heat shock at 42 °C for 45 seconds, followed by a 2-minutes incubation on ice. Subsequently, 1 ml of fresh LB media devoid of antibiotics was added to the mixture, and the bacterial culture was incubated at 37 °C with gentle agitation for 1 hour. Following this incubation period, the bacterial suspension was subjected to a 2-minute centrifugation at 5000 g. The supernatant was discarded, and the bacterial pellet was resuspended in a small amount of the remaining LB media. The transformed bacterial suspension was evenly spread onto culture plates containing antibiotics tailored to the specific experimental requirements, either LB-kanamycin or LB-ampicillin plates, depending on the context. These plates were then

incubated overnight at 37 °C to facilitate the selection and proliferation of transformed bacterial colonies.

## **5. Colony PCR**

A single bacterial colony was selected from a freshly grown bacterial culture using a sterile pipette tip and transferred to LB media supplemented with an appropriate antibiotic selection marker. Then the culture was incubated overnight at 37 °C in a bacteria shaker. Subsequently, plasmid isolation was carried out using mini-prep plasmid isolation kit (described in method 6) and PCR amplification using specific primers.

## **6. Plasmid isolation**

In this research, plasmid isolation was carried out in accordance with the suppliers' protocol using the QIAprep® Miniprep Kit from Qiagen Inc. (Valencia, CA, USA) for all plasmid isolation steps, except when preparing plasmids for microinjection. For microinjection-ready plasmid preparation, the PureLink™ Quick Plasmid Miniprep Kit by Thermo Fisher Scientific, MA, U.S. was employed to acquire higher levels of purity and quality.

### **6.1 The protocol for QIAprep® miniprep Kit**

The overnight bacterial culture (1-5 ml) was centrifuged 10 mins at 5000 rpm, and the supernatants were removed. The pelleted bacterial cells were resuspended in 250 µl of Buffer P1, ensuring that RNase A had been added to Buffer P1. The absence of visible cell clumps after pellet resuspension was confirmed. Complete resuspension of the bacteria was achieved by either vortexing or pipetting up and down until no cell clumps remained. Subsequently, 250 µl of Buffer P2 was added, and the tube was thoroughly mixed by inverting it 4–6 times. Gentle mixing by tube inversion was employed. Following this, 350 µl of Buffer N3 was added, and immediate and thorough mixing was accomplished by inverting the tube 4–6 times, resulting in a cloudy solution. The mixture was then centrifuged for 10 minutes at 13,000 rpm using a tabletop microcentrifuge, leading to the formation of a compact white pellet. A volume of 800 µl of the supernatant from step 4 was pipetted onto the QIAprep 2.0 Spin Column, followed by

centrifugation for 30–60 seconds. The flow-through was subsequently discarded. To wash the QIAprep 2.0 Spin Column, 0.75 ml of Buffer PE was added, and centrifugation for 30–60 seconds was carried out. The flow-through was discarded, and an additional 1-minute centrifugation at full speed was performed to remove residual wash buffer. Finally, the QIAprep 2.0 Spin Column was placed into a clean 1.5 ml microcentrifuge tube. For DNA elution, 30 µl of Buffer EB (10 mM Tris·Cl, pH 8.5) or water was added to the centre of each QIAprep 2.0 Spin Column, allowed to stand for 1 minute, and then centrifuged for 1 minute.

## **6.2 The protocol for PureLink™ Quick Plasmid Miniprep Kit**

The overnight bacteria culture (1-5 ml) was centrifuged. All medium was removed. The cell pellet was resuspended in 250 µl of Resuspension Buffer (R3) with RNase A until it was homogeneous. Then, 250 µl of Lysis Buffer (L7) was added, and the mixture was gently mixed by inverting the capped tube until it became homogeneous. The tube was incubated at room temperature for 5 minutes. Afterward, 350 µl of Precipitation Buffer (N4) was added, and the mixture was immediately mixed by inverting the tube until it was homogeneous. The lysate was centrifuged at 10,000 rpm for 10 minutes. The supernatant was loaded onto a spin column in a 2-ml wash tube. The column was centrifuged at 10,000 rpm for 1 minute, and the flowthrough was discarded. The column was then placed back into the wash tube. Next, 500 µl of Wash Buffer (W10) with ethanol was added to the column, and the column was incubated for 1 minute at room temperature. The column was centrifuged at 10,000 rpm for 1 minute, and the flowthrough was discarded. The column was once again placed back into the wash tube. Following that, 700 µl of Wash Buffer (W9) with ethanol was added to the column, and the column was centrifuged at 10,000 rpm for 1 minute. The flowthrough was discarded, and the column was placed into the wash tube. The column was then centrifuged at 10,000 rpm for 1 minute, and the wash tube with the flowthrough was discarded. Finally, the Spin Column was placed in a clean 1.5-mL elution tube. Thirty microliters of H<sub>2</sub>O was added to the centre of the column to elute the plasmid, and the column was incubated for 1 minute at room temperature. The column was centrifuged at 10,000 rpm for 2 minutes.

## **7. Purification methods**

### **7.1 PCR purification**

PCR purification was conducted using QIAquick PCR Purification Kit according to supplier's protocol (Qiagen Inc, Valencia, CA, USA). Five volumes of Buffer PB were combined with one volume of the PCR reaction and mixed. For DNA binding, the sample was applied to the QIAquick column within a provided 2 ml collection tube and centrifuged for 30–60 minutes at 13,000 rpm. Subsequently, the flow-through was discarded, and the QIAquick column was repositioned into the same tube. To initiate the washing step, 750 µl of Buffer PE was added to the QIAquick column and subjected to centrifugation for 30–60 minutes. The QIAquick column was centrifuged once more in the provided 2 ml collection tube for 1 minute to eliminate any remaining wash buffer. Each QIAquick column was then placed into a clean 1.5 ml microcentrifuge tube. For DNA elution, 30 µl of Buffer EB was introduced to the centre of the QIAquick membrane, allowed to stand for 1 minute, and then centrifuged.

### **7.2 Gel extraction method**

The gel extraction method was conducted using QIAquick Gel Extraction Kit (Qiagen Inc, Valencia, CA, USA) according to supplier's protocol. PCR samples were loaded into a 0.8% agarose gel with 1 kb NEB DNA (New England Biolabs, MA, US) ladder and run for 25 minutes at 150V. The gel was cut under a UV illuminator. The gel slice was then weighed in a colourless tube, and 3 volumes of Buffer QG were added to 1 volume of gel (100 mg gel was approximately equal to 100 µl) and incubated at 50 °C for 10 minutes (or until the gel slice had completely dissolved), with the tube being vortexed every 2–3 minutes to aid in the dissolution of the gel. Following that, 1 gel volume of isopropanol was added to the sample, and thorough mixing was performed. A QIAquick spin column was placed in a provided 2 ml collection tube and centrifuged for 1 minute at 13,000 rpm, with the flow-through being discarded. Subsequently, 500 µl of Buffer QG was added to the QIAquick column, and it was centrifuged for 1 minute at 13,000 rpm, with the flow-through being discarded. For the washing step, 750 µl of Buffer PE was added to the QIAquick column, and it was centrifuged for 1 minute at 13,000 rpm, with the flow-through being discarded. The QIAquick column was centrifuged in the provided 2 ml collection tube for 1 minute to eliminate residual wash buffer. The QIAquick column was then placed into a clean 1.5 ml microcentrifuge tube. To elute DNA, 20 µl of Buffer

EB (10 mM Tris·Cl, pH 8.5) was added, left for 2 minutes, and then centrifuged for 1 minute at 13,000 rpm.

## **8. Gene expression level analysis**

### **8.1 Worm lysis**

A simplified approach for worm lysis and DNA extraction, involving the utilization of a small volume reaction in the lid of a PCR tube, was employed. This method, commonly known as the "HotShot" or "PCR-based lysis" method, was utilized for expedited DNA extraction from individual worms or small quantities of worms, primarily for genotyping purposes. The procedure began by preparing a mixture of 0.5 µl Proteinase K and 9.5 µl worm lysis buffer within the lid of a PCR tube, ensuring thorough mixing for homogeneity. Subsequently, a single worm (or a small number of worms) was selected using a worm pick or platinum wire loop and was transferred to the mixture in the PCR tube lid, with care taken to prevent the introduction of excess liquid or contamination. The lid of the PCR tube was securely sealed to prevent sample loss during centrifugation. The PCR tube was then subjected to high-speed micro-centrifugation (e.g., 12,000-16,000 x g) for 10 seconds to promote effective mixing and lysis of the worm sample. Following centrifugation, the tube was transferred to a thermal cycler or heating block, where a series of temperature incubation steps was executed. This included an incubation at 65 °C for 19 minutes to facilitate Proteinase K-mediated protein digestion and DNA release, followed by an increase in temperature to 95 °C for an 11-minute incubation to deactivate Proteinase K and denature any residual proteins. After the temperature incubation steps, the sample was prepared for downstream applications, such as PCR genotyping or other molecular analyses, and if necessary, the DNA was used immediately or stored at -20 °C until further use.

### **8.2 Single worm PCR for genotyping**

The PCR method for genotyping was employed (Table 25), utilizing worm lysate (described in method 8.1) as the DNA template. In this method, a reaction mixture was prepared, which included 5 µl of GoTaq® G2 Green Master Mix 2x (Promega, Wisconsin, US),

0.3  $\mu$ l of 10  $\mu$ M forward primer, 0.3  $\mu$ l of 10  $\mu$ M reverse primer, 0.7  $\mu$ l of DNA, and 3.7  $\mu$ l of ddH<sub>2</sub>O. The samples were subsequently analysed through agarose gel electrophoresis.

**Table 25: Single worm lysis PCR conditions**

<i>Temperature [°C]</i>	<i>Time [sec.]</i>	<i>Number of cycles</i>
94	60	1
94	15	
<i>Depends of primer set</i>	<i>Depends of primer set</i>	35
72	90	
4	$\infty$	1

### 8.3 RNA interference (RNAi) assay

The gene of interest was subjected to knockdown via an RNA interference (RNAi) assay. In this experimental setup, 90 mm NGM RNAi plates, enriched with 1 mM IPTG and 50  $\mu$ g/ml ampicillin, were utilized. When required, the *ama-1* RNAi vector served as a vital tool to assess the functionality of RNAi plates. This approach is rooted in the fact that *ama-1*, being a subunit of RNAPII, is extremely sensitive to AMAnitin inhibition, resulting in lethality when targeted via RNAi. If the *ama-1* RNAi works (resulting in a lethal phenotype), it confirms that the RNAi pathway is functional in the experiment. The nutritional source for the animals was comprised of an RNAi clone enclosed within an L4440 plasmid, ampicillin resistance (Amp<sup>R</sup>), which was transported by the HTT15 *E. coli*, tetracycline resistance (Tet<sup>R</sup>), bacterial strain. The desired RNAi clone employed in this investigation was sourced from the Ahringer Library which is stored at the Laboratory of Animal Model Organisms, Institute of Bioorganic Chemistry PAS in Poznań. For the purpose of a negative control, an empty L4440 plasmid was introduced into HTT15 bacteria. The bacteria, carrying both the double-stranded RNA clone and the empty plasmid, underwent separately overnight cultivation in LB media with the addition of ampicillin (final concentration: 50  $\mu$ g/ml) and tetracycline (final concentration: 12.5  $\mu$ g/ml). The subsequent day, the bacterial culture was incubated in freshly prepared LB with ampicillin (in 1:20 dilution) for 5 hours. A portion of 750  $\mu$ l of the overnight bacterial culture was distributed onto the 90 mm RNAi plates and allowed to air-dry overnight. Following these preparations, bleach-synchronized ~ 1500-2000 L1-stage animals were placed onto the RNAi plates and transferred to an incubation chamber set at 20 °C. Upon attaining the desired

developmental stage, the animals were collected for the analysis of gene expression levels or for the execution of downstream processes such as phenotypic characterization or observation.

#### **8.4 RNA isolation from *C. elegans***

Approximately 1,000 to 2,000 synchronized worms were harvested in a 15 ml tube and washed three times with M9. The worm pellet was resuspended in 700  $\mu$ l of TRIzol, transferred to a 1.6 ml tube, and frozen in liquid nitrogen, with the option to store it at -80 °C. Subsequently, the tube was incubated at 42 °C. When thawing was initiated, it was vortexed for 10 seconds and frozen in liquid nitrogen. This process was repeated five times, except for freezing in the fifth repetition. Then, 140  $\mu$ l of chloroform was added, followed by extensive shaking for 20 seconds, and the mixture was kept at room temperature for 2-5 minutes. Afterward, centrifugation was performed at 12,000 g for 10 minutes at 4 °C. The aqueous phase was then transferred to a 1.6 ml tube (the white or pink phase was not included), and the supernatant was transferred to a new 1.6 ml tube.

To isolate RNA the Direct-zol RNA Miniprep Kit (Zymo Research, California, US) was used, according to the manufacturer's protocol, which was as follows: an equal volume of ethanol (95-100%) was added to a sample lysed in trizol, and thorough mixing was carried out. The mixture was then transferred into a Zymo-Spin™ IICG Column2 in a Collection Tube and subjected to centrifugation. The column was transferred into a new collection tube, and the flow-through was discarded. For DNase I treatment, 400  $\mu$ l of RNA Wash Buffer was added to the column and centrifuged. In an RNase-free tube, 5  $\mu$ l of DNase I (6 U/ $\mu$ l), along with 75  $\mu$ l of DNA Digestion Buffer, was added and mixed. The mixture was added directly to the column matrix and incubated at room temperature (20-30 °C) for 15 minutes. Subsequently, 400  $\mu$ l of Direct-zol™ RNA PreWash was added to the column, followed by centrifugation. The flow-through was discarded, and this step was repeated. Then, 700  $\mu$ l of RNA Wash Buffer was added to the column and centrifuged for 2 minutes to ensure complete removal of the Wash Buffer. The column was carefully transferred into an RNase-free tube. To elute RNA, 100  $\mu$ l of DNase/RNase-Free water was added directly to the column matrix and subjected to centrifugation. Alternatively, for highly concentrated RNA,  $\geq 50$   $\mu$ l elution was used. The resulting RNA could be used immediately or stored frozen at  $\leq -70$  °C.

## 8.5 Complementary DNA (cDNA) synthesis

To perform the reverse transcription assay, 100 ng of RNA was employed in accordance with the High-Capacity cDNA Reverse Transcription Kit (Thermo Fisher Scientific, MA, U.S.) protocol. The master mix composition example (Table 26) and reverse transcription program details (Table 27) are presented in the tables below. For the generation of a cDNA library from mRNAs, oligo(dT)18 primers were utilized, whereas for cDNA synthesis from general RNAs, random hexamers were employed. Each individual sample had a total volume of 20  $\mu$ l, consisting of 10  $\mu$ l of master mix, 10  $\mu$ l of DNase/RNase-free water, and 100 ng of RNA. Subsequently, the resulting cDNA was subjected to dilution, with a 1:10 dilution for the gene of interest and a 1:100 dilution for *act-1* (actin) analysis.

**Table 26: cDNA synthesis master mix components (1x)**

<i>Component</i>	<i>Amount</i>
<i>10x RT Buffer</i>	<i>2 <math>\mu</math>l</i>
<i>20x Oligo(dT)18 primer</i>	<i>1 <math>\mu</math>l</i>
<i>40 U/<math>\mu</math>l RiboLock RNase Inhibitor</i>	<i>0.5 <math>\mu</math>l</i>
<i>MultiScribe Reverse Transcriptase</i>	<i>1 <math>\mu</math>l</i>
<i>DNase/RNase-free H<sub>2</sub>O</i>	<i>10.5 <math>\mu</math>l</i>
<i>100 ng/<math>\mu</math>l total RNA</i>	<i>5 <math>\mu</math>l</i>

**Table 27: Program for reverse transcription**

<i>Temperature [°C]</i>	<i>Time [min.]</i>
25	10
37	120
85	5
4	$\infty$

## 8.6 Real-time quantitative PCR (qPCR)

The analysis of the expression levels of selected genes was carried out using real-time quantitative PCR (RT-qPCR), with the utilization of the PowerUp™ SYBR™ Green Master Mix (Thermo Fisher Scientific, MA, U.S.). The reaction components (Table 28) and conditions (Table 29) are described in the tables below. The melting curve stage was only used for new primers. It confirmed target amplification by detecting a distinct melting temperature ( $T_m$ ) peak, identified non-specific amplification or primer-dimer formation through unusual curve profiles, and served as a quality control step to ensure high-quality PCR products. Ct values were determined using the QuantStudio™ 3 (Thermo Fisher Scientific, MA, U.S.) instrument, and the fold change was estimated through the delta-delta Ct method. Statistical analysis for all RT-qPCR experiments was performed using GraphPad Prism 8.

**Table 28: RT-qPCR mixture (1x)**

<i>Components</i>	<i>Volume</i>
<i>2x PowerUp™ SYBR™ Green Master Mix</i>	<i>12.5 <math>\mu</math>l</i>
<i>1 <math>\mu</math>M forward primer</i>	<i>1.75 <math>\mu</math>l</i>
<i>1 <math>\mu</math>M reverse primer</i>	<i>1.75 <math>\mu</math>l</i>
<i>DNase/RNase-free H<sub>2</sub>O</i>	<i>3 <math>\mu</math>l</i>
<i>cDNA</i>	<i>6 <math>\mu</math>l</i>
<i>Total</i>	<i>25 <math>\mu</math>l</i>

**Table 29: Program for RT-qPCR.**

<i>Temperature [°C]</i>	<i>Time [sec.]</i>	<i>Number of cycles</i>
50	120	1
95	120	
95	15	40
60	60	
95	15	<i>Continuous data collection (melt curve)</i>
60	60	
95	15	
4	∞	

## 9. Brood Size assay

The investigation into brood size regulation in *C. elegans* involved a comprehensive experimental procedure. To compare different *C. elegans* strains, they were cultured on nematode growth medium (NGM) agar plates seeded with OP50 bacteria as the primary food source. These plates were carefully maintained at a consistent temperature of 20 °C to ensure uniform growth conditions. To initiate the investigation, synchronized populations of gravid adult hermaphrodites were meticulously selected and individually placed on NGM plates. A total of 20 plates were prepared for this purpose, providing a solid foundation for subsequent statistical analysis. Hermaphrodites were allowed to deposit their eggs, enabling the development of embryos into hatched larvae. Following this incubation period, each NGM plate underwent a thorough examination, with precise enumeration conducted for both eggs and hatched larvae across all experimental groups and conditions. This data collection process was vital for accurately determining and comparing brood sizes among the various strains and conditions under investigation. The accumulated data analysed using one-way ANOVA, aimed at assessing and quantifying any significant differences between the diverse groups or conditions under study. This analytical approach was designed to yield valuable insights into

the underlying mechanisms and influencing factors governing brood size regulation in *C. elegans*, thereby enhancing our understanding of this crucial biological process.

## **10. Embryonic Survival Assay**

The hatched embryos were counted by placing multiple gravid worms (The required quantity of animals varied depending on the RNAi condition, e.g., under *puf-8* RNAi, there was a significant reduction in brood size, necessitating the placement of a larger number, like 50 animals, on the plate to reach the desired egg count. In contrast, in other conditions, 5-6 animals were sufficient to achieve the target number of eggs.) on a 60mm NGM plate and allowing approximately 100 eggs to be laid. After the worms were positioned on the plate, a waiting period was ensued, during which approximately 100 eggs were allowed to be laid by the gravid worms. Subsequently, the gravid worms were removed from the plate to ensure an unobstructed view and access to the laid eggs. Following this step, the number of hatched embryos was counted. Two-way ANOVA statistical analysis was conducted to evaluate distinctions between groups or experimental conditions.

## **11. Statistics**

Statistical analysis for all experiments was performed using the statistical methodologies described in the figure legends, and GraphPad Prism version 8 or 9 software was utilized for this purpose. Error bars in all figures denote the standard error of the mean (SEM). The significance levels were represented as follows: "ns" for not significant, "\*" for p-values less than or equal to 0.05, "\*\*" for p-values less than or equal to 0.01, "\*\*\*" for p-values less than or equal to 0.001, and "\*\*\*\*" for p-values less than or equal to 0.0001. RNAi assays, developmental observations, and RT-qPCR analyses were conducted with a minimum of three biological replicates. Microscopy analyses involved a minimum of two biological replicates.

## RESULTS AND DISCUSSIONS

### 1. Developmental significances of XRN-2

Essential roles of XRN-2 throughout the developmental stages of *C. elegans*, encompassing embryogenesis, larval development, and reproduction, were previously demonstrated by our group. This was achieved through the utilization of a temperature-sensitive *xrn-2* mutant (*xrn-2ts*) strain (Figure 7), which also unveiled its ubiquitous expression [Miki et al., 2014c]. While the degradation of miRNA [Chatterjee and Grosshans, 2009; Miki et al., 2014c, b], pre-mRNA processing [Miki et al., 2016], and the termination of RNAPII transcription on specific genes [Miki et al., 2017] in *C. elegans* have been attributed to XRN-2, the precise significance of these functions in development remains unclear. Challenges arise due to the ubiquitous expression pattern and multifunctionality of XRN-2, hindering the establishment of clear links between specific molecular pathways and distinct developmental processes. In the pursuit of gaining insights into the developmental role of XRN-2, a comprehensive investigative approach employing two distinct methodologies was utilized. The primary objective was to elucidate the genetic suppressors (Figure 6A) linked to XRN-2 during the developmental process, aiming to discern the specific role played by XRN-2 in this context. Through the identification of these suppressors, the unravelling of molecular interactions and regulatory mechanisms underlying the developmental function of XRN-2 was sought after.

Furthermore, the secondary approach was undertaken to identify synthetic lethality partners of XRN-2. Synthetic lethality denotes a genetic interaction where the concurrent loss of two genes results in cell death or severe growth impairments, while the loss of each gene independently remains tolerable [O'Neil et al., 2017] (Figure 6B). The objective was to uncover synthetic lethality partners associated with XRN-2 within the developmental processes, aiming to shed light on the functional interplay between XRN-2 and these partners. This approach was driven by the rationale of achieving a more comprehensive understanding of XRN-2's developmental role by exploring the functional repercussions of its interactions with other genes operating within the same pathway.

The convergence of these two investigative strategies was geared towards revealing the intricate molecular network within which XRN-2 functioned during development. By identifying genetic suppressors and synthetic lethality partners, an endeavour was undertaken to illuminate the precise functions and regulatory mechanisms through which XRN-2

contributed to the intricate processes underlying development. The implications of these findings are poised to enhance our grasp of developmental biology, furnishing invaluable insights into the intricate interplay of genes and molecular pathways pivotal to this fundamental biological process.

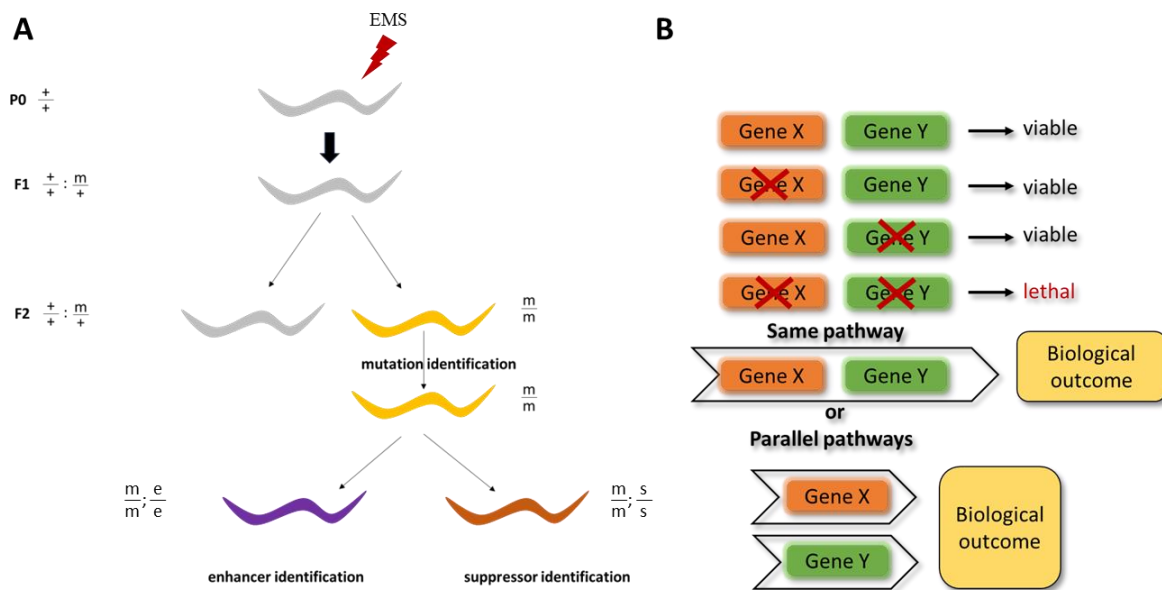


**Figure 6: Schematic illustration of synthetic lethality and modifier screen.** (A) Normally, each gene independently supports cell survival. However, when either gene is disrupted alone, the cell remains viable. Strikingly, simultaneous disruption of both genes induces cell death. Inspired by O'Neil et al., 2017. (B) This schematic outlines the basic steps of a simple F2 screen in genetic research. It begins with the search for a specific phenotype of interest in the F2 generation, derived from P0 animals exposed to a chemical mutagen, such as EMS (Ethyl methanesulfonate). The subsequent step involves pinpointing the mutation (m) responsible for the observed phenotype. Following this, the identified mutants can be further employed in modifier screens to uncover enhancer mutations (e) or suppressor mutations (s), enabling a more comprehensive understanding of the genetic mechanisms at play. Inspired by Singh, 2021

### 1.1 Screening suppressors of *xrn-2* sterility

To gain deeper insights into the diverse functions of XRN-2 in *C. elegans* development, genetic suppressor screens were initiated, targeting the developmental defects stemming from

*xrn-2* inactivation. The power of conditional mutants was harnessed, aiming to identify genetic modifiers associated with this essential gene. As previously mentioned, the existence of temperature-sensitive alleles of *xrn-2* (*xrn-2ts*) (Figure 7) in *C. elegans* was reported by our group [Miki et al., 2014c, 2016, 2017]. It has a point mutation to destabilize the XRN-2 protein at high temperature. Defective embryogenesis, larval development, and fertility were exhibited by these mutant animals at restrictive temperatures. However, previous endeavours to identify suppressor mutations beyond *xrn-2* itself using these mutants yielded no success. Given the ubiquitous expression of *xrn-2* throughout development [Miki et al., 2014c], the speculation arose that a single allele might not sufficiently suppress the diverse developmental defects occurring across various tissues or cells of *xrn-2* mutant animals. Consequently, the decision was made to narrow the focus to germline development.

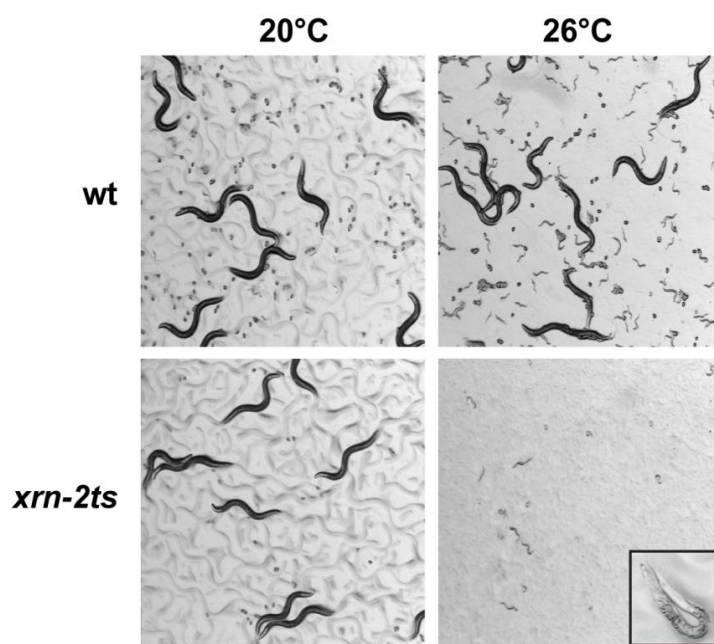


**Figure 7: Developmental comparison of *xrn-2* temperature-sensitive mutant (*xrn-2ts*) and wild-type worms.** Under favourable temperature conditions (20 °C), *xrn-2ts* mutant worms develop almost normally, similar to wild-type worms. However, when exposed to an elevated temperature (26 °C), the *xrn-2ts* mutant worms exhibit larval arrest due to the inactivation of the XRN-2 protein [Miki, et al., 2014].

### 1.1.1 Creating germline-specific *xrn-2* conditional mutants

The germline-specific temperature-sensitive mutant of *xrn-2* (referred to as *xrn-2ts<sup>germ</sup>*) was generated utilizing the MosSCI technique [Frøkjær-Jensen et al., 2008] by dr. habil. Takashi Miki. Employing this approach, a functional *xrn-2* transgene fused with green fluorescent protein (GFP) (*xrn-2::gfp*) was expressed in the somatic cells of *xrn-2(xe31)*, a temperature-sensitive mutant of *xrn-2* (*xrn-2ts*). The expression of *xrn-2::gfp* was governed by the *dpy-18* promoter for somatic cell rescue. Animals carrying the *xrn-2::gfp* transgene under the control of the *dpy-18* promoter (*Pdpy-18::xrn-2::gfp*) were cultured at 20 °C and observed using fluorescent microscopy, resulting in the detection of the XRN2-GFP signal in hypodermal and other somatic cells, excluding the intestine and the gonad (Figure 8A). For embryo rescue, the *pes-2.1* promoter, which activates gene expression specifically in embryos, was harnessed. Animals harbouring the *xrn-2::gfp* transgene driven by the *pes-2.1* promoter (*Ppes-2.1::xrn-2::gfp*) were incubated at 20 °C and observed using fluorescent microscopy. Notably, GFP fluorescence was confined to embryos (Figure 8B).

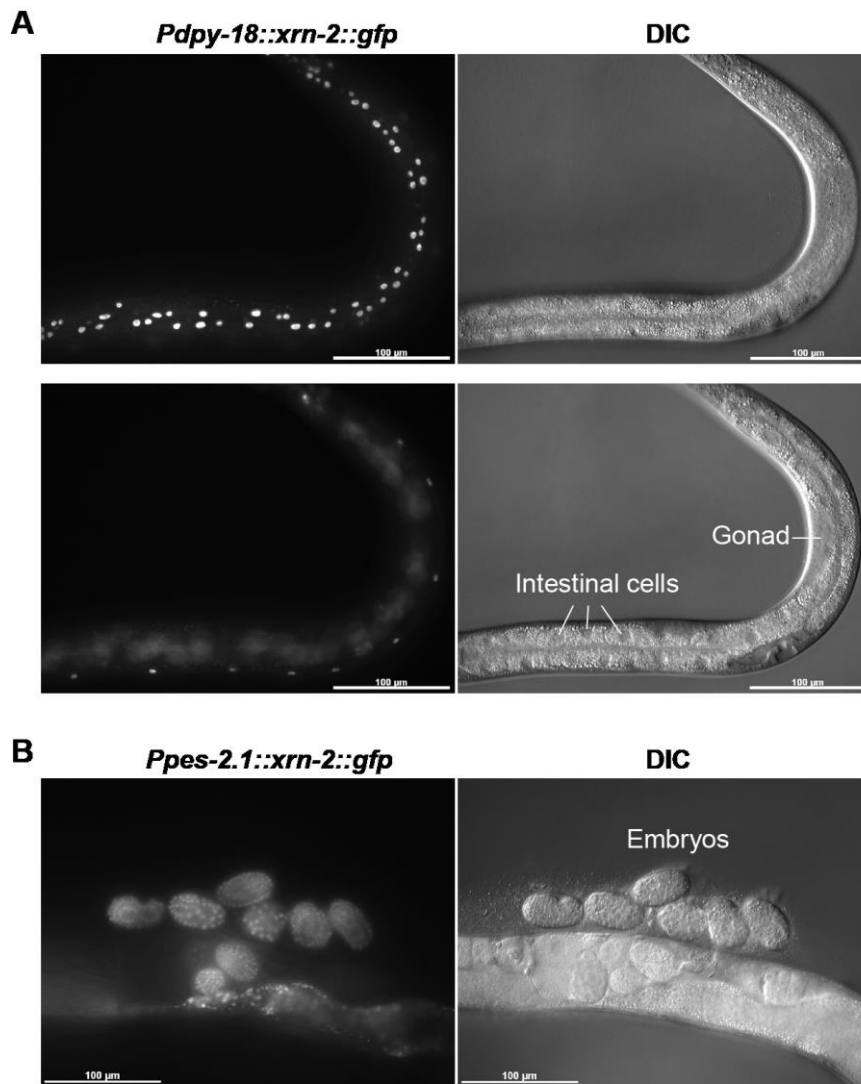


**Figure 8: Germline-specific *xrn-2* temperature-sensitive mutant (*xrn-2ts<sup>germ</sup>*)** (A) Animals carrying the *xrn-2::gfp* transgene driven by the *dpy-18* promoter (*Pdpi-18::xrn-2::gfp*) were incubated at 20 °C and examined. Fluorescent microscopy revealed GFP expression in hypodermal cells (top) while excluding the intestine and gonad (bottom). Corresponding DIC images are provided (right). (B) Animals harbouring the *xrn-2::gfp* transgene driven by the *pes-2.1* promoter (*Ppes-2.1::xrn-2::gfp*) were incubated at 20 °C and examined. GFP fluorescence was observed specifically in embryos. Corresponding DIC images are provided (right) [Aygün et al., 2023].

### 1.1.2 Phenotypic characterization of *xrn-2ts<sup>germ</sup>*

To evaluate the suitability of *xrn-2ts<sup>germ</sup>* animals, temperature shift experiments were performed. Following the transition from the permissive temperature (20 °C) to the restrictive

temperature (26 °C), a noticeable alteration in the reproductive capacity of the *xrn-2ts<sup>germ</sup>* animals was observed. Under favourable temperature conditions, these animals progressed through normal developmental stages, achieving adulthood and displaying successful reproduction from the initial larval (L1) stage. However, exposure to the restrictive temperature induced sterility (100%) in the *xrn-2ts<sup>germ</sup>* animals, indicating *xrn-2ts<sup>germ</sup>* strain can serve as a valuable tool for identifying genetic suppressors that counteract sterility resulting from XRN-2 inactivation within the germline (Figure 9A).

To gain insights into the specific developmental stages reliant on XRN-2 for fertility, targeted temperature shifts were conducted at various time points using *xrn-2ts<sup>germ</sup>* animals. Intriguingly, when the temperature increase was initiated from the mid-L4 stage, the animals maintained their fertility and exhibited unimpaired reproductive capacity (Figure 9B). Conversely, when the temperature shift was initiated from the L2 stage, the animals completely failed to sustain their reproductive ability. These observations underscore the crucial involvement of XRN-2 in germline development preceding the mid-L4 stage, with its functional presence during this developmental window being indispensable for ensuring fertility.

In conclusion, the transition of *xrn-2ts<sup>germ</sup>* L2-stage animals from a permissive temperature to a restrictive one induced sterility, highlighting the significant role of XRN-2 in modulating reproductive outcomes. The *xrn-2ts<sup>germ</sup>* strain offers a valuable experimental resource for exploring genetic suppressors associated with sterility resulting from XRN-2 inactivation. Moreover, through targeted temperature shifts, the developmental dependence of XRN-2 for fertility has been identified, shedding light on the critical role played by XRN-2 in germline development before the mid-L4 stage.

These findings are consistent with earlier studies conducted by Miki et al., [2014], thus it is validating the importance of XRN-2. The distinct response of the *xrn-2ts<sup>germ</sup>* strain to permissive and restrictive temperatures underscores its potential as a valuable tool for conducting genetic suppressor screens aimed at elucidating the molecular basis of germline-specific sterility resulting from XRN-2 inactivation.

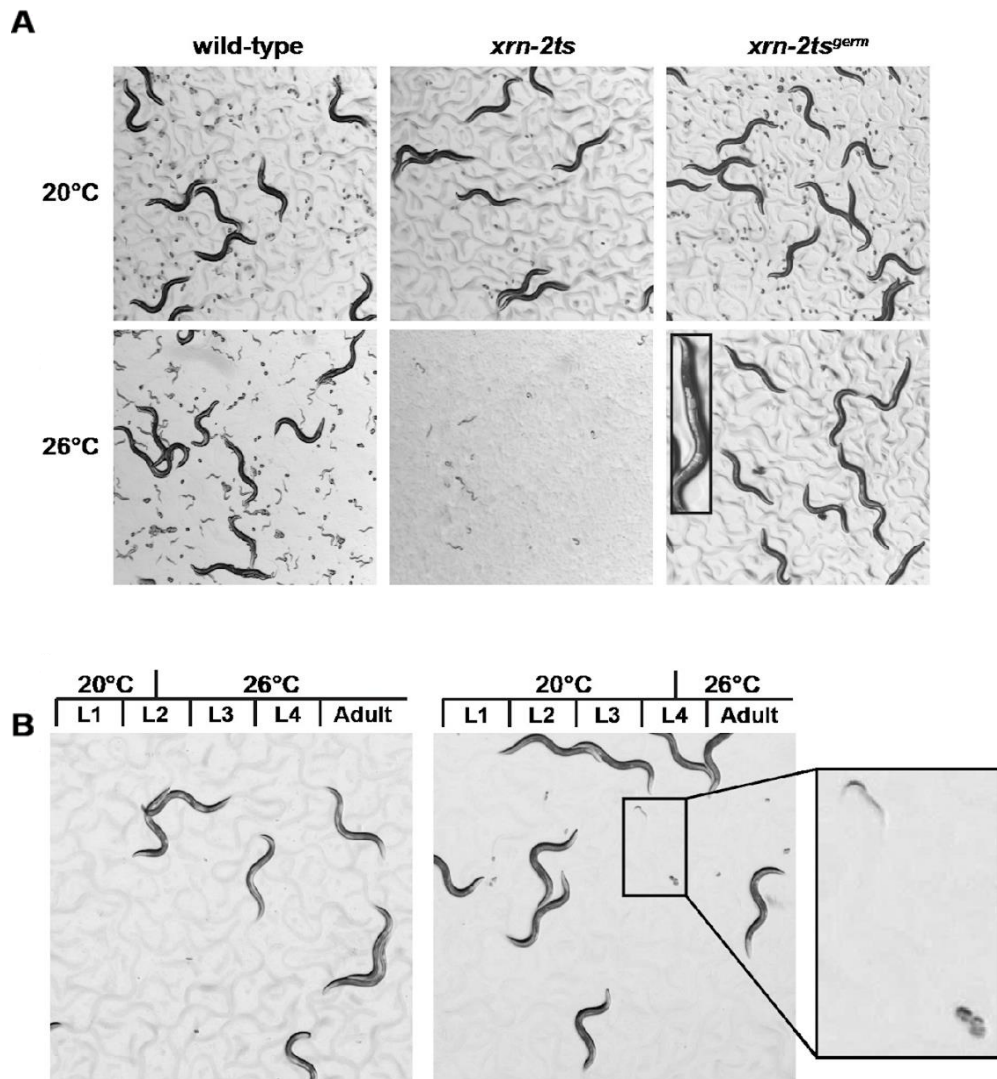


**Figure 9: Phenotypic characterization of *xrn-2ts*<sup>germ</sup>.** (A) Wild-type, *xrn-2ts*, and *xrn-2ts*<sup>germ</sup> animals were cultured at 20 °C or 26 °C from the L1 stage for 72 hours and monitored using stereomicroscopy under the same magnification (25x). An inset displays an adult animal lacking embryos, shown at higher magnification (100x). (B) *xrn-2ts* germ animals were cultured at 20 °C from the L1 stage until the middle of the L2 (left) or L4 (right) stage, followed by incubation at 26 °C until adulthood. The animals were observed using stereomicroscopy at the same magnification. An inset displays embryos and a hatched larva [Aygün et al., 2023].

### 1.1.3 The genes *dpy-10*, *osr-1*, *ptr-6*, and *C34C12.2* were identified as genetic suppressors of *xrn-2ts*<sup>germ</sup>

To gain further insights into the molecular basis of *xrn-2*'s involvement in germline development, ethyl methanesulfonate (EMS) mutagenesis was employed previously by dr.

habil. Takashi Miki, on *xrn-2ts<sup>germ</sup>* animals, resulting in the isolation of four distinct strains capable of successful reproduction at 25.5 °C. The presence of oocytes and embryos was observed in these strains, but not in *xrn-2ts<sup>germ</sup>* (Figure 10A). By performing genomic DNA sequencing (at FMI Functional Genomics Facility, Basel, Switzerland) and subsequent mutation mapping on these strains, the presence of recessive alleles within the *dpy-10*, *osr-1*, *ptr-6*, and *C34C12.2* genes was unravelled (Table 30).

The *dpy-10* gene, encoding a collagen protein crucial for cuticle formation [Levy et al., 1993], revealed a missense mutation within the *dpy-10(kid6)* allele, resulting in a dumpy phenotype in the mutant animals. Meanwhile, *osr-1*, previously implicated in osmotic stress resistance [Solomon et al., 2004], exhibited a nonsense mutation in the *osr-1(kid1)* allele. Notably, *ptr-6*, encoding a member of the patched family proteins vital for various developmental processes [Kuwabara and Labouesse, 2002; Zugasti et al., 2005; Daggubati et al., 2022], displayed an amino acid substitution within the evolutionarily conserved extracellular ligand binding site of the *ptr-6(kid4)* allele. An additional *ptr-6* allele, harbouring a missense mutation was recovered but subsequently lost due to extreme difficulties in cryopreservation [Choi et al., 2016]. Lastly, the uncharacterized gene *C34C12.2* carried the *C34C12.2(kid2)* allele, disrupting splicing by altering the guanine at the 5' splice site of the fourth intron to alanine.

Considering the nature of these alleles, it was anticipated that they would either diminish or abolish the functions of their respective genes. To validate this hypothesis, RNAi-mediated knockdown of each gene was conducted, resulting in the restoration of fertility in *xrn-2ts<sup>germ</sup>* animals at a restrictive temperature (25.5 °C). Notably, the presence of oocytes and embryos was observed in all RNAi conditions, and these embryos subsequently hatched and developed normally (Figure 10B, 10C). These findings strongly indicate that the four identified genes, either directly or indirectly, counteract the function of *xrn-2* during germline development.

This comprehensive characterization of genetic suppressors in the *xrn-2ts<sup>germ</sup>* strain not only enhances our understanding of the regulatory network involved in germline development but also sheds light on the intricate interplay between *xrn-2* and these specific genetic modifiers. Further investigations into the precise molecular mechanisms underlying these interactions hold immense potential for deciphering the intricacies of germline development and its associated regulatory pathways.

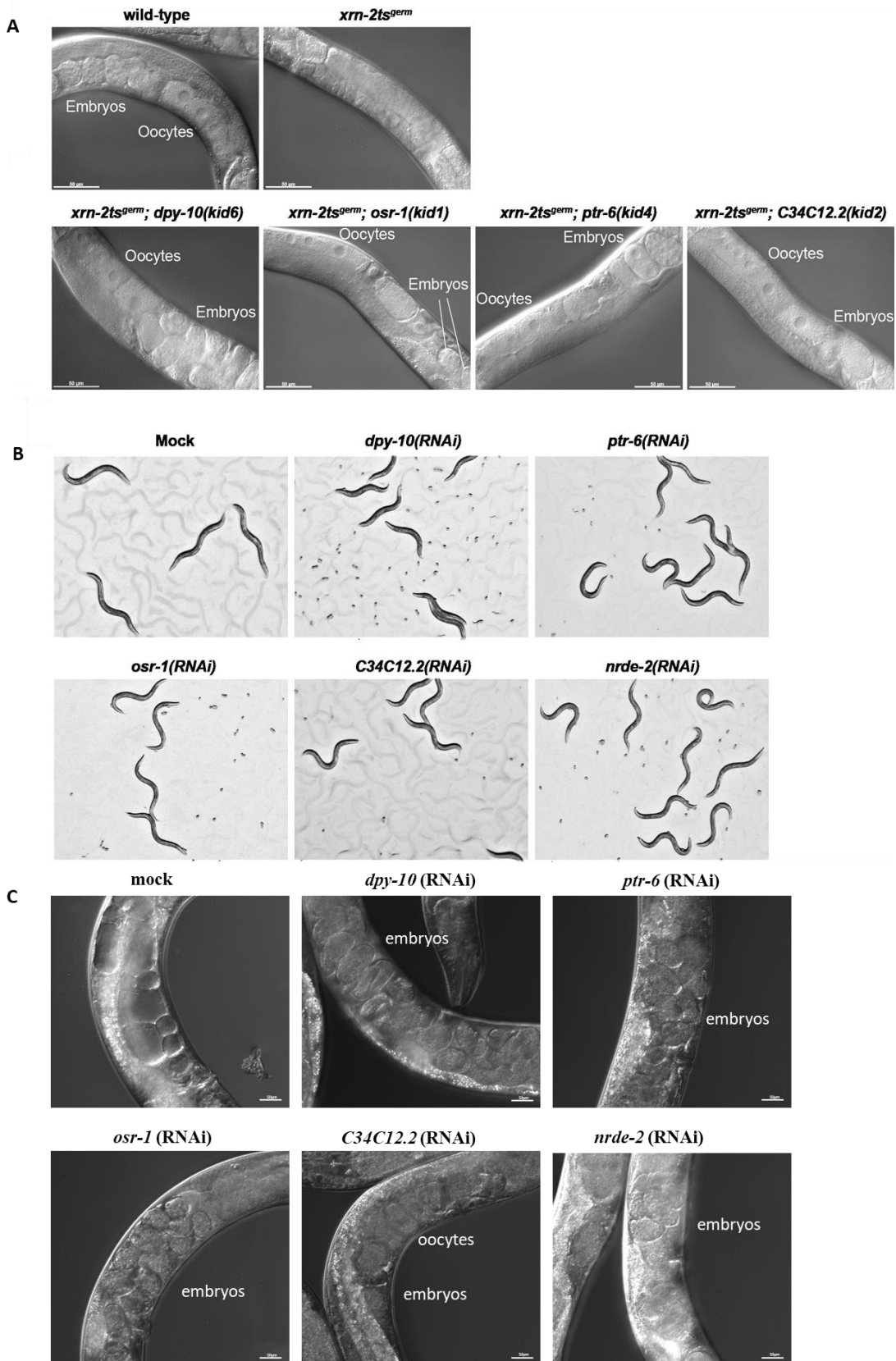


**Figure 10: Identification of genetic suppressors: *dpy-10*, *osr-1*, *ptr-6*, and *C34C12.2* counteracting *xrn-2ts<sup>germ</sup>*.** (A) Animals of indicated genotypes were incubated at a temperature of 25.5 °C starting from

the L1 stage for 72 hours and observed. Oocytes and embryos were found in all strains except *xrn-2ts<sup>germ</sup>*. (B) *xrn-2ts<sup>germ</sup>* animals were exposed to either mock RNAi or RNAi targeting specific genes, starting from the L1 stage and continuing until adulthood at 25.5 °C and observed by stereomicroscopy at the same magnification. Embryos were found in all conditions except mock RNAi [Aygün et al., 2023]. (C) *xrn-2ts<sup>germ</sup>* animals subjected to RNAi treatment, imaged at the same magnification. With the exception of the mock, embryos were observed in all the animals.

**Table 30: Alleles recovered from the screen.**

Gene(allele)	Type of mutation	Nucleotide change	Codon change	Amino acid change
<i>dpy-10(kid6)</i>	Missense	G → A	GGA → AGA	G131R
<i>osr-1(kid1)</i>	Nonsense	C → T	CAA → TAA	Q239Stop
<i>ptr-6(kid4)</i>	Missense	G → A	GGA → GAA	G223E
<i>C34C12.2(kid2)</i>	Splice site	G → A*	n/a	n/a

\*5' splice site of intron 4

n/a: not applicable

#### 1.1.4 DPY-10, OSR-1, and PTR-6 regulate the accumulation of glycerol

During extensive exploration of the scientific literature, a plethora of valuable insights were encountered that significantly expand the understanding of the complex regulatory mechanisms governing glycerol-3-phosphate dehydrogenase (*gpdh-1*) and its impact on fertility. In a groundbreaking genome-wide RNAi screen aimed at identifying genes involved in the activation of the *gpdh-1* promoter, several key players including *dpy-10*, *osr-1*, and *ptr-6* emerged as positive regulators [Lamitina et al., 2006].

Motivated by these intriguing findings, a series of RNAi experiments were conducted, at 25 °C, upon to elucidate the functional consequences of *dpy-10*, *osr-1*, and *ptr-6* silencing in wild-type animals. Remarkably, a substantial elevation in *gpdh-1* mRNA levels was observed upon the knockdown of any of the three genes (Figure 11A). When compared to the mock control, the knockdown of *dpy-10* resulted in a substantial approximately 17-fold increase in the expression of *gpdh-1* mRNA. In contrast, *osr-1* exhibited an approximately 6.5-fold increase, and *ptr-6* displayed a roughly 10-fold elevation in *gpdh-1* mRNA expression. Notably,

mutants with *C34C12.2* knockdown did not exhibit a significant change in *gpdh-1* mRNA expression levels under the same conditions. This observation strongly suggested a direct correlation between the upregulation of *gpdh-1* expression and the restoration of fertility in *xrn-2ts<sup>germ</sup>* animals, the RNAi treatments not only restored fertility but also exhibited a remarkable parallel correlation with the extent of *gpdh-1* upregulation. (Figure 11B).

DPY-10, OSR-1, and PTR-6 serve as negative regulators of *gpdh-1* expression. The depletion of any of these regulators results in the de-repression of *gpdh-1*, leading to an increase in glycerol levels, ultimately contributing to the restoration of fertility in *xrn-2ts<sup>germ</sup>* animals. In conclusion, the subsequent elevation in glycerol levels were likely to restore fertility in *xrn-2ts<sup>germ</sup>* animals, which underscored the significant role of glycerol modulation in reproductive processes.

This intriguing discovery prompted further research to explore the potential of glycerol uptake in restoring fertility in *xrn-2ts<sup>germ</sup>* animals (Figure 11C). To achieve this, a series of meticulously controlled experiments was devised, involving the incubation of wild-type, *xrn-2ts*, and *xrn-2ts<sup>germ</sup>* animals on culture plates supplemented with varying glycerol concentrations (2%, 16%, or 64%) at a constant temperature of 26 °C. The incubation period spanned from the L1 stage and persisted for 72 hours, ensuring sufficient exposure to the glycerol environment. Subsequent to this incubation, all animals underwent thorough examination using stereomicroscopy at a standardized magnification. However, the attempts to restore fertility in *xrn-2ts<sup>germ</sup>* animals through the external provision of glycerol from culture plates ultimately proved unsuccessful. This may be attributed to the animals' apparent reluctance to actively assimilate the externally provided glycerol. Hence, the endeavour to restore fertility in *xrn-2ts<sup>germ</sup>* animals by externally providing glycerol from culture plates was unsuccessful, potentially due to the animals' hesitancy in taking in exogenously provided glycerol.

These remarkable findings not only shed light on the intricate network of genes and molecular pathways involved in glycerol regulation but also provide a potential avenue for therapeutic interventions targeting fertility restoration. The detailed understanding of the mechanisms underlying the regulation of *gpdh-1* expression opens up new possibilities for developing strategies aiming at manipulating glycerol levels to overcome fertility-related challenges in diverse biological systems. Further exploration of the interplay between these

regulatory factors and their downstream effects will deepen our comprehension of the intricate molecular tapestry that governs reproductive processes.

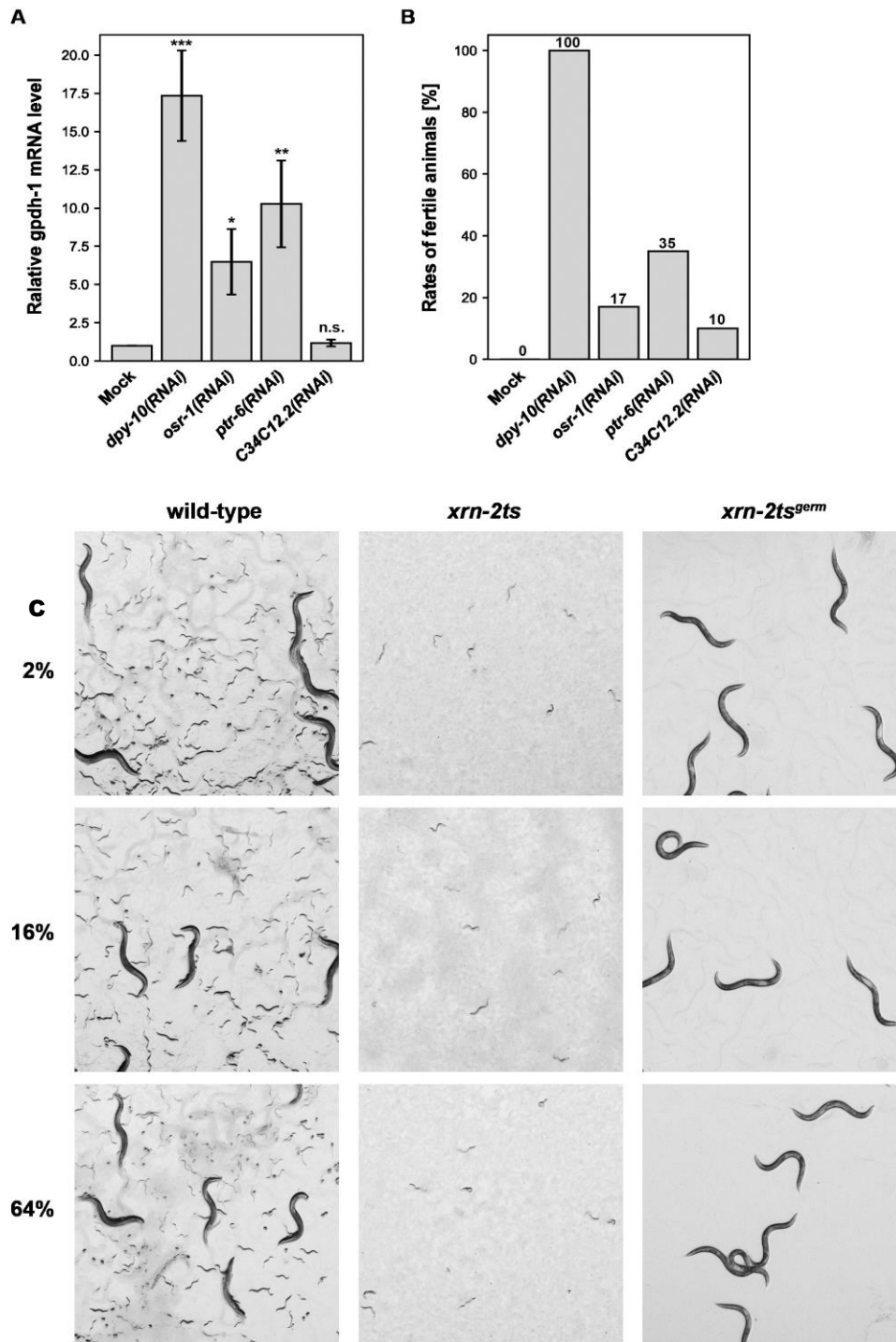


**Figure 11: Significant increases in *gpdh-1* expression were observed upon knockdown of *dpy-10*, *osr-1*, *ptr-6*, or *C34C12.2* genes. (A) To evaluate the impact of gene knockdown, wild-type animals**

were subjected to either mock RNAi or RNAi targeting the specific genes from the L1 stage to adulthood at 25 °C. Quantification of *gpdh-1* mRNA levels was performed using RT-qPCR and normalized to *act-1* mRNA levels. The values were expressed relative to the mock-treated animals, which were assigned a value of 1 (n = 5, means ± SEM). Statistical analysis was conducted using a two-sided paired t-test, and the resulting p-values were indicated as follows: \*p < 0.05, \*\*p < 0.01, \*\*\*p < 0.001, n.s. not significant. The detailed numerical values can be found in Table 31. (B) In *xrn-2ts<sup>germ</sup>* animals, exposure to either mock RNAi or RNAi targeting the indicated genes from the L1 stage to adulthood at 26 °C allowed assessment of fertility restoration rates (n=100 for each condition, across two independent experiments). (C) wild-type, *xrn-2ts*, and *xrn-2ts<sup>germ</sup>* animals were incubated on culture plates supplemented with varying concentrations of glycerol (2%, 16%, or 64%) at 26 °C from the L1 stage for 72 hours. The animals were then examined using stereomicroscopy at a consistent magnification. While *xrn-2ts<sup>germ</sup>* animals developed into adults, they exhibited sterility, in contrast to the wild-type animals that successfully reproduced. Furthermore, *xrn-2ts* animals ceased their development at the L1 stage [Aygün et al., 2023].

**Table 31: *gpdh-1* RT-qPCR data**

Treatment	Repeat 1	Repeat 2	Repeat 3	Repeat 4	Repeat 5	Mean	SEM	p-value
Mock	1	1	1	1	1	1	0	0
<i>dpy-10</i> (RNAi)	14.840 98	26.346 17	8.2232 92	17.857 73	19.463 33	17.346 3	2.9601 26	0.0002 79
<i>osr-1</i> (RNAi)	3.8939 4	5.6199 18	2.3814 54	5.8629 68	14.662 14	6.4840 85	2.1395 52	0.0167 4
<i>ptr-6</i> (RNAi)	4.9838 17	15.985 94	3.0426 2	10.129 17	17.197 92	10.267 89	2.8360 77	0.0056 96
<i>C34C12.2</i> (RNAi)	0.6910 02	0.7939 35	1.0363 31	1.8880 86	1.4711 5	1.1761 01	0.2230 34	0.2262 72

### 1.1.5 The depletion of *dpy-10*, *osr-1*, or *ptr-6* did not alleviate the larval arrest phenotype observed in *xrn-2ts* animals

Glycerol, along with glycine betaine, proline, trehalose, and other compounds, plays a pivotal role in enhancing the adaptability of various life forms to a wide range of environments. When confronted with extreme conditions such as high salinity or desiccation, cells actively accumulate osmolytes, with glycerol emerging as a prominent component in this process. Glycerol assumes a central role as a sentinel in the defence mechanisms of cells. As cells

accumulate glycerol in response to stress, it serves as a protective shield for proteins through intricate interactions. Glycerol forms hydrogen bonds with water and protein surfaces, fortifying native protein structures and preventing unfolding. Moreover, glycerol displaces water molecules, averting disruptive protein interactions. This dual role underscores glycerol's significance in maintaining protein stability under duress [Wang and Bolen, 1997; Sebollela et al., 2004].

Considering the possibility that elevated glycerol levels could potentially stabilize mutant XRN-2 in both germ cells and somatic cells of *xrn-2ts* animals, promoting their development, further investigations were conducted. It was hypothesized that if this mechanism was effective, knockdown of *dpy-10*, *osr-1*, or *ptr-6*, which are involved in glycerol accumulation, could rescue the *xrn-2ts* animals from larval arrest.

Also, due to the often partial depletion of target proteins through RNAi, an investigation was conducted to examine the effect of constitutive gene deletion by crossing *osr-1(ok959)*, a loss-of-function allele of *osr-1* [Wheeler and Thomas, 2006], with *xrn-2ts (osr-1(ok959); xrn-2ts)* (worm crossing conducted by Alicja Rzepczak, MSc, a project developer at Laboratory of Animal Model Organisms, IBCH PAN). The purpose of this experiment was to gain insights into the consequences of complete removal of *xrn-2* and *osr-1* genes.

Contrary to the hypothesis, the depletion of *dpy-10*, *osr-1*, or *ptr-6*, at 25 °C, did not lead to rescue of *xrn-2ts* animals from their larval arrest phenotype (Figure 12A). Furthermore, when subjected to incubation at 25 °C from the L1 stage, it was observed that all *osr-1(ok959); xrn-2ts* animals experienced developmental arrest during the larval stage, thereby exhibiting no developmental advantage over *xrn-2ts* animals (Figure 12B).

The results strongly suggest that the rescue is not attributed to the stabilization of XRN-2. Instead, the upregulation of glycerol emerges as a relevant factor in the restoration of germline development in *xrn-2ts<sup>germ</sup>* animals. These compelling findings highlight that the upregulation of *gpdh-1* restores fertility in *xrn-2ts* germ animals through mechanisms distinct from the stabilization of the mutant XRN-2 protein at elevated temperatures. As suggested by a previous study [Davis et al., 2017], an increase in glycerol accumulation may serve as an adaptive response to osmotic stress in the *C. elegans* germline, maintaining germ cell and oocyte quality. This is in line with the observation that animals lacking *gpdh-1* and *gpdh-2*

genes exhibit reduced brood size under osmotic stress compared to wild-type animals [Lamitina et al., 2006]. The possibility arises that XRN-2 functions to regulate osmolality in the germline through an unidentified mechanism. In such a scenario, elevated glycerol levels could act as a chemical chaperone, safeguarding XRN-2-inactivated germ cells from osmotic stress by stabilizing proteins and other structures.

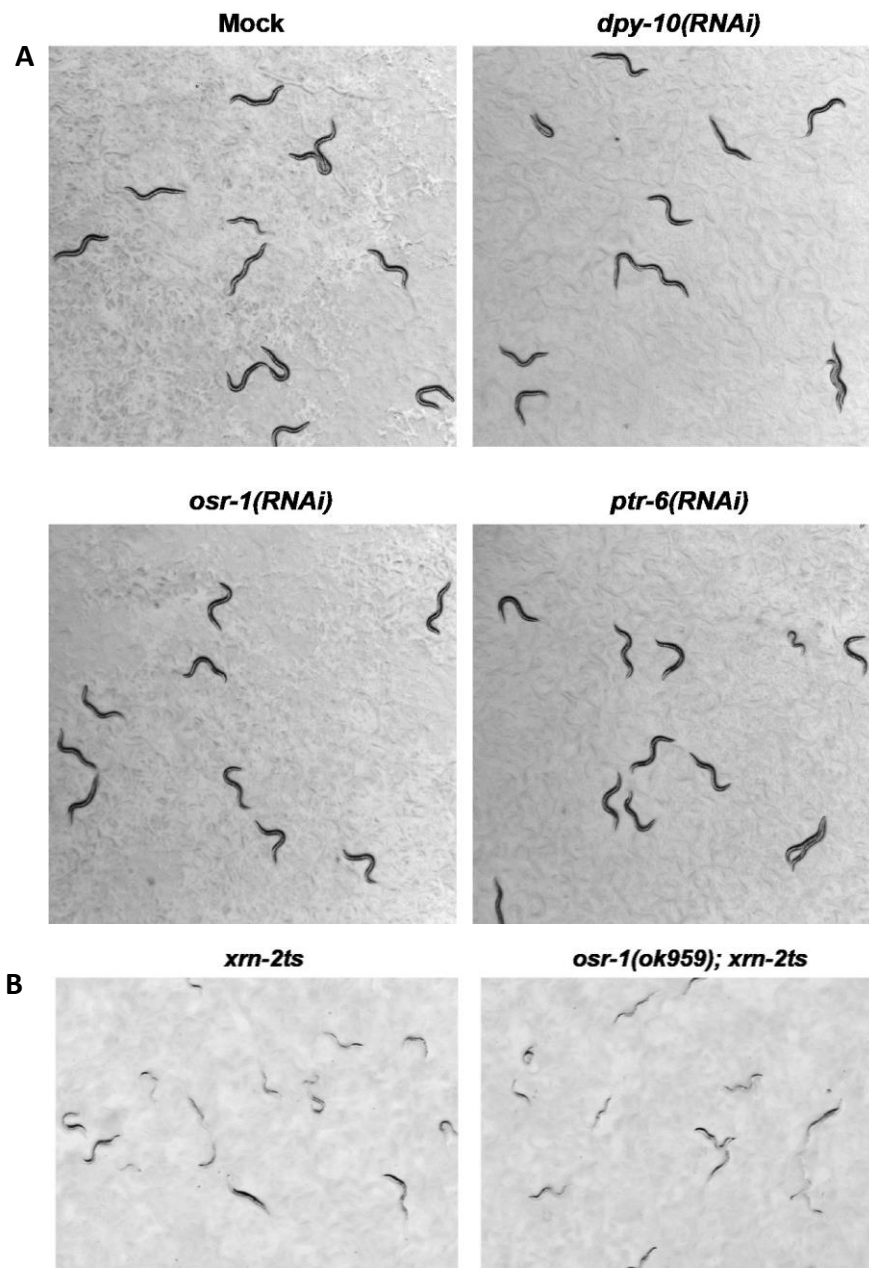


**Figure 12: The knockdown of *dpy-10*, *osr-1*, or *ptr-6* did not result in the rescue of *xrn-2ts* animals from their larval arrest phenotype. (A) *xrn-2ts* animals were subjected to RNAi targeting the specified**

genes, along with a control group exposed to mock RNAi. The RNAi treatment was initiated at the L1 stage and lasted for 48 hours at a temperature of 25 °C and observed using stereomicroscopy at the same magnification. All animals displayed arrested development and remained in the larval stage. (B) Animals with specific genotypes were cultured at 25 °C from the L1 stage for 72 hours and observed using stereomicroscopy at the same magnification. All animals displayed arrested development and remained in the larval stage [Aygün et al., 2023].

### **1.1.6 The primary localization of C34C12.2 is within the nucleolus of germ cells**

In contrast to the three other genes identified in the screen (*dpy-10*, *osr-1* and *ptr-6*), knockdown of *C34C12.2* did not elicit any discernible effect on *gpdh-1* expression (Figure 11 A). Consequently, it is likely that the *C34C12.2* allele restores fertility in *xrn-2ts* germ animals through a distinct mechanism from those involving the *dpy-10*, *osr-1*, and *ptr-6* alleles. The functional characteristics and developmental roles of *C34C12.2* have remained largely unexplored to date. To examine the subcellular localization of *C34C12.2* in germ cells, a transgenic strain expressing a GFP-fused *C34C12.2* was generated using the MosSCI technique. Intriguingly, the imaging analysis unveiled the predominant localization of *C34C12.2* within the germ cell nucleoli (Figure 13). This distinctive localization pattern strongly supports the notion of potential involvement of *C34C12.2* in germline development. Moreover, *C34C12.2* displayed widespread expression across germ cells, encompassing oocytes and sperm, as well as other tissues like the hypodermis and intestine.

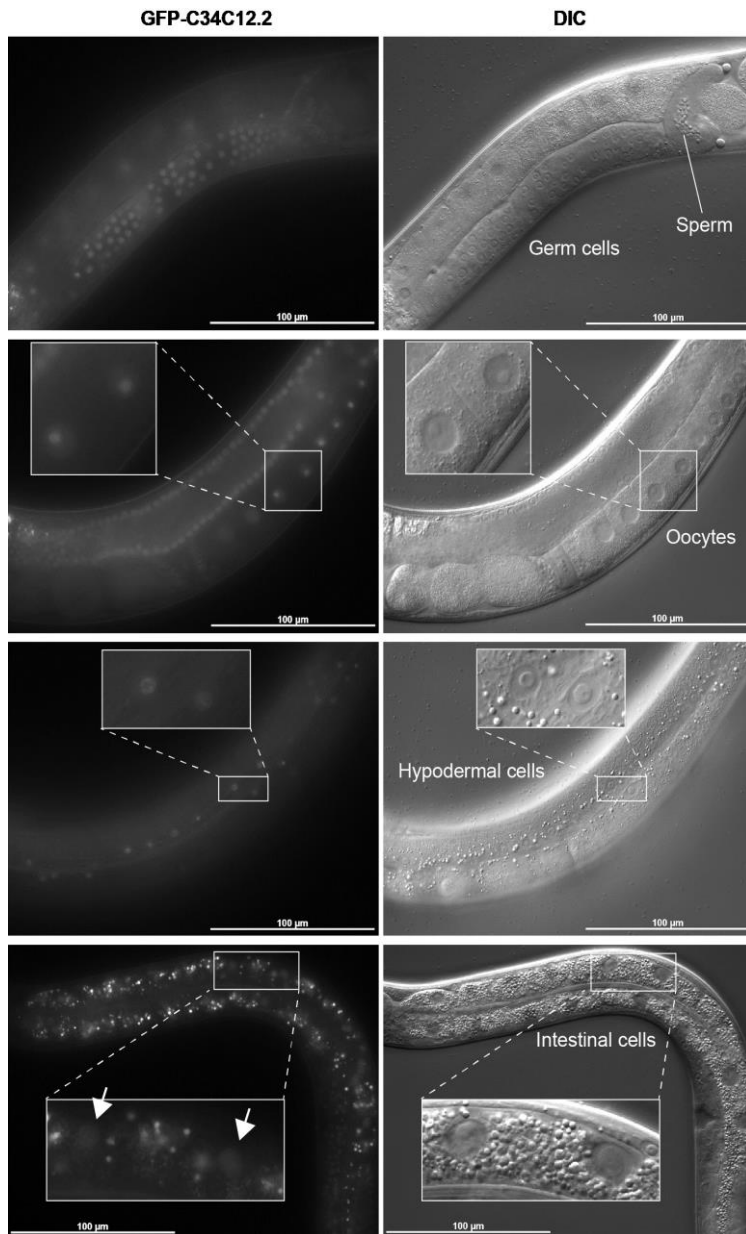


**Figure 13: The predominant localization of C34C12.2 within the nucleolus is demonstrated.** Animals carrying a transgene of *gfp::C34C12.2* incubated at 20 °C and observed. Insets provide higher magnification images of cell nuclei. GFP signal was detected within the nucleolus of various cell types, including germ cells, oocytes, sperm, hypodermal cells, and intestinal cells. The corresponding DIC images are also presented (right) [Aygün et al., 2023]. The punctate signal observed in the intestine corresponds to the autofluorescence emitted by gut granules, as previously described [Coburn and Gems, 2013].

### 1.1.7 The depletion of NRDE-2 led to the restoration of fertility in *xrn-2<sup>germ</sup>* animals

To shed light on the potential molecular function of C34C12.2, a protein homology search was carried out using Position-Specific Iterated BLAST (National Centre for Biotechnology Information, Bethesda, MA, USA), which revealed an intriguing similarity between C34C12.2 and *S. cerevisiae* Net1 (Figure 14). In *S. cerevisiae*, the role of Net1 involves functioning as a core subunit within the regulator of nucleolar silencing and telophase exit (RENT) complex (Straight et al., 1999). This complex plays a crucial role in facilitating the attachment of the RENT complex to ribosomal DNA (rDNA) within the nucleolus, thus enabling gene silencing through the collaborative action of NAD-dependent deacetylase Sir2, another constituent of the complex.

In our group's previous investigation [Miki et al., 2014b], the presence of C34C12.2 in XRN-2-containing complexes purified from whole-worm lysates could not be detected. This finding suggests that these two proteins may function independently of each other without forming stable physical interactions within germ cell nuclei. Wan and colleagues identified C34C12.2 in NRDE-2-containing complexes, in *C. elegans*, through immunoprecipitation mass spectrometry, although the specific function of C34C12.2 was not addressed in their study [Wan et al., 2020].

NRDE-2 serves as an effector protein, in *C. elegans*, in the nuclear RNAi pathway, wherein Argonaute protein, NRDE-3 in the soma or HRDE-1 in the germline, binds to endogenous siRNA species known as 22G RNA. Subsequently, NRDE-3 translocates from the cytoplasm to the nucleus, where it recruits NRDE-1, NRDE-2, and NRDE-4 to nascent pre-mRNA molecules. This recruitment leads to the inhibition of RNAPII elongation and the deposition of repressive histone H3K9 trimethylation marks [Guang et al., 2008, 2010; Burkhart et al., 2011; Ashe et al., 2012; Buckley et al., 2012; Luteijn et al., 2012]. This pathway plays a critical role in maintaining germline integrity by silencing transposons, regulating gene expression, and facilitating epigenetic inheritance. Intriguingly, the same machinery is involved in repressing the expression of pre-rRNA [Zhou et al., 2017; Liao et al., 2021].

Since C34C12.2 has been identified in NRDE-2-containing complexes [Wan et al., 2020], the aim of the experiment was to see whether this protein is indeed in complex with NRDE-2 in *xrn-2<sup>germ</sup>* strain. If C34C12.2 collaborates with NRDE-2, either directly or indirectly, to counteract the role of XRN-2 in germ cells, the knockdown of *nrde-2* should result

in the restoration of fertility in *xrn-2ts<sup>germ</sup>* animals. Remarkably, our findings demonstrate that *xrn-2ts<sup>germ</sup>* animals depleted of NRDE-2 indeed regained fertility (Figure 10). This observation suggests a potential functional interaction between C34C12.2 and NRDE-2, highlighting their significance in modulating the role of XRN-2 in germline.

The findings of the study reveal exciting prospects for further investigation into the functional significance of C34C12.2 and its intricate involvement in germline development. Future research efforts should be directed towards uncovering the precise molecular mechanisms governing the unique role of C34C12.2 within the nucleolus, as well as its potential interactions with other components of the regulatory machinery. By elucidating the intricate dynamics of C34C12.2, deeper insights into the complex regulatory networks that govern germline development can be obtained, thereby expanding our understanding of the broader field of developmental biology.

## Net1p [*Saccharomyces cerevisiae* YJM1399]

Sequence ID: [AJV44886.1](#) Length: 1195 Number of Matches: 1

Range 1: 775 to 1189 [GenPept](#) [Graphics](#)

[▼ Next Match](#) [▲ Previous Match](#)

Score	Expect	Identities	Positives	Gaps
55.1 bits(131)	1e-06	99/446(22%)	165/446(36%)	49/446(10%)
Query 92	ARQAKISQNLTKTSETASTSSPVRQVQKTEIVPRVS--QRTIVKTQALPRVNA--PVLS	146		
Sbjct 775	+++ + KTS+++ T S + +Q+ P ++ Q K + P A PV+S	834		
Sbjct 775	SQKKSVMSESFKTSQSSVTDSKISEQMAKSFYPNLNKKQNEATKVETKPATQASFFPVVS			
Query 147	SVPAKNPLPPKFVYINTAGLKRKRDDDKNTPTSTNSITLNPSSRGDQTQFIVHLQRTIER	206		
Sbjct 835	P+ + T G ++ N + ++ + Q + T R	877		
Sbjct 835	GAPS-----VATKGTSSFNEE-----GNRKNVTKAKNESAIQIDRQQKETTSTR			
Query 207	LEKEKAALT--EKLTMREDEIKVFSVEFVNIQKENVK--LMKENKAKESQISNQSIQVRN	262		
Sbjct 878	+ K+A E L + + K NIQ N K L ++ +K Q+S + +++ +	937		
Sbjct 878	VTDLKSANIGGEDLNKKAEGSKEPEKASANIQDANDKNNLKEKEDSKSKQVSQKCLKMTD			
Query 263	SWKFAD--LFKKEIQSRKDVSEVKKWIKIDKIEKKVGI----KKPTPRKKPDVKLI--NPE	314		
Sbjct 938	K + L K KD+ + K+ K GI K + D + E	996		
Sbjct 938	HLKEGNVQLPKPSANDKLDL-KAKFTNSKTLVPPGIISNEKNSSANDDDSSSSSGSSTE			
Query 315	DISLMSDRTQDGEDSSDFGSLAKYLKPDQPSTSSACYGKPFYFESTSSSSRKPITASPG	374		
Sbjct 997	D S S + D E S+ + P +P SS+ E+ S S K I A+P	1050		
Sbjct 997	DESSSSSSSDEETSTSRKARRVVNTPREPVRSS-----KIEAPSPSVNKKINATPD			
Query 375	PPGRTQISDQLNTGEVRYVWNSGKPFNFSSSESNRNLKIPGYIKRPEFRYIKPEGFTSA	434		
Sbjct 1051	TQ+ D + V+ S N SS + K+ P + + G	1103		
Sbjct 1051	KIPVTQLMDMSSPPSVKSKTTS----NPSSILHDLPRKVRPSLSSLSLSD---LVSRGIPDV			
Query 435	SYKAQSEGMSFLKTGSSATPENSKKSAHFDMPD-ISSTPYKSHVVVEDEMNSSSSTIG	493		
Sbjct 1104	K S K SS+ E+S S D+S + S +SD+ SS	1163		
Sbjct 1104	KEKTSKSNESQTKASSSSDDESSSDSDSNSSSDSVSDSSSDSKESDSDSDSDGSDDDGK			
Query 494	GFSEKKGNGALGSQKSPMPDIATAL 519			
Sbjct 1164	F S K + ALG +K P A+ +	1189		
Sbjct 1164	SFISAKSASAALGKKKKPSGGFASLI 1189			

**Figure 14: The homology between C34C12.2 and *S. cerevisiae* Net1.** The complete sequence of the C34C12.2 protein (identified as NCBI accession ID: NP\_497712) was subjected to analysis using PSI-BLAST, employing default algorithm parameters with the exception of selecting "no adjustment" for compositional adjustments [Aygün et al., 2023].

## 1.2 Identifying potential synthetic lethality partners of *xrn-2*

In order to identify genetic modifiers of *xrn-2*, an alternative approach was employed through an extensive RNAi-based synthetic lethality screen. This screen encompassed approximately 500 RNA-regulating factors, which were systematically targeted in the *xrn-2ts* mutant (by dr. habil. Takashi Miki). The screen was conducted at a permissive temperature (20°C), wherein the mutant animals exhibited reduced XRN-2 activity but did not manifest any overt phenotypes. Out of 500 RNA regulatory factors, 17 mRNA regulators were identified as potential synthetic lethality partners of *xrn-2* (Table 32).

**Table 32: mRNA regulators as putative synthetic lethality partner of *xrn-2***

Gene name	Human ortholog	Process (predicted)
<i>cpf-2</i> (Cleavage and polyadenylation factor)	CSTF2/CstF64	pre-mRNA 3' end processing
<i>clpf-1</i> (Cleavage/polyadenylation factor subunit)	CLP1	pre-mRNA 3' end processing
<i>cpsf-1</i> (Cleavage and polyadenylation specificity factor)	CPSF160	pre-mRNA 3' end processing
<i>cpsf-2</i> (Cleavage and polyadenylation specificity factor)	CPSF100	pre-mRNA 3' end processing pre-mRNA splicing
<i>hrp-1</i> (human HnRNP A1 ortholog)	HNRNPA1	pre-mRNA 3' end processing
<i>nono-1</i> (NONO (conserved nuclear protein) ortholog)	NONO	pre-mRNA splicing
<i>prp-38</i> (yeast PRP (splicing factor) related)	PRPF38A	pre-mRNA splicing
<i>rbm-42</i> (RNA binding motif protein ortholog)	RMB42	pre-mRNA splicing
<i>rnp-4</i> (RNP (RRM RNA binding domain) containing)	RBM8A	pre-mRNA splicing
<b>R08D7.1</b>	BUD13	pre-mRNA splicing
<i>oma-2</i> (Oocyte maturation defective)		mRNA stability/translation regulation
<i>puf-3</i> ( PUF (Pumilio/FBF) domain-containing)	PUM1/2	mRNA stability/translation regulation
<i>puf-8</i> ( PUF (Pumilio/FBF) domain-containing)	PUM1/2	mRNA stability/translation regulation
<i>puf-9</i> ( PUF (Pumilio/FBF) domain-containing)	PUM1/2	mRNA stability/translation regulation
<i>cel-1</i> (mRNA capping enzyme like)	RNGTT	mRNA capping
<i>ell-1</i> (ELL transcription elongation factor ortholog)	ELL	mRNA transcription elongation
<i>ain-1</i> (ALG-1 interacting protein)	TNRC6A	miRNA-induced mRNA silencing

### 1.2.1 *puf-9* was identified as a synthetic lethality partner of *xrn-2*

Among the potential synthetic lethality partners of *xrn-2* that have been identified, *puf-9*, an ortholog of Drosophila Pumilio and human PUM1/2, emerged as a compelling and noteworthy candidate. The Pumilio family is renowned for its pivotal role in governing RNA regulation, lending particular significance to *puf-9* (Table 32). Although *puf-9* has demonstrated its involvement in mRNA regulation [Nolde et al.,2007], many aspects of its specific mechanisms in *C. elegans* development remain elusive. Consequently, our research endeavoured to extensively characterize *puf-9* and to explore potentially shared functions with *xrn-2*.

By employing knockdown techniques, at 20 °C, on *puf-9* in *xrn-2ts* animals (Figure 15A), or vice versa, i.e., knockdown of *xrn-2* in *puf-9* mutant animals (Figure 15B), a striking

phenotype became evident, characterized by a noticeable decline in vitality, as evidenced by pronounced sluggishness in behaviour, in both cases. Furthermore, phenotypes such as blister formation and molting defects, observed in *xrn-2* mutant animals, were exacerbated in the *puf-9/xrn-2* double mutant. Importantly, when subjected to the same *puf-9* knockdown, wild-type animals exhibited no discernible phenotypic alterations. These observations strongly indicate that *puf-9* acts as a genetic enhancer of *xrn-2*, making a substantial contribution to its functional modulation. The elucidation of this interaction sheds light on the intricate regulatory mechanisms governing the interplay between *puf-9* and *xrn-2*, thereby holding promising implications for further investigations into their respective roles in biological processes.

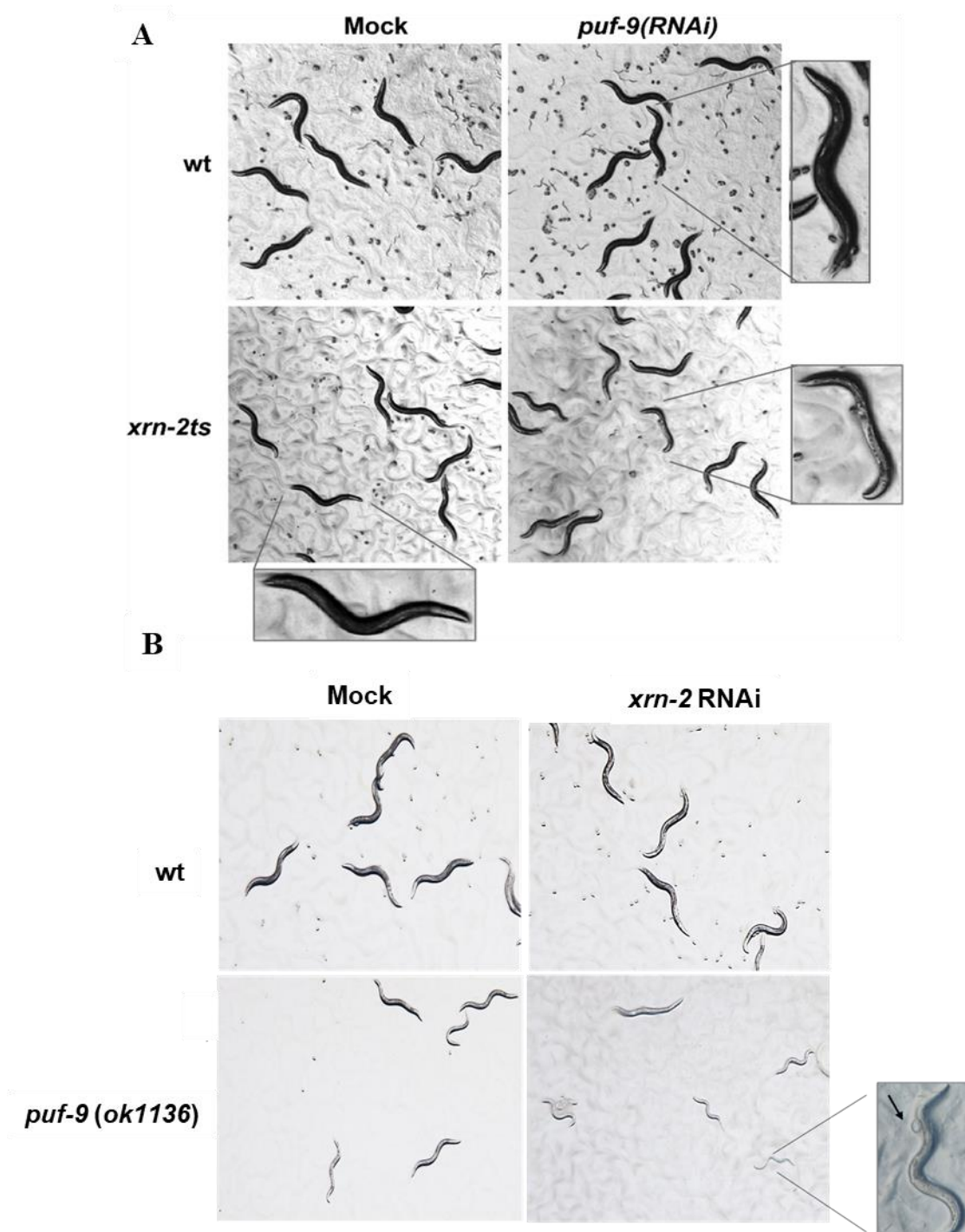


**Figure 15: *puf-9* was identified as a genetic enhancer of *xrn-2*.** (A) Experiments conducted subjecting both groups to mock or *puf-9* RNAi treatment to wild-type and *xrn-2ts* animals from the first larval stage, lasting for 72 hours at 20 °C and observed using stereomicroscopy. Upon *puf-9* RNAi treatment, *xrn-2ts* animals displayed sickness, evident through a clear and sluggish phenotype, while wild-type animals showed no discernible phenotypic changes under the same conditions. (B) *xrn-2* RNAi was applied to *puf-9* mutant worms, at 20 °C, revealing severe phenotypes such as developmental delay,

reduced progeny, and increased vulval bursting and blistering, while wild-type worms exhibited no noticeable phenotype.

### **1.2.2 PUF-9 is expressed in both germline and soma during development**

Post-transcriptional gene expression regulation plays a crucial role in modulating protein production rates through precise control of mRNA levels and translation. Within diverse eukaryotes, RNA-binding proteins (RBPs) exert regulatory influence by selectively binding to the 3' untranslated regions (3'UTRs) of mRNA, impacting crucial factors such as mRNA stability, translation, biogenesis, and cellular localization. Notably, the Pumilio/FBF family an evolutionarily conserved group of eukaryotic post-transcriptional regulators [Wickens et al., 2002], was initially identified as Pumilio (DmPUM) in *Drosophila melanogaster* and as a fem-3-binding factor (FBF) in *C. elegans*, collectively referred to as PUF or PUM-HD proteins [Zamore, et al., 1997].

PUF family members play vital roles in diverse biological processes, including oogenesis, spermatogenesis [Kraemer et al., 1999], neuronal function, stem cell maintenance [Lehmann and Nüsslein-Volhard, 1987] and organelle biogenesis [García-Rodríguez et al., 2007]. Their regulatory actions involve mechanisms such as deadenylation, direct binding to the cap structure, and occasional recruitment of cap-binding factors [Wreden et al., 1997] to control target mRNA stability and translation. These regulatory processes culminate in translational repression or mRNA decay. In *C. elegans*, the ten identified PUF proteins are categorized into four subfamilies based on amino acid sequence similarities: PUF-8/9, FBF-1/2, PUF-3/11/4, and PUF-5/6/7 [Wickens et al., 2002].

Significantly, FBF-1, FBF-2, PUF-8, PUF-3, and PUF-11 display enriched expression in germline stem cells, promoting stem cell maintenance and germline development, including dedifferentiation of primary spermatocytes and facilitating the sperm/oocyte switch [Ariz and Subramaniam, 2009]. PUF-5/6/7, on the other hand, control oocyte formation [Hubstenberger et al., 2012]. Given that each subfamily recognizes and regulates distinct sets of mRNAs, unravelling the precise functions of these proteins will enhance our understanding of their roles within complex developmental processes.

Despite considerable progress in comprehending PUF proteins, knowledge gaps endure, particularly concerning PUF-9. Although a study has unveiled its role in controlling epidermal stem cell differentiation in the soma [Nolde et al., 2007], the specific functions of PUF-9 in germline or developmental processes remain elusive. Extensive investigations are warranted to fully uncover the multifaceted functions of PUF-9 and its significance across various biological contexts.

The main objective of the study was to thoroughly analyse PUF-9's role in *C. elegans* development in order to identify its common roles with XRN-2. In order to ascertain the localization of the PUF-9 protein in *C. elegans*, GFP label was initially inserted into the *puf-9* gene using CRISPR/Cas9 in worms (GFP-PUF-9) (PHX2148) which was commercially obtained from SunyBiotech (Fujian, China). These worms were compared to wild-type worms, and their development was inspected, using a stereomicroscope, to ensure that the GFP tagging had no effect on the PUF-9 protein's functionality (Figure 16A). As anticipated, no developmental changes were observed even under *xrn-2* RNAi conditions, indicating that the localization of PUF-9 could be determined using this strain. The worms were incubated at 20 °C, and observed through fluorescent microscopy. Intriguingly, PUF-9's expression was observed in the proximal region of the gonad (Figure 16B), suggesting the potential role of PUF-9 in germline development. Additionally, PUF-9 exhibited widespread expression in various tissues, including the hypodermis, intestine, and pharynx (Figure 16B). The pattern of *puf-9* expression during development, was analysed based on data obtained from a study conducted by Meeuse et al., [2020]. The derived graph strongly indicates continuous PUF-9 expression throughout the entire developmental process (Figure 16C).

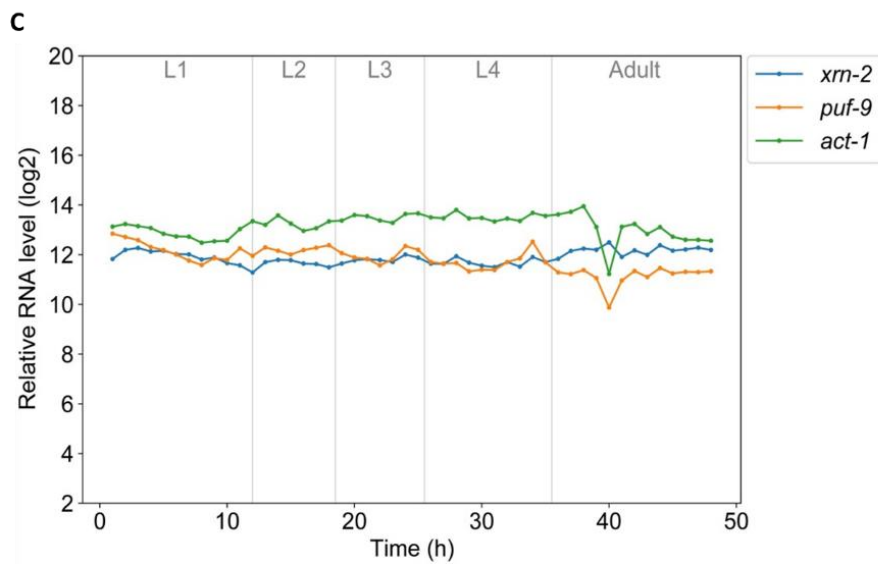
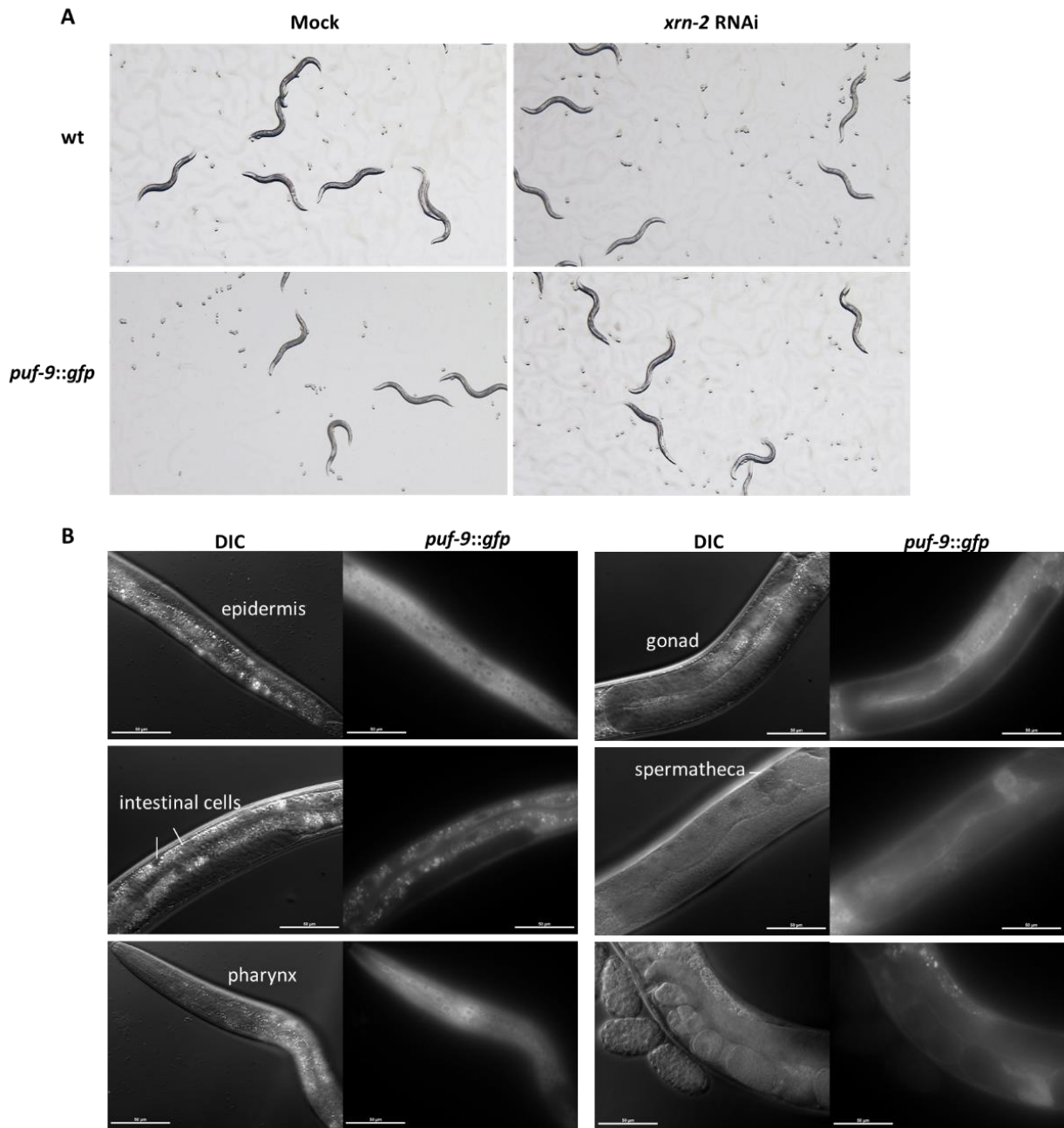


**Figure 16: PUF-9 is expressed in several tissues throughout *C. elegans* development.** (A) *puf-9::gfp* worms were examined using stereomicroscopy, and their developmental changes were compared with wild-type worms under both mock and *xrn-2* RNAi conditions at 20 °C. No significant developmental changes were observed. (B) Detection of the PUF-9 protein was achieved through fluorescent microscopy, unveiling its localization within the proximal region of the gonad, hypodermis, intestine, and pharynx. Corresponding DIC images are included on the right for reference. (C) The graph displays relative RNA levels on the y-axis, correlated with the developmental stages of the worms on the x-axis. Comparative analysis includes *puf-9* RNA levels alongside *xrn-2* and *act-1*. The graph underscores the consistent expression of *puf-9* throughout distinct developmental stages [Meeuse et al., 2020].

### 1.2.3 A *puf-9* mutation leads to developmental delay and vulval bursting

To comprehensively understand the developmental role of PUF-9, an investigation was undertaken, involving the utilization of *puf-9* null mutant animals (ok1136). A comparative analysis was carried out, aligning their phenotypes with wild-type worms. The findings, consistent with the research conducted by Nolde et al., [2007], furnished compelling evidence for the critical engagement of PUF-9 in development. Notably, at 25 °C, an approximate 12-hour developmental delay was observed in *puf-9* mutant animals in comparison to the wild-type (Figure 17A). This delay was observed across multiple developmental stages spanning from L1 to L4, thereby suggesting that PUF-9 plays a pivotal role in the regulation of diverse developmental processes.

Furthermore, a distinct and prominent phenotype termed "vulval bursting" was also demonstrated by the *puf-9* null mutant animals, in line with Nolde et al.'s research [2007], accounting for nearly 25% of occurrences (Figure 17B). Characterized by an explosive breach through the vulva, this phenotype led to the death of the animals. The presence of vulval bursting within the *puf-9* mutants further accentuated the significance of *puf-9* in ensuring proper developmental signalling and the maintenance of tissue integrity.

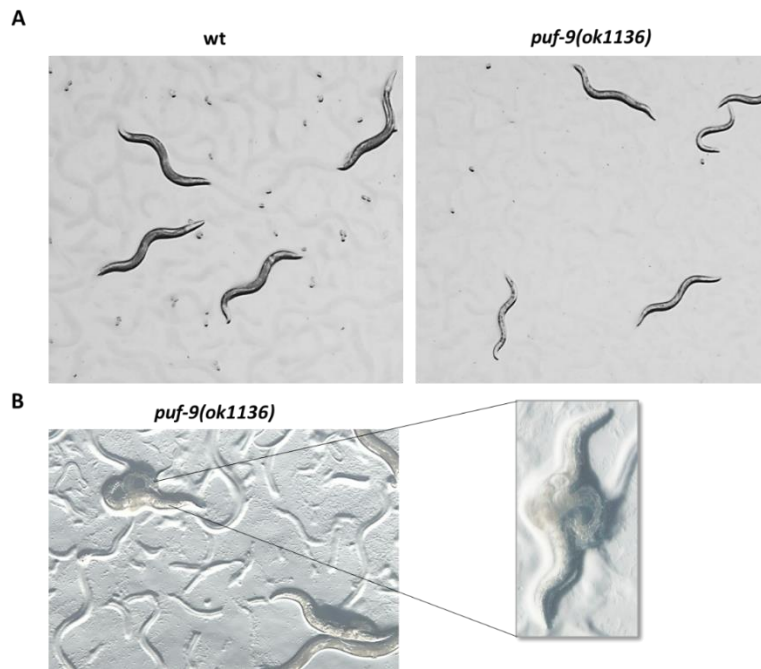


**Figure 17: *puf-9* mutation causes developmental delay and striking phenotype in worms.** (A) Comparison of developmental changes observed through stereomicroscopy between wild-type animals (left) and *puf-9* mutant animals (right). The *puf-9* mutants display an approximate 12-hour developmental delay, at 25 °C. (B) Characterization of *puf-9* mutants reveals distinctive phenotypes, including a sluggish behaviour and the occurrence of vulval bursting.

#### 1.2.4 *puf-9* mutant worms showed brood size reduction and germline deficiencies

In the study focusing on the nematode *C. elegans*, brood size represents the number of offspring generated by a hermaphroditic adult worm throughout its reproductive lifespan [Hodgkin, and Barnes,1991]. The principal aim of this study was to analyse prospective variations in offspring quantity among organisms exhibiting mutations in the *puf-9* gene, based on the empirical observations of nematodes. To accomplish this, two distinct strains of *puf-9* null alleles, *puf-9(ok1136)* and *puf-9(tm1520)*, were used. To minimize confounding factors stemming from additional mutations, the mutant strains were subjected to three consecutive rounds of backcrossing before commencing the experimental analysis. Remarkably, both strains of *puf-9* mutant animals exhibited approximately 50% reduction of brood size compared to wild-type animals, at 25 °C, (Figure 18A). Moreover, during the comprehensive investigation, meticulous observations of the nematodes' germline were conducted, revealing notable deficiencies in oocyte development such as abnormal enlargement of oocytes

formations, impaired migration of the gonads, and a consequential occurrence of sterility (approximately 20%) in certain individuals within the worm population (Figure 18B). This intriguing finding suggests a crucial role for the *puf-9* gene in germline development. Notably, previous research has exclusively explored the somatic function of *puf-9*, making this study a pioneering contribution towards elucidating the germline function of this gene. Building upon the existing knowledge of *puf-9*'s somatic function, these novel findings serve as a foundation for further exploration into the intricate processes underlying its involvement in germline function.

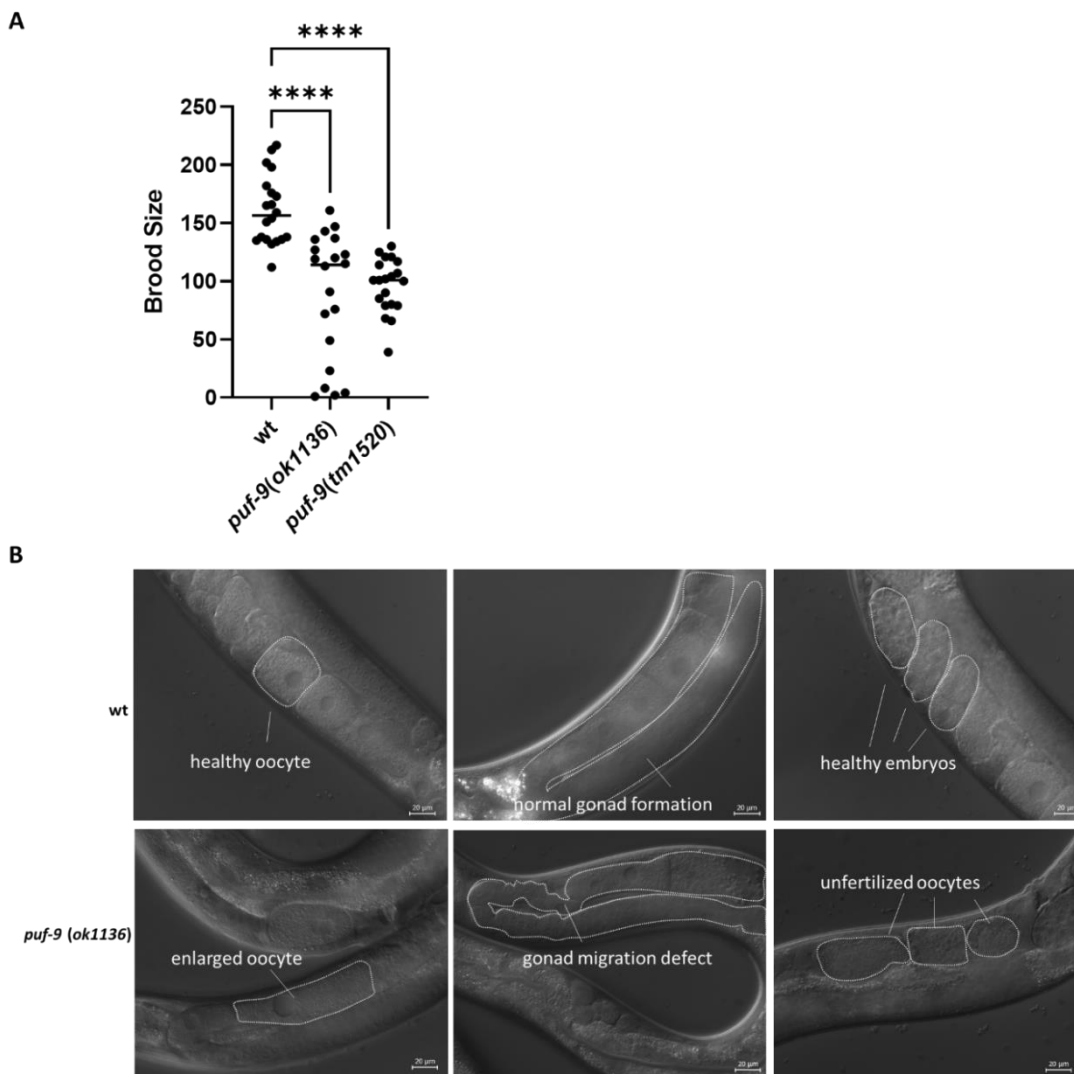


**Figure 18: *puf-9* mutation causes reduction of brood size and abnormal germline development in *C. elegans*.** (A) Both *puf-9* mutant strains exhibited a significant reduction in brood size, at 25 °C, when

compared to the control group. Statistical analysis was performed using one-way ANOVA, with each dot (.) representing an individual worm (n=20), and the line (-) indicating the average number of brood size. Significance levels are denoted by asterisks, \*\*\*\*p< 0.0001. (B) Comparison between wild-type and *puf-9* mutant germlines. *puf-9* worms exhibit enlarged oocyte formations, compromised gonad migration, and subsequent sterility in specific individuals within the worm population.

### **1.2.5 *puf-3* and *puf-8* were identified as synthetic lethality partners of *puf-9***

With the observation of numerous germline defects in *puf-9* mutant animals, an investigation was undertaken to uncover the primary functions of *puf-9* in germline development. The focus was on identifying potential partners for synthetic lethality with *puf-9*. To achieve this, a small-scale RNAi screening was conducted, at 25 °C, using *puf-9* mutant animals, where wild-type animals served as control. This relatively high temperature was chosen to accelerate *C. elegans* germ cell development, rendering processes with redundant factors more susceptible to the impact of individual factor loss, as established in prior studies [Subramaniam and Seydoux 2003; Ariz and Subramaniam, 2009]. The screening was focused on candidate genes with recognized roles in *C. elegans* germline development, encompassing members of the PUF family (*puf-3*, *puf-5*, *puf-6*, *puf-7*, *puf-8*) and other germline protein families, such as *oma-1*, *oma-2* (involved in oocyte maturation, vital for mature egg development in *C. elegans*) and *gld-1* (key factor in germline development and sex determination in *C. elegans*, regulating the development of sperm and egg cells). The outcome of this RNAi screening revealed two candidate genes, namely *puf-3* and *puf-8*, exhibiting a potential synthetic lethal interaction with *puf-9*. Notably, knockdown of either *puf-3* or *puf-8* within *puf-9* mutant organisms yielded significant developmental anomalies in the germline, as compared to the effects observed in wild-type animals (Figure 19A).

In this investigation, in wild-type worms under *puf-3* RNAi conditions, at 25 °C, DIC imaging unveiled anomalies in oocyte formation, including oocytes featuring two nuclei and less cytoplasm. Importantly, these anomalies did not impair embryo viability or strain maintenance. However, these abnormalities were markedly severer in *puf-9* mutant animals, resulting in highly diminutive and disorganized oocytes. This, in turn, led to embryonic lethality or compromised egg hatching. Contrastingly, wild-type animals did not exhibit such aberrant outcomes. Likewise, *puf-8* RNAi induced fertility-related defects in wild-type animals due to its substantial roles in germline maintenance. However, in *puf-9* mutant animals, *puf-8* RNAi

yielded considerably more pronounced phenotypes, profoundly impacting germ cell formation and culminating in sterility (Figure 19B).

To facilitate a comprehensive investigation, a comparative analysis was conducted, at 25 °C, encompassing various genetic conditions, including control conditions, *puf-3* RNAi, and *puf-8* RNAi, in both *puf-9* mutant and wild-type *C. elegans*. The primary endpoint of this analysis was the quantification of hatched embryos across all experimental conditions. This systematic approach aimed to provide a holistic understanding of the distinct effects of each condition on embryonic development, shedding light on the intricate interplay among these genetic factors within the context of germline development. The specific manipulation of *puf-3* through RNAi yielded intriguing findings. Notably, *puf-3* RNAi resulted in complete embryonic lethality, with a striking 100% incidence observed exclusively in *puf-9* mutant worms (Figure 19C), while wild-type worms displayed normal embryonic development under the same conditions. This outcome underscores a pivotal interaction between *puf-9* and *puf-3* in the intricate web of genetic determinants governing germline development. Furthermore, this interaction was accentuated by their shared roles in oogenesis, as corroborated by data obtained through DIC imaging (Figure 19C).

Embryonic lethality is a multifaceted phenomenon rooted in a myriad of factors that can compromise germline development. Errors during meiosis or mitosis within the germline can culminate in chromosomal abnormalities within the developing embryo. These aberrations, in turn, can trigger profound disruptions in the typical course of development, ultimately leading to embryonic lethality. Additionally, deviations from the normal meiotic process can significantly contribute to embryonic lethality. Meiosis, responsible for the division of germline cells to produce oocytes and sperm, is particularly susceptible to errors. Nondisjunction and improper chromosome segregation during meiosis can result in the formation of nonviable embryos.

Our in-depth investigation leads to the proposition that *puf-3* may represent a putative synthetic lethality partner of *puf-9*, implying that the absence of both genes synergistically induces embryonic lethality. This discovery opens an avenue for further exploration into the intricacies of germline development, offering insights into the potential cooperative mechanisms underlying the genetic regulation of this critical biological process.

In addition to primary investigation, complementary study was conducted to assess the impact of *puf-8* knockdown on brood size. PUF-8's critical role in oogenesis is well-documented, and prior research has illustrated that *puf-8* mutation diminishes brood size (Xu et al., 2021). Notably, RNAi-induced knockdown differs from null mutations in terms of effects. RNAi acts post-transcriptionally via small RNA molecules, leading to relatively rapid effects. In contrast, null mutations bring about more profound and enduring gene function changes by altering genes at the DNA level before transcription. RNAi induces partial effects, whereas null mutations induce substantial disruptions. Interestingly, when *puf-9* mutant worms were subjected to *puf-8* RNAi, a considerable fraction of these worms displayed a severe phenotype, leading to nearly 80% sterility, while the remaining 20% exhibited extremely low brood sizes, typically ranging between 5 and 20 progeny per worm (Figure C,D). This finding suggests a potential partnership of synthetic lethality between *puf-8* and *puf-9*, particularly in the context of oogenesis.

These outcomes highlight the intricate interplay among genetic factors, specifically *puf-3*, *puf-8*, and *puf-9*, in regulating germline development, with a particular emphasis on their roles in oogenesis..

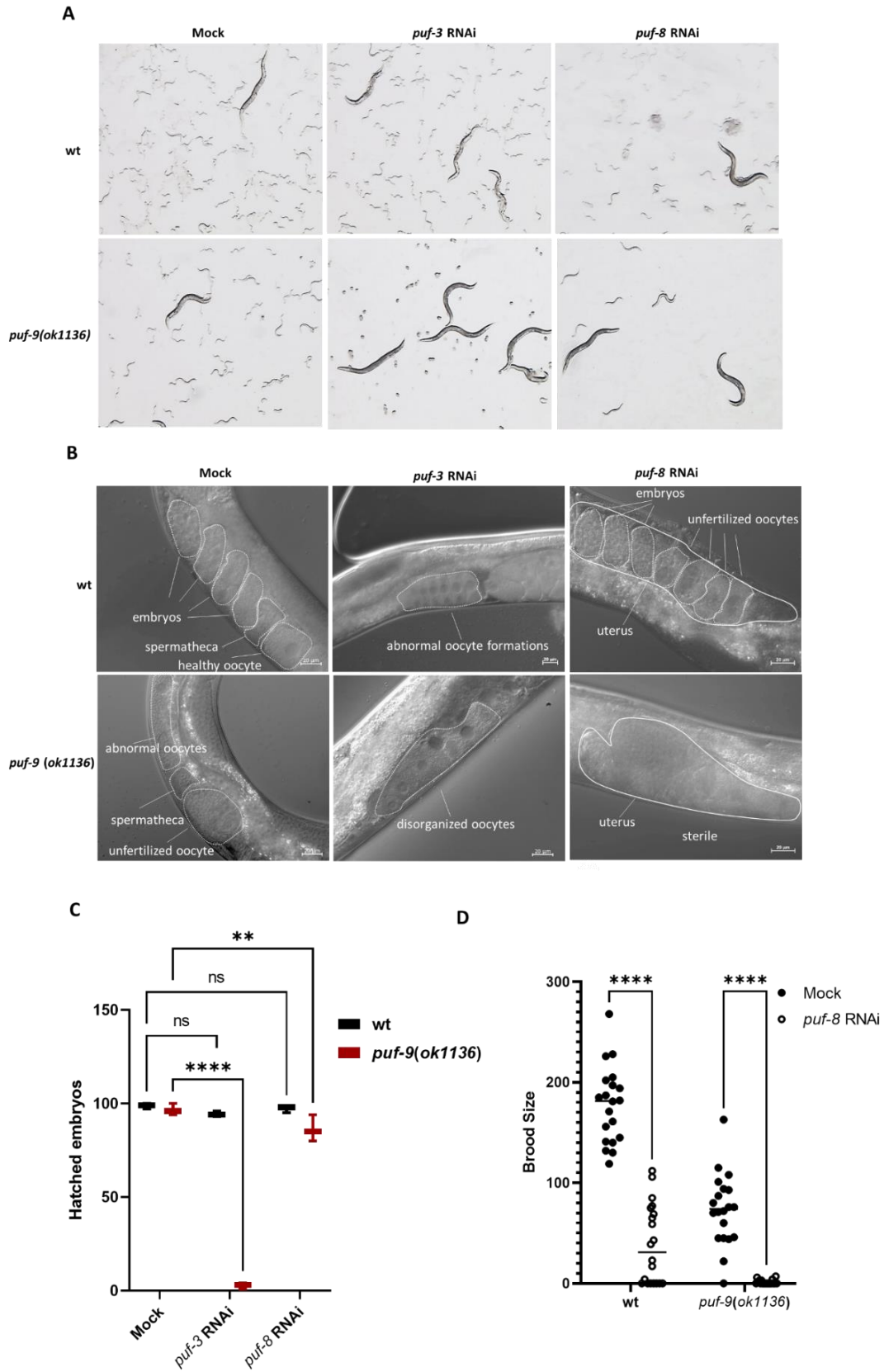


**Figure 19: Genetic interactions of *puf-9* with *puf-3* and *puf-8* in germline development.** (A) Stereomicroscopic examination was conducted on *puf-9* mutant worms (*ok1136*), and their

developmental changes were juxtaposed with those of wild-type worms under conditions involving mock, *puf-3*, and *puf-8* RNAi. In *puf-9* mutant animals, the introduction of either *puf-3* or *puf-8* yielded severe defects in germline development, while wild-type worms exhibited comparatively milder defects. wt= wild-type (B) *puf-9(ok11360)* and wild-type worms were subjected to *puf-3* and *puf-8* RNAi treatments. A discerning analysis revealed that *puf-9* mutant animals displayed substantial defects in oocyte formation compared to wild-type animals. These defects led to outcomes of embryonic lethality and sterility. (C) An embryonic lethality assay was executed, wherein *puf-9* mutant animals were juxtaposed with their wild-type counterparts under conditions involving mock, *puf-3*, and *puf-8* RNAi. Particularly noteworthy, *puf-3* RNAi within *puf-9* mutants culminated in absolute embryonic lethality. The data underwent rigorous analysis via two-way ANOVA, and the significance levels are indicated by asterisks (\*\*p < 0.01, \*\*\*\* p<0.0001). ns=statistically non-significant. (n=100). (D) As part of a complementary study, the effects of *puf-8* RNAi on brood size were meticulously examined. A profound phenotype was observed when *puf-9(ok11360)* worms were subjected to *puf-8* RNAi, 80% of worms exhibiting sterility. The data were meticulously analysed using two-way ANOVA, with significance levels indicated by asterisks (\*\*\*\* p<0.0001) (n=20).

### 1.2.6 *puf-9* and *xrn-2* share same or parallel functions in germline development

Substantial insights into the putative functions of *puf-9* in germline development, particularly in oogenesis, were gained, leading to an investigation into whether common or parallel functions are shared between *puf-9* and *xrn-2* in this vital process. To address potential limitations associated with the partial depletion of target proteins through RNAi, the impact of complete gene deletion was explored by performing a genetic cross between two distinct strains: *puf-9(ok11360)*, representing a null mutation, and *xrn-2ts (puf-9(ok1136); xrn-2ts)*. The primary objective of this study was to acquire valuable insights into the consequences associated with the total removal of the *puf-9* gene.

A brood size assay was employed for each single mutant (*puf-9(ok1136)* and *xrn-2ts*), as well as the double mutant at 20 °C (Figure 20). The results obtained from this multifaceted investigation revealed a significant decrease in brood size in the double mutant compared to both single mutants. The double mutant exhibited a 2.7-fold decrease in brood size compared to *xrn-2ts* and an almost 1.5-fold decrease compared to the *puf-9* single mutant. This intriguing finding suggests that both *puf-9* and *xrn-2* play roles in germline development. The pronounced

reduction in brood size in the double mutant underscores the potential functional interdependence between these two genes in governing the reproductive capacity of *C. elegans*.

This investigation has not only highlighted the consequences of completely removing of *puf-9* gene but has also unveiled potential functional interactions between *puf-9* and *xrn-2* in germline development, specifically in the realms of oogenesis and the regulation of reproductive capacity. The substantial reduction in brood size observed in the double mutant underscores their potential functional interdependence in governing critical aspects of germline development, underscoring the pivotal roles of these genes in orchestrating essential reproductive processes in *C. elegans*.

Similar roles for these two genes in the reproductive processes of *C. elegans* have been evidenced, adding depth to our understanding of the intricate regulatory mechanisms governing protein expression and the coordination of reproductive events. Our current knowledge of the complex and finely tuned protein regulation mechanisms underlying germline development and reproductive processes in the model organism *C. elegans* is significantly contributed to by these noteworthy findings. Exciting avenues for further investigations into their molecular pathways and potential shared targets are provided by the potentially functional interactions between *puf-9* and *xrn-2*. Considerable promise is held for not only advancing our understanding of fundamental developmental biology but also for potential applications in broader contexts, including the exploration of conserved mechanisms in other organisms, including humans. The significance of these findings in the broader landscape of developmental biology is underscored by the importance of continued research efforts to unravel the intricate molecular networks governing essential biological processes.

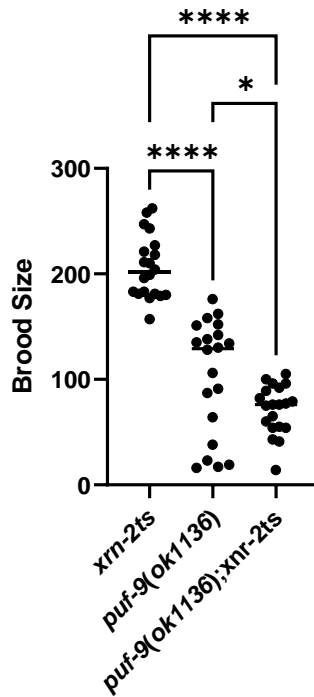


**Figure 20: Investigating the shared functions of *puf-9* and *xrn-2* in germline development through brood size analysis.** Brood size analysis conducted for each single mutant (*puf-9(ok1136)* and *xrn-2ts*) and the double mutant (*puf-9;xrn-2*) at 20 °C. Significant decrease in brood size in the double mutant compared to both single mutants at the permissive temperature. Statistical analysis was performed using one-way ANOVA, and significance levels are denoted by asterisks ( \* $p < 0.05$ , \*\*\*\* $p < 0.0001$ ).

## 2. Mechanisms of mRNA degradation by XRN-2

The remarkable capacity of XRN-2 to regulate multiple RNAs through degradation and trimming mechanisms has given rise to an intriguing scientific inquiry. Within this investigation, efforts were being made to identify the specific mRNA targets that are subject to the regulatory influence of XRN-2. Particular attention was being directed towards uncovering the intricate details of the RNA degradation mechanisms employed by XRN-2. The ongoing exploration was driven by a quest to reveal the molecular underpinnings of XRN-2's versatile RNA-modulating activities. This comprehensive investigation aimed to provide valuable insights into the complex networks that govern cellular RNA dynamics. Such insights, once attained, have the potential to advance our understanding of fundamental cellular processes, with implications spanning various fields, from molecular biology to potential applications in therapeutics.

## 2.1 XRN-2 ensures the integrity of gene expression by transcription termination

The comprehensive time-course RNA expression analysis using RNA-sequencing (RNA-seq) on the *xrn-2ts* mutant, conducted by dr. habil. Takashi Miki, aimed to investigate the effects of *xrn-2* inactivation [Miki et al., 2016]. Inactivation of *xrn-2* was induced at the onset of the fourth larval stage (0 h) by subjecting *xrn-2ts* animals to a temperature shift, and the observation of RNA expression occurred every hour until young adulthood (10 h) via poly(A)-RNA-seq. In order to assess the impact of *xrn-2* inactivation on gene expression, a comparison was made between *xrn-2* and wild-type animals (Figure 21A). The distinct sets of upregulated RNAs were discerned in response to *xrn-2* inactivation (Figure 21B). Upon closer scrutiny, it was noted that the majority of upregulated genes appeared to be influenced by transcription read-through events originating from their upstream genes. This phenomenon stems from *xrn-2* functional inactivation, enabling RNAPII to persist in gene transcription, resulting in increased downstream gene expression. Furthermore, the inactivation of *xrn-2* resulted in the identification of discrete subsets of downregulated RNAs, a consequence of the collisions between RNAPII molecules (Figure 21C). Inactivation of *xrn-2* leads to the prolonged presence of RNAPII during gene transcription, thereby promoting the occurrence of collisions between RNAPII molecules, particularly when the involved genes exhibit divergent transcriptional orientations. This collision phenomenon subsequently culminates in the downregulation of gene expression due to the interference caused by RNAPII collisions.

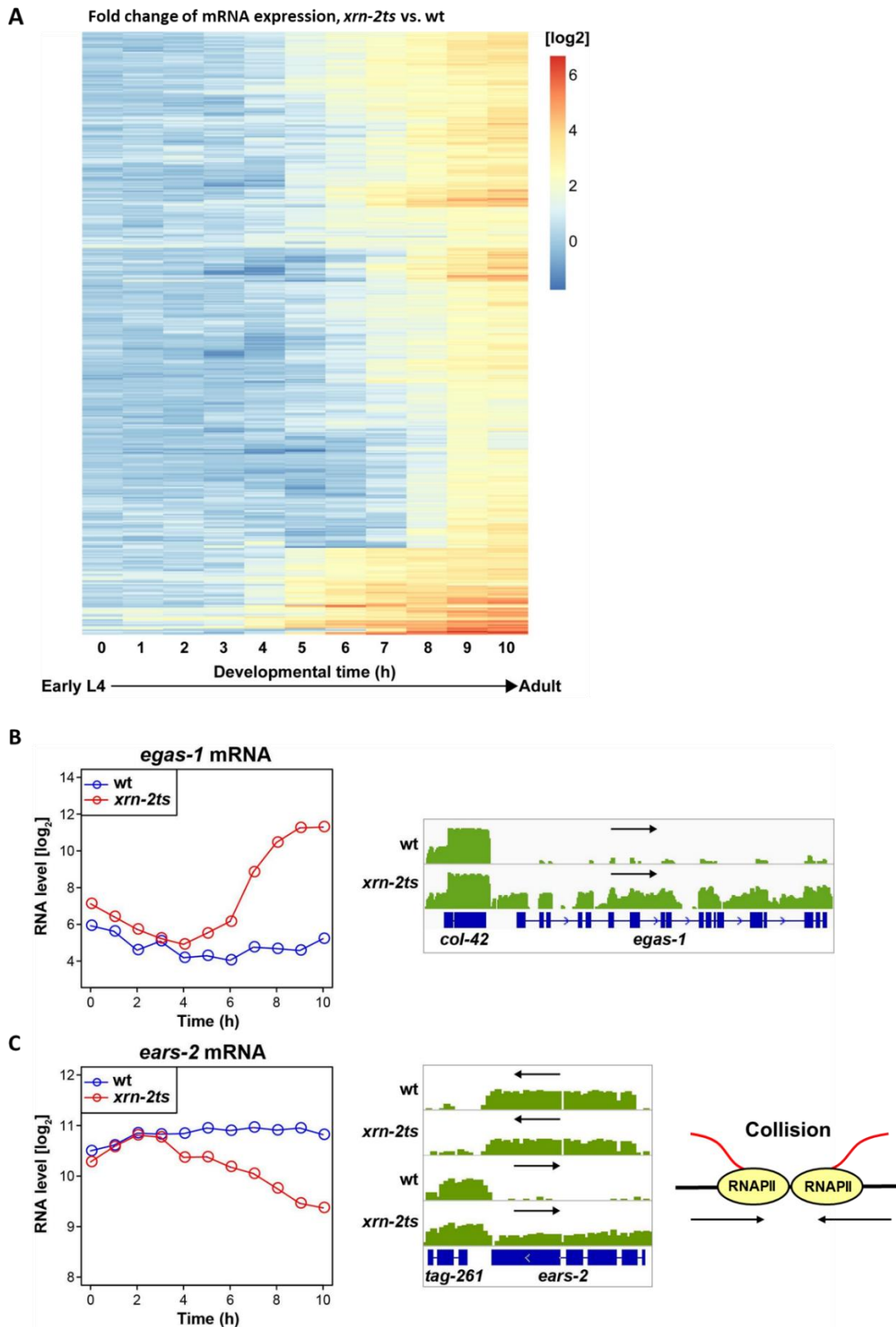


**Figure 21: mRNA expression changes and transcriptional effects in *xrn-2ts* mutant *C. elegans*.** (A) Heatmap displaying logarithmic alterations in mRNA expression across *C. elegans* development, contrasting *xrn-2ts* mutant worms with the wild-type counterparts. (B) Exemplary illustration of gene

mRNA level data, accompanied by corroborative snapshot data that elucidates the accumulation of polyadenylation signals (PAS) under *xrn-2* knockdown conditions. This phenomenon leads to transcriptional read-through from upstream genes. (C) Representative depiction of gene mRNA level data, bolstered by snapshot data that underscores gene downregulation resulting from collisions among RNAPII complexes [Miki et al., 2016].

## **2.2 XRN-2 repressed expression of *ceh-99* by causing premature transcription termination of RNAPII**

Upon an in-depth examination of the analysed *xrn-2ts* RNA sequencing data, a significant discovery was made concerning a gene denoted as *ceh-99*. Interestingly, following *xrn-2* inactivation, an increase in *ceh-99* expression was observed (Figure 22A), although this increase could not be attributed to transcription read-through from its upstream genes. This intriguing observation sparked interest, prompting the selection of *ceh-99* as a prime candidate for unravelling the mechanisms underlying XRN-2-mediated regulation. In terms of its genetic features, *ceh-99* is a putative homeobox gene, characterized by the presence of four homeodomains. Due to its proximity to *ceh-100* on chromosome II, it is plausible that *ceh-99* might have emerged as a recent paralog [Reilly et al., 2020]. Considering the established role of homeodomain proteins as transcription factors, specifically their capacity to bind to DNA, the putative characterization of *ceh-99* as a homeobox gene amplifies its significance in the context of regulation by XRN-2. After identifying *ceh-99* as a candidate gene, it underwent a thorough examination, uncovering the presence of a single TC1 insertion within the first intron. This finding underscores the significance of investigating the regulatory interplay between XRN-2 and TC1 through the *ceh-99* gene.

To evaluate *ceh-99* expression levels, in *xrn-2* knockdown condition, quantitative RT-qPCR was employed for quantifying its relative mRNA levels. Consistent with the outcomes from RNA-seq data, under *xrn-2* RNAi, at 20 °C, *ceh-99* expression also exhibited upregulation (~25 fold), supporting the result of RNA-seq (Figure 22B). To elucidate the regulatory mechanisms governing *ceh-99* expression by XRN-2, a thorough analysis of RNAPII chromatin immunoprecipitation sequencing (ChIP-seq) data, as previously generated by dr. habil. Takashi Miki [Miki et al., 2017] (Figure 22C), was conducted. This exploration allowed for formulating of novel insights and hypotheses concerning the interplay between *ceh-99* and XRN-2

This result brought to light compelling evidence indicating that XRN-2 functions as a repressor of *ceh-99* expression by facilitating premature transcription termination of RNAPII. Specifically, under *xrn-2* RNAi conditions, at 20 °C, a significant accumulation of RNAPII originating from the second exon of *ceh-99* was observed, in contrast to the absence of RNAPII accumulation in normal conditions from the second exon of the gene. This revelation provides critical insights into the intricate regulation of *ceh-99* expression by XRN-2, wherein premature termination of RNAPII plays a central role in suppressing *ceh-99* expression under normal physiological conditions. These novel findings establish the foundation for subsequent investigations into the precise molecular interplay between XRN-2 and *ceh-99*, unveiling the underlying regulatory networks and signalling pathways governing gene expression.

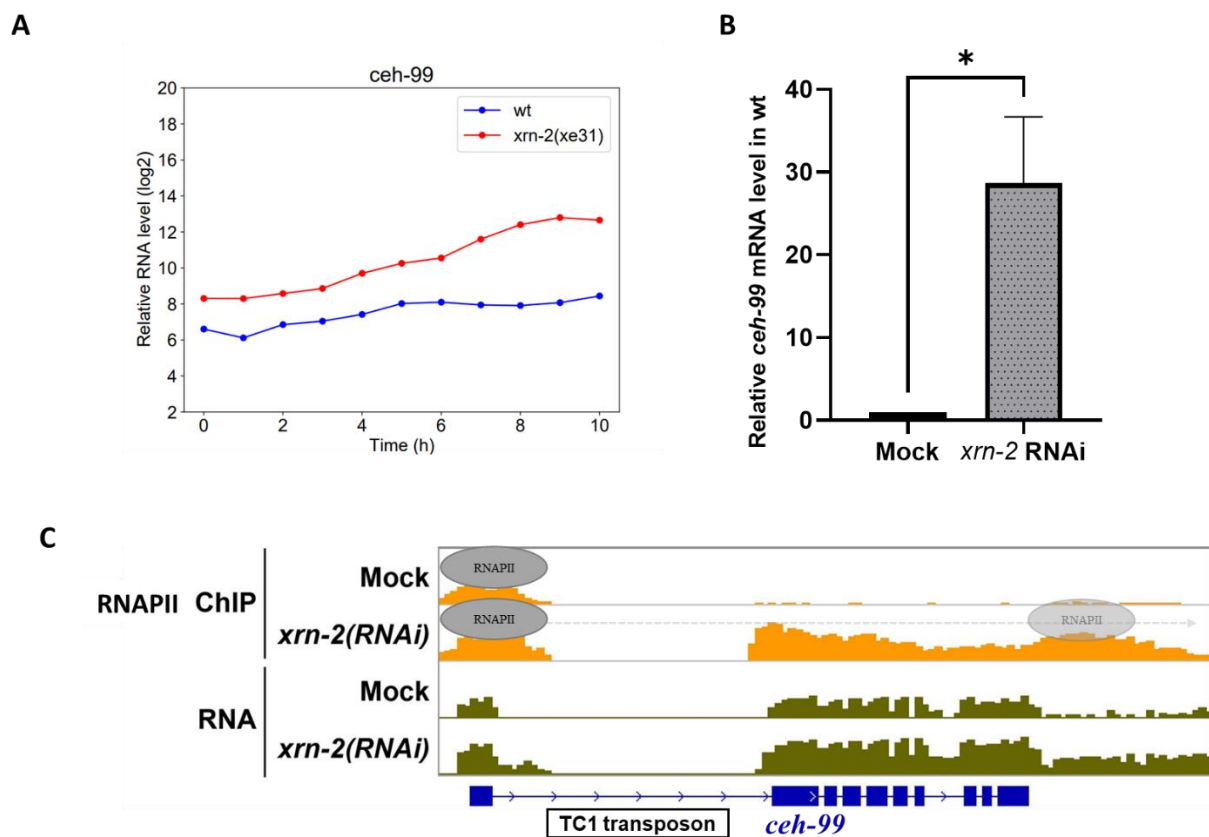


**Figure 22: XRN-2 mediates transcriptional repression of *ceh-99* through premature transcription termination of RNAPII.** (A) mRNA sequencing data graph illustrating the upregulation of *ceh-99* following *xrn-2* inactivation. The blue line represents the mRNA expression level of wild-type *ceh-99*, while the red line represents the *ceh-99* mRNA level in the context of *xrn-2* inactivation. (B) qPCR analysis demonstrates that *xrn-2* knockdown, at 20 °C, significantly increases the expression level of

*ceh-99*. The statistical analysis was performed using an unpaired t-test, and asterisks denote the level of significance (\* $p < 0.05$ ). (C) RNAPII chromatin immunoprecipitation sequencing (ChIP-seq) analysis and *ceh-99* RNA-seq snapshot data representation. In wild-type conditions, the RNAPII signal diminishes after the first intron of the *ceh-99* gene. In the context of *xrn-2* inactivation, the RNAPII signal persists throughout the *ceh-99* gene. This observation aligns with the RNA-seq snapshot data of *ceh-99*, illustrating an elevated RNA expression level under *xrn-2* inactivation conditions. The absence of an RNA signal in the TC1 insertion region is due to the multiple copies of TC1 in *C. elegans*, making mapping impossible [Miki et al., 2017].

### **2.3 Upstream region of *ceh-99* is responsible for regulation by XRN-2**

To elucidate the mechanisms underlying the recognition of *ceh-99* by XRN-2, the role of *ceh-99* gene's upstream region in this regulatory process was examined. For this purpose, a commercially available *mir-77* (n4286) strain, recognized for a substantial deletion in the upstream and promoter regions of *ceh-99*, was utilized (Figure 23A). Taking advantage of this mutant strain, RNAi was employed, at 20 °C, to knock down *xrn-2*, and a thorough comparison was conducted with the wild-type strain under identical conditions. Despite the considerable deletion within the promoter region of *ceh-99* in the mutant strain, *ceh-99* mRNA levels remained virtually unchanged, compared to those in the wild-type strain, under normal conditions. This finding strongly suggests that the remaining portion of the promoter region likely contains critical promoter elements that are essential for maintaining *ceh-99* expression levels. Notably, upon *xrn-2* inactivation, *ceh-99* mRNA expression levels were increased by approximately 25-fold in the wild-type strain (Figure 23B). On the other hand, in the mutant strain with the deleted upstream region, this regulatory effect was entirely abolished, unequivocally confirming the requirement of the upstream region for XRN-2-mediated regulation of *ceh-99*. The findings unequivocally demonstrated that the upstream region of *ceh-99* plays a pivotal role in its regulation by XRN-2.

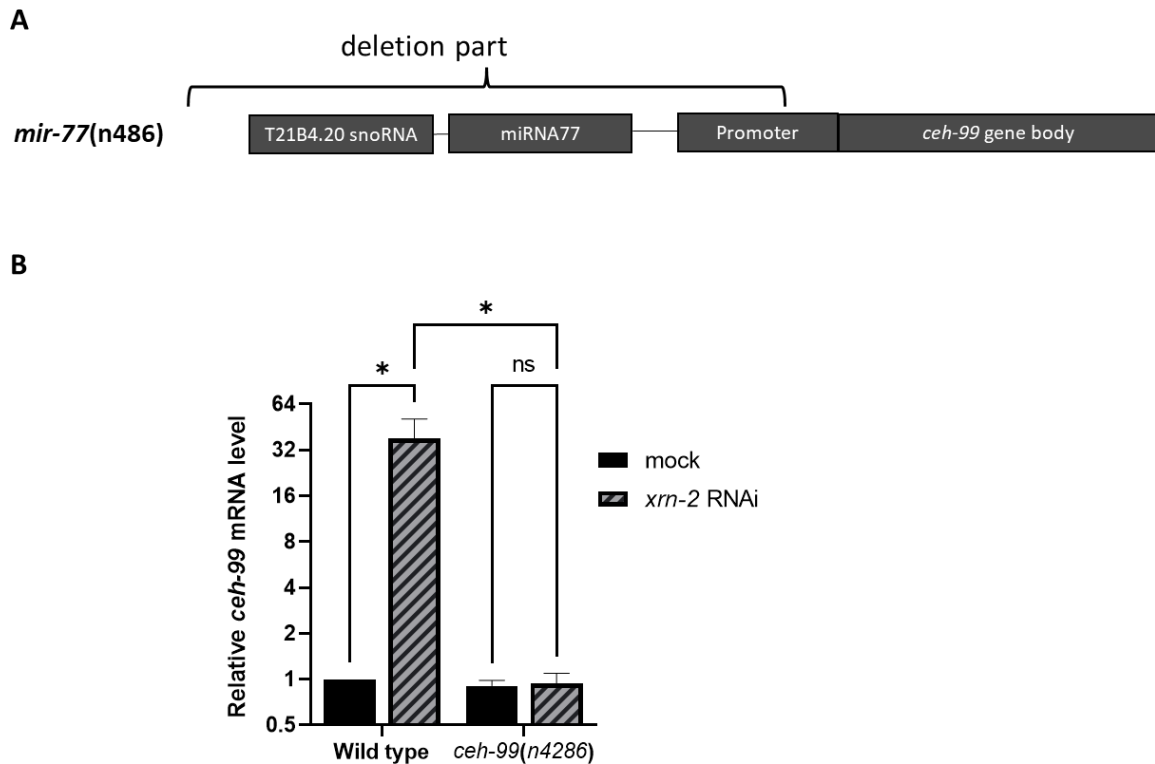


**Figure 23: *ceh-99* upstream region has crucial role for *xrn-2* mediated regulation.** (A) Schematic representation of the *mir77* (n4286) strain illustrating a large deletion in the upstream region of *ceh-99*. (B) RNAi was performed, at 20 °C, using a commercially available strain with substantial deletions in the upstream and promoter regions of *ceh-99* (n4286). The effects of XRN-2 knockdown were compared between the wild-type strain and the mutant strain. Knockdown of *xrn-2* led to a significant increase in *ceh-99* mRNA expression levels (~25-fold) in the wild-type strain. However, in the mutant strain with the deleted upstream region, this regulatory effect was completely abolished. Despite the substantial deletion in the promoter region of *ceh-99* in the mutant strain, *ceh-99* mRNA levels remained unchanged compared to the wild-type strain under normal conditions. Statistical analysis was conducted using the two-way ANOVA method, and significance is denoted by asterisks (\* $p < 0.05$ ).

#### 2.4 The crucial elements for XRN-2-mediated regulation are identified within the *ceh-99* promoter region

To provide insights into the critical region of *ceh-99* responsible for XRN-2-mediated regulation, the MosSCI [Frøkjær-Jensen et al., 2008] technique was employed to generate several transgenic worm strains (Methods 3.1.3). Accordingly, six transgenic constructs were designed, each tagged with GFP, to assess their impact on gene expression. The transgenic

constructs consisted of different combinations of key elements, including snoRNA and miRNA sequences from the upstream region, and a TC1 insertion within the first intron, all of which were present in the *ceh-99* gene locus. The purpose of constructing elements that encompass the upstream region of the *ceh-99* gene was to ascertain whether the regulation of *ceh-99* by XRN-2 is influenced by transcription read-through from either TB21B4.10 snoRNA or miRNA77. The first construct was designed to harbour only the *ceh-99* promoter region, the second one included upstream elements (TB21B4.10 snoRNA and miRNA77) along with the promoter, the third one represented the full *ceh-99* gene construct encompassing the upstream elements, promoter, and gene body, while the fourth one shared the same construction as the normal gene, except for the absence of TC1 in the *ceh-99* body. The fifth one had promoter region and gene body with TC1 but not the upstream elements, and the last one had only the promoter and gene body without the TC1 region (Figure 21A). Their expression levels were evaluated by employing RT-qPCR to measure mRNA levels of each transgene. Initially, a comparison was made between the third and fifth transgenic strains, both containing identical gene constructs, but differing in the presence of the upstream region. Although the fifth strain lacked the upstream elements, *xrn-2* inactivation did not result in any observed indication of transcription read-through from the snoRNA or miRNA region. Moreover, in the fifth strain, the inactivation of *xrn-2* resulted in a significant increase in mRNA levels compared to the control condition, indicating the significance of the *ceh-99* promoter region in XRN-2 regulation (Figure 24B). Upon a comparative analysis of the other transgenic strains, no additional regulatory regions responsive to XRN-2 were identified.

Additionally, the total RNA expression levels of the snoRNA region, miRNA region, and the region between the promoter and miRNA region were examined. As expected, no significant increase in RNA expression from these regions was detected upon *xrn-2* inactivation (Figure 24C).

In conclusion, *ceh-99* expression was upregulated upon *xrn-2* inactivation, yet this effect was not due to transcription read-through from the upstream region. Instead, the crucial element for XRN-2 recognition and regulation appeared to reside within the *ceh-99* promoter region.

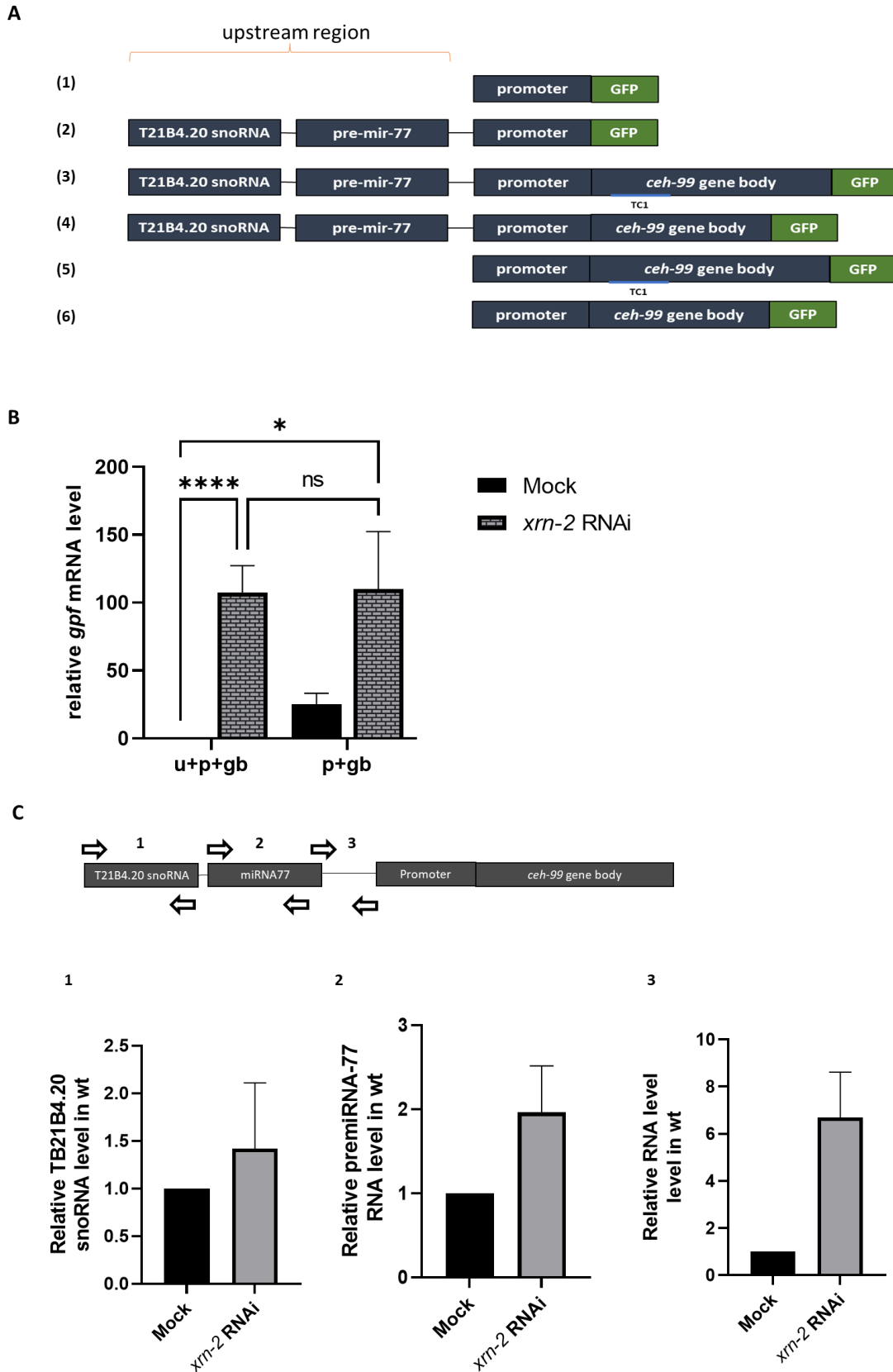


**Figure 24: XRN-2 regulates *ceh-99* through its promoter region.** (A) Schematic illustration of transgenic constructs employed for MosSCI insertion. (B) Comparative analysis between the third and

fifth transgenic strains under normal and *xrn-2* RNAi conditions, both harbouring gene constructs identical to the normal gene but differing in the presence of the upstream elements (u=upstream, p=promoter, gb=gene body). XRN-2 regulation remained consistent for both transgenes. *xrn-2* inactivation led to increased GFP expression in the fifth strain. The data analysed with two-way ANOVA. The asterisks indicate statistical significance (\* $p < 0.01$ , \*\*\*\* $p < 0.0001$ ) (C) Total RNA expression levels were assessed in the upstream elements; snoRNA region, miRNA region, and the region between the promoter and miRNA. Notably, no significant increase in RNA expression was detected from these regions upon XRN-2 inactivation. Analyses were conducted using an unpaired t-test.

## 2.5 Alternative transcription start sites have been identified in the *ceh-99* gene

In the WormBase database [WormBase : Nematode Information Resource, n.d.], a putative transcription start site (TSS) for *ceh-99* is annotated (TSS1). Nevertheless, other study [Saito et al., 2013] on *C. elegans* TSS, identified another major TSS (ATCATTTTCGT---) (TSS2), differing from the annotated TSS in WormBase (TTTGTGTCGA---). Consequently, two potential *ceh-99* transcripts arise, with one 23 base pairs longer than the other. Crucially, it is essential to highlight that TSS2 is situated downstream of a substantial genomic deletion within the *mir-77*(n2486) strain, while TSS1 is found within this deleted region. This deletion has unveiled a pivotal regulatory area that is governed by XRN2, signifying that TSS1, and not TSS2, is subject to regulation by XRN-2 (Figure 25A).

A significant structural difference between the transcripts of TSS1 and TSS2 was detected through structural RNA analysis conducted using the RNAfold web server [RNAfold Web Server, n.d.]. Specifically, TSS1 was found to produce an extended stem-loop structure (Figure 25D), whereas TSS2 did not exhibit this structural motif. Stem-loops are widely acknowledged as influential regulatory elements that exert a significant influence on gene expression. These structural motifs emerge through the intramolecular folding of single-stranded RNA or DNA, leading to the formation of stable hairpin-like structures, wherein a segment of the sequence pairs with its complementary region. Stem-loops, frequently identified in the untranslated regions (UTRs) of mRNA molecules and upstream regions of genes, significantly impact gene expression through interactions with nucleases, including XRN-2. It is noteworthy that nucleases exhibit a preference for double-stranded regions within stem-loops, resulting in the precise cleavage of RNA molecules [Dehé and Gaillard, 2017]. The

outcome of endonuclease-mediated cleavage is contingent on the location and sequence of the stem-loop. For instance, when a stem-loop is positioned within an mRNA molecule, endonuclease cleavage may lead to transcript degradation, ultimately reducing gene expression.

These findings suggest a plausible scenario where XRN-2 predominantly degrades transcripts that originate from TSS1 underscoring its preferential regulation of the isoform with an extended 5' UTR. In other words, only the longer transcript contains a stem-loop structure, which might serve as a target for XRN2-mediated degradation.

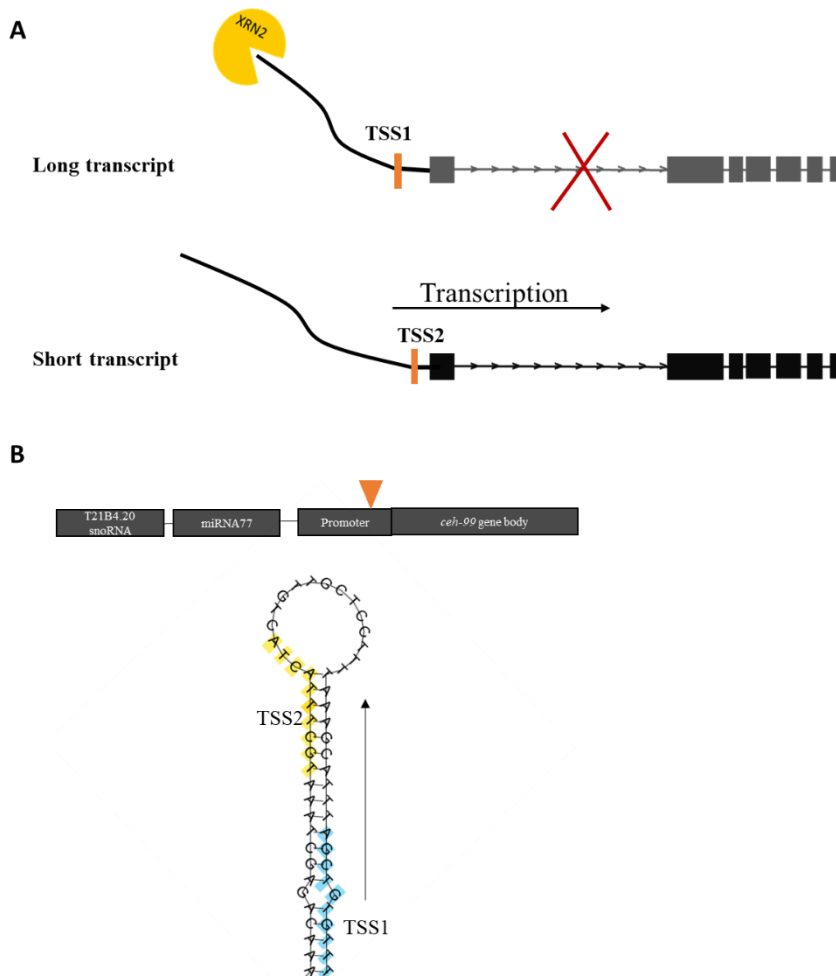


**Figure 25: Alternative TSS of *ceH-99* identified.** (A) Schematic representation of the two transcription start sites identified in the *ceH-99* gene. (B) Possible stem-loop structure at the promoter region of the *ceH-99* gene using MFE (Minimum Free Energy) analysis. The analysis was conducted at the optimal temperature of *C. elegans* (25 °C). Blue colour indicates the region of TSS1, yellow colour indicates the region of TSS2. RNA modelling was performed based on the Turner model, 2004.

## 2.6 XRN-2 mediates repression of TC1 transposon through *ceh-99* locus

As previously mentioned (Figure 22C), a TC1 insertion is contained in the first intron region of *ceh-99*. An autonomous DNA transposon, TC1, is abundantly found in the genome of *C. elegans*, comprising 33 copies and belonging to the Tc1/mariner superfamily of transposons. Notably, TC1 can be mobilized within the genome through a "cut-and-paste" mechanism [Muñoz-López and García-Pérez, 2010], wherein it is excised from one location and inserted into another, potentially causing disruptions to genes or regulatory regions.

Strikingly, it was observed that an increase in TC1 expression levels occurred upon *xrn-2* inactivation (Figure 26A, 26B), along with a corresponding rise in TC1 relative mRNA expression level upon *xrn-2* knockdown, at 20 °C. Among the 33 TC1 copies in the *C. elegans* genome, only five genes, including *ceh-99*, have TC1 insertions in their intronic regions, oriented in the same transcriptional direction (Figure 26C). Interestingly, the expression levels of these genes, except for *ceh-99*, did not increase upon XRN-2 inactivation, suggesting that *ceh-99* may play a crucial role in mediating TC1 regulation by XRN-2.

To investigate the potential link between *ceh-99* and TC1 regulation, an examination was conducted to determine whether a strain overexpressing *ceh-99* would exhibit altered TC1 expression levels compared to the wild-type strain. To achieve this, a transgenic strain with increased *ceh-99* expression relative to the wild-type was utilized (Figure 26D), and TC1 levels in this strain were quantified, comparing it to the wild-type. Remarkably, in the *ceh-99* overexpression strain, TC1 expression levels increased by approximately two-fold (Figure 26E). This compelling result suggests that XRN-2 exerts regulatory control over TC1, at least in part, through the *ceh-99* locus.

Considering the presence of 33 copies of TC1 in *C. elegans*, this 2 fold increase in TC1 expression indicates that *ceh-99* significantly contributes to the regulation of TC1 by XRN-2. As a result, a notable association between *ceh-99* and TC1 regulation by XRN-2 is revealed by these findings. The upregulation of TC1 expression upon XRN-2 inactivation, combined with the impact of *ceh-99* overexpression on TC1 levels, provides compelling evidence that *ceh-99* plays a pivotal role in mediating the regulatory effects of XRN-2 on TC1. These findings shed

light on the intricate interplay between XRN-2 and transposons like TC1, contributing to our understanding of the molecular mechanisms underlying gene and transposon regulation.

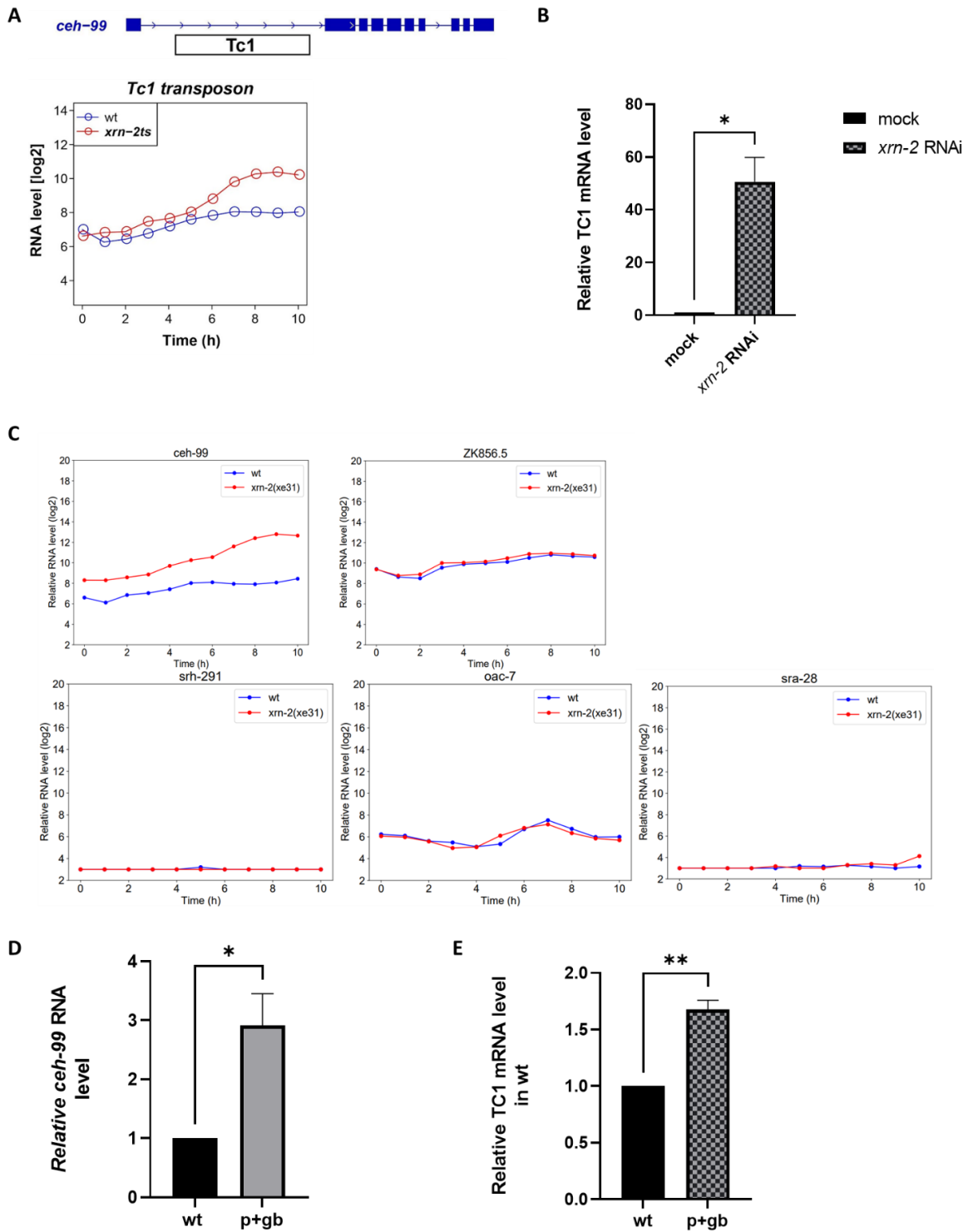


**Figure 26: XRN-2 is involved in the regulatory control of the TC1 transposon via the *ceh-99* locus.** (A) Left: Analysis of TC1 transposon RNA levels in *xrn-2ts* RNA-seq data reveals an increase upon *xrn-2* inactivation. Right: Relative TC1 mRNA levels show upregulation upon *xrn-2* knockdown using *xrn-2* RNAi. Paired t-test analysis was employed. (B) RNA level graphs for selected genes harbouring TC1 in their intronic region with the same direction of transcription. Among them, only *ceh-99* expression is significantly regulated upon *xrn-2* inactivation. (C) *ceh-99* RNA level comparison between

the wild-type and a transgenic line. The transgenic line exhibits higher *ceh-99* expression. Unpaired t-test was used for analysis. (D) TC1 level comparison between the wild-type and a transgenic line overexpressing *ceh-99*. TC1 mRNA level is elevated in the *ceh-99* overexpression line. Unpaired t-test was used for analysis. Asterisks indicate significance (\* $p < 0.01$ , \*\* $p < 0.01$ ). p=promoter, gb=gene body.

## CONCLUSIONS

This thesis has investigated the role of XRN-2 in *C. elegans* development using a variety of genetic and molecular approaches. The key findings are summarized below:

### **XRN-2 is essential for *C. elegans* fertility**

*xrn-2<sup>ts<sup>germ</sup></sup>* animals were observed to exhibit sterility at restrictive temperatures, rendering them a valuable resource for the investigation of XRN-2's role in *C. elegans* germline development. The importance of XRN-2 in germline development was underscored by these observations, particularly emphasizing the necessity of its presence in a functional state before the mid-L4 stage to ensure fertility. Four specific genes, namely *dpy-10*, *osr-1*, *ptr-6*, and *C34C12.2*, were identified as genetic suppressors of *xrn-2* in germline development. The function of XRN-2 during germline development was found to be countered either directly or indirectly by these suppressors. Fertility restoration in *xrn-2<sup>ts<sup>germ</sup></sup>* animals at restrictive temperatures was achieved through the utilization of RNAi of these four genes. Among these genes, *dpy-10*, *osr-1*, and *ptr-6* were implicated in the regulation of glycerol levels, functioning as positive regulators of *gpdh-1* expression, a key enzyme in glycerol biosynthesis. A notable increase in *gpdh-1* mRNA levels and subsequent fertility restoration in *C. elegans* were observed following the knockdown of *dpy-10*, *osr-1*, or *ptr-6*. Additionally, *C34C12.2*, a nuclear protein that partially shares homology with *S. cerevisiae* Net1, known for its role in tethering the RENT complex to rDNA for gene silencing, was implicated in the potential regulation of rRNA maturation. Fertility restoration in *xrn-2<sup>ts<sup>germ</sup></sup>* animals was demonstrated following the depletion of NRDE-2, a putative interacting partner of *C34C12.2*. NRDE-2 functions as an effector of the nuclear RNAi machinery, primarily involved in the negative regulation of pre-mRNA and pre-rRNA expression. Based on these findings, it is conjectured that *C34C12.2*, through its interaction with the nuclear RNAi machinery via NRDE-2, represses pre-rRNA expression, ultimately resulting in elevated rRNA levels. These findings collectively suggest that rRNA maturation represents a crucial function of XRN-2 in germline development.

### ***puf-9* is a synthetic lethality partner of *xrn-2***

It was observed that PUF-9 plays a vital role in *C. elegans* development, as evidenced by the severe developmental delay and distinctive "vulval bursting" phenotype observed in *puf-9* null mutant animals. Knockdown of *puf-9* in *xrn-2<sup>ts</sup>* animals resulted in a notable decline in

vitality and sluggish behaviour, as well as exacerbated phenotypes such as blister formation and molting defects. Additionally, PUF-9 was found to be essential for germline development, as *puf-9* mutant worms exhibited a reduction in brood size and significant germline deficiencies such as abnormal oocyte development, impaired gonad migration, and sterility. Furthermore, PUF-9 was found to be a synthetic lethality partner with PUF-3 and PUF-8, suggesting a possible genetic interaction. Knockdown of either *puf-3* or *puf-8* in *puf-9* mutant animals resulted in significant germline developmental abnormalities, further supporting the importance of PUF-9 in this process. A brood size assay comparing the *puf-9* and *xrn-2* single mutants to the *puf-9/puf-9;xrn-2/xrn-2* double mutant revealed a decrease in brood size in the double mutant compared to each single mutant. This observation suggests that *xrn-2* and *puf-9* share similar or parallel functions in *C. elegans* germline development.

### **XRN-2 regulates *ceh-99* gene expression via premature transcription termination of RNAPII**

The study prominently highlights the critical regulatory role of XRN-2 in maintaining gene expression. *xrn-2* inactivation brought about changes in RNA expression, driven by either RNAPII read-through, leading to the upregulation of specific genes, or collisions between RNAPII molecules, resulting in the downregulation of another set of genes. Notably, the study identified *ceh-99* as an upregulated gene, and this upregulation does not appear to be due to transcription readthrough but is more likely a result of premature termination of RNAPII. Crucially, XRN-2 seems to specifically control the *ceh-99* transcript with a longer 5' UTR. Furthermore, the study reveals that *ceh-99*'s first intron contains a TC1 insertion, and TC1 expression is upregulated upon *xrn-2* inactivation. Overexpressing *ceh-99* led to a twofold increase in TC1 expression, highlighting XRN-2's regulatory influence through *ceh-99*. The research reaffirms the pivotal role of the *ceh-99* promoter region in XRN-2 regulation, without identifying any additional responsive regions in transgenic constructs.

## LIST OF FIGURES

Figure 1: XRN2 targets different types of RNA for varied purposes.....	20
Figure 2: Processing and quality control mechanisms mediated by XRN2 play crucial roles in mammalian pre-rRNA maturation .....	23
Figure 3: Schematic representation of XRN2 functions in RNAPII transcription termination.....	27
Figure 4: <i>C. elegans</i> life cycle and germline development .....	31
Figure 5: Schematic representation of example of Gateway MultiSite recombination cloning .....	58
Figure 6: Schematic illustration of synthetic lethality and modifier screen .....	78
Figure 7: Developmental comparison of <i>xrn-2</i> temperature-sensitive mutant ( <i>xrn-2ts</i> ) and wild-type worms .....	79
Figure 8: Germline-specific <i>xrn-2</i> temperature-sensitive mutant ( <i>xrn-2ts<sup>germ</sup></i> ) .....	81
Figure 9: Phenotypic characterization of <i>xrn-2ts<sup>germ</sup></i> .....	83
Figure 10: Identification of genetic suppressors: <i>dpy-10</i> , <i>osr-1</i> , <i>ptr-6</i> , and <i>C34C12.2</i> counteracting <i>xrn-2ts<sup>germ</sup></i> .....	85
Figure 11: Significant increases in <i>gpdh-1</i> expression were observed upon knockdown of <i>dpy-10</i> , <i>osr-1</i> , <i>ptr-6</i> , or <i>C34C12.2</i> genes .....	88
Figure 12: The knockdown of <i>dpy-10</i> , <i>osr-1</i> , or <i>ptr-6</i> did not result in the rescue of <i>xrn-2ts</i> animals from their larval arrest phenotype .....	91
Figure 13: The predominant localization of <i>C34C12.2</i> within the nucleolus is demonstrated. ....	93
Figure 14: The homology between <i>C34C12.2</i> and <i>Saccharomyces cerevisiae</i> <i>Net1</i> .....	96
Figure 15: <i>puf-9</i> was identified as a genetic enhancer of <i>xrn-2</i> .....	99
Figure 16: PUF-9 is expressed in several tissues throughout <i>C. elegans</i> development ..	103
Figure 17: <i>puf-9</i> mutation causes developmental delay and striking phenotype in worms. ....	104
Figure 18: <i>puf-9</i> mutation causes reduction of brood size and abnormal germline development in <i>C. elegans</i> .....	105
Figure 19: Genetic interactions of <i>puf-9</i> with <i>puf-3</i> and <i>puf-8</i> in germline development .....	109
Figure 20: Investigating the shared functions of <i>puf-9</i> and <i>xrn-2</i> in germline development through brood size analysis. ....	112
Figure 21: mRNA expression changes and transcriptional effects in <i>xrn-2ts</i> mutant <i>C. elegans</i> .....	114

<b>Figure 22: XRN-2 mediates transcriptional repression of <i>ceh-99</i> through premature transcription termination of RNAPII.....</b>	<b>116</b>
<b>Figure 23: <i>ceh-99</i> upstream region has crucial role for <i>xrn-2</i> mediated regulation. ....</b>	<b>118</b>
<b>Figure 24: XRN-2 regulates <i>ceh-99</i> through its promoter region.....</b>	<b>120</b>
<b>Figure 25: Alternative TSS of <i>ceh-99</i> identified .....</b>	<b>122</b>
<b>Figure 26: XRN-2 is involved in the regulatory control of the TC1 transposon via the <i>ceh-99</i> locus .....</b>	<b>125</b>

## LIST OF TABLES

<b>Table 1: Chemicals used in this research</b> .....	34
<b>Table 2: Reagents and kits used in the study</b> .....	35
<b>Table 3: Antibiotics used in the research</b> .....	36
<b>Table 4: Restriction enzymes used in the study</b> .....	36
<b>Table 5: Bacteria strains used in this study</b> .....	36
<b>Table 6: RNAi clones that used in this research</b> .....	37
<b>Table 7: Buffers and media used in this research</b> .....	38
<b>Table 8: Equipment used in this research</b> .....	39
<b>Table 9: Software used in this research</b> .....	41
<b>Table 10: Online tools utilized in this study</b> .....	41
<b>Table 11: Consumables used in this research</b> .....	41
<b>Table 12: Primers used in this research</b> .....	42
<b>Table 13: Oligos used in this research</b> .....	46
<b>Table 14: Plasmids used in this research</b> .....	47
<b>Table 15: <i>C. elegans</i> strains used in this research</b> .....	49
<b>Table 16: Transgenes construct details</b> .....	57
<b>Table 17: Cloning inserts obtained via PCR and commercial sources</b> .....	59
<b>Table 18: PCR conditions for insert preparation</b> .....	60
<b>Table 19: PCR conditions for attaching “attB” sites to the insert</b> .....	60
<b>Table 20: Gateway BP reaction (1-4,1-2,2-3)</b> .....	62
<b>Table 21: Colony PCR conditions</b> .....	62
<b>Table 22: Restriction enzyme digestion</b> .....	63
<b>Table 23: Gateway LR reaction</b> .....	63
<b>Table 24: Injection mixture components</b> .....	64
<b>Table 25: Single worm lysis PCR conditions</b> .....	71
<b>Table 26: cDNA synthesis master mix components (1x)</b> .....	73
<b>Table 27: Program for reverse transcription</b> .....	73
<b>Table 28: RT-qPCR mixture (1x)</b> .....	74
<b>Table 29: Program for RT-qPCR</b> .....	75
<b>Table 30: Alleles recovered from the screen</b> .....	86
<b>Table 31: <i>gpdh-1</i> RT-qPCR data</b> .....	89

**Table 32: mRNA regulators as putative synthetic lethality partner of *xrn-2* ..... 97**

## REFERENCES

1. A Transparent window into biology: A primer on *Caenorhabditis elegans*. (n.d.). [http://www.wormbook.org/chapters/www\\_celegansintro/celegansintro.html](http://www.wormbook.org/chapters/www_celegansintro/celegansintro.html)
2. Aldrich, T.L., Di Segni, G., McConaughy, B.L., Keen, N.J., Whelen, S. and Hall, B.D. (1993) Structure of the yeast TAP1 protein: dependence of transcription activation on the DNA context of the target gene. *Mol. Cell. Biol.* 13, 3434–3444
3. Amberg DC, Goldstein AL and Cole CN (1992) Isolation and characterization of RAT1: An essential gene of *Saccharomyces cerevisiae* required for the efficient nucleocytoplasmic trafficking of mRNA. *Genes Dev* 6:1173-1189.
4. Ariz, M., Mainpal, R., & Subramaniam, K. (2009). *C. elegans* RNA-binding proteins PUF-8 and MEX-3 function redundantly to promote germline stem cell mitosis. *Developmental biology*, 326(2), 295-304.
5. Arraiano, C. M., Andrade, J. M., Domingues, S., Guinote, I. B., Malecki, M., Matos, R. G., ... & Viegas, S. C. (2010). The critical role of RNA processing and degradation in the control of gene expression. *FEMS microbiology reviews*, 34(5), 883-923.
6. Arraiano, C. M., Yancey, S. D., & Kushner, S. R. (1988). Stabilization of discrete mRNA breakdown products in *ams pnp rnb* multiple mutants of *Escherichia coli* K-12. *Journal of bacteriology*, 170(10), 4625-4633.
7. Ashe A, Sapetschnig A, Weick EM, Mitchell J, Bagijn MP, Cording AC, Doebley AL, Goldstein LD, Lehrbach NJ, Le Pen J *et al* (2012) piRNAs can trigger a multigenerational epigenetic memory in the germline of *C. elegans* *Cell* 150:88-99.
8. Aygün, I., & Miki, T. S. (2021). Nuclear RNA regulation by XRN2 and XTBD family proteins. *Cell Structure and Function*, 46(2), 73-78.
9. Aygün, I., Rzepczak, A., & Miki, T. S. (2023). A germline-targeted genetic screen for *xrn-2* suppressors identifies a novel gene C34C12. 2 in *Caenorhabditis elegans*. *Genetics and Molecular Biology*, 46, e20220328.
10. Ballarino, M., Pagano, F., Girardi, E., Morlando, M., Cacchiarelli, D., Marchioni, M., Proudfoot, N.J. and Bozzoni, I. (2009) Coupled RNA processing and transcription of intergenic primary microRNAs. *Mol. Cell. Biol.* 29, 5632–5638.
11. Banerjee, A., Sammarco, M.C., Ditch, S., Wang, J. and Grabczyk, E. (2009) A novel tandem reporter quantifies RNA polymerase II termination in mammalian cells. *PLoS ONE* 4, e6193
12. Barton, M. K., & Kimble, J. (1990). *fog-1*, a regulatory gene required for specification of spermatogenesis in the germ line of *Caenorhabditis elegans*. *Genetics*, 125(1), 29-39.
13. Boix, E., Acquati, F., Leonidas, D., & Pulido, D. (2020). role of ribonucleases in immune response regulation during infection and Cancer. *Frontiers in immunology*, 11, 236.
14. Boo, S. H., & Kim, Y. K. (2020). The emerging role of RNA modifications in the regulation of mRNA stability. *Experimental & molecular medicine*, 52(3), 400-408.
15. Boulianne, B., & Feldhahn, N. (2018). Transcribing malignancy: transcription-associated genomic instability in cancer. *Oncogene*, 37(8), 971-981.
16. Bousquet-Antonelli, C., Presutti, C. and Tollervey, D. (2000) Identification of a regulated pathway for nuclear pre-mRNA turnover. *Cell* 102, 765–775.

17. Brannan, K., Kim, H., Erickson, B., Glover Cutter, K., Kim, S., Fong, N., Kiemele, L., Hansen, K., Davis, R., Lykke Andersen, J. and Bentley, D.L. (2012) mRNA decapping factors and the exonuclease Xrn2 function in widespread premature termination of RNA polymerase II transcription. *Mol. Cell.* 46, 311–324.
18. Brenner S (1974) The genetics of *Caenorhabditis elegans* *Genetics* 77:71-94.
19. Buckley BA, Burkhart KB, Gu SG, Spracklin G, Kershner A, Fritz H, Kimble J, Fire A and Kennedy S (2012) A nuclear Argonaute promotes multigenerational epigenetic inheritance and germline immortality. *Nature* 489:447-451.
20. Burkhart KB, Guang S, Buckley BA, Wong L, Bochner AF and Kennedy S (2011) A pre-mRNA-associating factor links endogenous siRNAs to chromatin regulation. *PLoS Genet* 7:e1002249.
21. Castro, J., Ribó, M., Vilanova, M., & Benito, A. (2021). Strengths and Challenges of Secretory Ribonucleases as AntiTumor Agents. *Pharmaceutics* 2021, 13, 82.
22. Chanfreau, G., Rotondo, G., Legrain, P. and Jacquier, A. (1998) Processing of a dicistronic small nucleolar RNA precursor by the RNA endonuclease Rnt1. *EMBO J.* 17, 3726–3737.
23. Chang, J.H., Jiao, X., Chiba, K., Oh, C., Martin, C.E., Kiledjian, M., and Tong, L. 2012. Dxo1 is a new type of eukaryotic enzyme with both decapping and 5'-3' exoribonuclease activity. *Nat. Struct. Mol. Biol.*, 19: 1011–1017.
24. Chatterjee S and Grosshans H (2009) Active turnover modulates mature microRNA activity in *Caenorhabditis elegans* *Nature* 461:546-549.
25. Chen, Y.L., Tao, J., Zhao, P.J., Tang, W., Xu, J.P., Zhang, K.Q. and Zou, C.G. (2019) Adiponectin receptor PAQR-2 signaling senses low temperature to promote *C. elegans* longevity by regulating autophagy. *Nat Commun*, 10, 2602.
26. Cheng, Z. F., & Deutscher, M. P. (2005). An important role for RNase R in mRNA decay. *Molecular cell*, 17(2), 313-318.
27. Choi MK, Son S, Hong M, Choi MS, Kwon JY and Lee J (2016) Maintenance of membrane integrity and permeability depends on a patched-related protein in *Caenorhabditis elegans* *Genetics* 202:1411-1420.
28. Christofi, T., & Zaravinos, A. (2019). RNA editing in the forefront of epitranscriptomics and human health. *Journal of translational medicine*, 17(1), 1-15..
29. Coburn C and Gems D (2013) The mysterious case of the *C. elegans* gut granule: Death fluorescence, anthranilic acid and the kynurenine pathway. *Front Genet* 4:151.
30. Consortium, C.e.S. (1998) Genome sequence of the nematode *C. elegans*: a platform for investigating biology. *Science*, 282, 2012-2018.
31. Couvillion MT, Bounova G, Purdom E, Speed TP and Collins K (2012) A *Tetrahymena* Piwi bound to mature tRNA 3' fragments activates the exonuclease Xrn2 for RNA processing in the nucleus. *Mol Cell* 48:509-520.
32. Daggubati V, Raleigh DR and Sever N (2022) Sterol regulation of developmental and oncogenic Hedgehog signaling. *Biochem Pharmacol* 196:114647.
33. Das, B., Butler, J.S. and Sherman, F. (2003) Degradation of normal mRNA in the nucleus of *Saccharomyces cerevisiae*. *Mol. Cell. Biol.* 23, 5502–5515.

34. Davidson, L., Kerr, A. and West, S. (2012) Co-transcriptional degradation of aberrant pre-mRNA by Xrn2. *EMBO J.* 31, 2566–2578.
35. Davis M, Montalbano A, Wood MP and Schisa JA (2017) Biphasic adaptation to osmotic stress in the *C. elegans* germ line. *Am J Physiol Cell Physiol* 312:C741-C748.
36. Dehé, P. M., & Gaillard, P. H. L. (2017). Control of structure-specific endonucleases to maintain genome stability. *Nature reviews Molecular cell biology*, 18(5), 315-330.
37. Dengl, S. and Cramer, P. (2009) Torpedo nuclease Rat1 is insufficient to terminate RNA polymerase II in vitro. *J. Biol. Chem.* 284, 21270–21279.
38. Di Segni, G., McConaughy, B.L., Shapiro, R.A., Aldrich, T.L. and Hall, B.D. (1993) TAP1, a yeast gene that activates the expression of a tRNA gene with a defective internal promoter. *Mol. Cell. Biol.* 13, 3424–3433
39. Eaton, J. D., & West, S. (2018). An end in sight? Xrn2 and transcriptional termination by RNA polymerase II. *Transcription*, 9(5), 321-326.
40. Eichler DC, Craig N. Processing of eukaryotic ribosomal RNA, *Prog. Nucleic Acid Res. Mol. Biol.*, 1994, vol. 49 (pg. 197-239)
41. El Hage, A., Koper, M., Kufel, J. and Tollervey, D. (2008) Efficient termination of transcription by RNA polymerase I requires the 5' exonuclease Rat1 in yeast. *Genes Dev.* 22, 1069–1081.
42. Fang F, Phillips S and Butler JS (2005) Rat1p and Rai1p function with the nuclear exosome in the processing and degradation of rRNA precursors. *RNA* 11:1574-1578.
43. Fang, F., Hoskins, J. and Butler, J.S. (2004) 5-Fluorouracil enhances exosome-dependent accumulation of polyadenylated rRNAs. *Mol. Cell. Biol.* 24, 10766–10776
44. Fong N, Brannan K, Erickson B, Kim H, Cortazar Michael A, Sheridan Ryan M, et al. Effects of Transcription Elongation Rate and Xrn2 Exonuclease Activity on RNA Polymerase II Termination Suggest Widespread Kinetic Competition. *Molecular Cell.* 2015;60(2):256–67. pmid:26474067.
45. Frand AR, Russel S and Ruvkun G (2005) Functional genomic analysis of *C. elegans* molting. *PLoS Biol* 3:e312.
46. Frezal, L. and Felix, M.A. (2015) *C. elegans* outside the Petri dish. *Elife*, 4.
47. Frøkjær-Jensen C, Davis MW, Hopkins CE, Newman BJ, Thummel JM, Olesen SP, Grunnet M and Jørgensen EM (2008) Single-copy insertion of transgenes in *Caenorhabditis elegans* *Nat Genet* 40:1375-1383.
48. García-Rodríguez, L. J., Gay, A. C., & Pon, L. A. (2007). Puf3p, a Pumilio family RNA binding protein, localizes to mitochondria and regulates mitochondrial biogenesis and motility in budding yeast. *The Journal of cell biology*, 176(2), 197-207.
49. Gateway Recombination Cloning Technology | Thermo Fisher Scientific - IE. (n.d.). <https://www.thermofisher.com/pl/en/home/life-science/cloning/gateway-cloning/gateway-technology.html>
50. Giunti, S., Andersen, N., Rayes, D. and De Rosa, M.J. (2021) Drug discovery: Insights from the invertebrate *Caenorhabditis elegans*. *Pharmacol Res Perspect*, 9, e00721.
51. Goh PY and Bogaert T (1991) Positioning and maintenance of embryonic body wall muscle attachments in *C. elegans* requires the *mup-1* gene. *Development* 111:667-681.

52. Granneman, S., Petfalski, E. and Tollervey, D. (2011) A cluster of ribosome synthesis factors regulate pre-rRNA folding and 5.8S rRNA maturation by the Rat1 exonuclease. *EMBO J.* 30, 4006–4019.
53. Grishok, A. (2013) Biology and Mechanisms of Short RNAs in *Caenorhabditis elegans*. *Adv Genet*, 83, 1-69.
54. Guang S, Bochner AF, Burkhart KB, Burton N, Pavelec DM and Kennedy S (2010) Small regulatory RNAs inhibit RNA polymerase II during the elongation phase of transcription. *Nature* 465:1097-1101.
55. Guang S, Bochner AF, Pavelec DM, Burkhart KB, Harding S, Lachowiec J and Kennedy S (2008) An Argonaute transports siRNAs from the cytoplasm to the nucleus. *Science* 321:537-541.
56. Handbook - Introduction. (n.d.). [www.wormatlas.org](http://www.wormatlas.org).  
<https://www.wormatlas.org/hermaphrodite/introduction/mainframe.htm>
57. Heyer, W.D., Johnson, A.W., Reinhart, U. and Kolodner, R.D. (1995) Regulation and intracellular localization of *Saccharomyces cerevisiae* strand exchange protein 1 (Sep1/Xrn1/Kem1), a multifunctional exonuclease. *Mol. Cell. Biol.* 15, 2728–2736
58. Hill KL, Harfe BD, Dobbins CA and L'Hernault SW (2000) *dpy-18* encodes an alpha-subunit of prolyl-4-hydroxylase in *Caenorhabditis elegans* *Genetics* 155:1139-1148.
59. Hodgkin, J., & Barnes, T. M. (1991). More is not better: brood size and population growth in a self-fertilizing nematode. *Proceedings of the Royal Society of London. Series B: Biological Sciences*, 246(1315), 19-24.
60. Houseley, J., & Tollervey, D. (2009). The many pathways of RNA degradation. *Cell*, 136(4), 763-776..
61. Hubstenberger, A., Cameron, C., Shtofman, R., Gutman, S., & Evans, T. C. (2012). A network of PUF proteins and Ras signaling promote mRNA repression and oogenesis in *C. elegans*. *Developmental biology*, 366(2), 218-231.
62. Hunt, P.R. (2017) The *C. elegans* model in toxicity testing. *J Appl Toxicol*, 37, 50-59.
63. Hwang, T., Park, C. K., Leung, A. K., Gao, Y., Hyde, T. M., Kleinman, J. E., ... & Weinberger, D. R. (2016). Dynamic regulation of RNA editing in human brain development and disease. *Nature neuroscience*, 19(8), 1093-1099.
64. Integrated DNA Technologies | IDT. (n.d.). Integrated DNA Technologies. <https://www.idtdna.com/pages>
65. Jimeno Gonzalez, S., Haaning, L.L., Malagon, F. and Jensen, T.H. (2010) The yeast 5–3 exonuclease Rat1p functions during transcription elongation by RNA polymerase II. *Mol. Cell* 37, 580–587
66. Johnson, A.W. (1997) Rat1p and Xrn1p are functionally interchangeable exoribonucleases that are restricted to and required in the nucleus and cytoplasm, respectively. *Mol. Cell. Biol.* 17, 6122–6130
67. Kamath RS and Ahringer J (2003) Genome-wide RNAi screening in *Caenorhabditis elegans* *Methods* 30:313-321.
68. Kawauchi, J., Mischo, H., Braglia, P., Rondon, A. and Proudfoot, N.J. (2008) Budding yeast RNA polymerases I and II employ parallel mechanisms of transcriptional termination. *Genes Dev.* 22, 1082–1092.

69. Kenna, M., Stevens, A., McCammon, M. and Douglas, M.G. (1993) An essential yeast gene with homology to the exonuclease-encoding XRN1/KEM1 gene also encodes a protein with exoribonuclease activity. *Mol. Cell. Biol.* 13, 341–350
70. Kim M, Vasiljeva L, Rando OJ, Zhelkovsky A, Moore C, Buratowski S. Distinct Pathways for snoRNA and mRNA Termination. *Molecular Cell.* 2006;24(5):723–34. <http://dx.doi.org/10.1016/j.molcel.2006.11.011>. [pmid:17157255](https://pubmed.ncbi.nlm.nih.gov/17157255/).
71. Kim, M., Ahn, S. H., Krogan, N. J., Greenblatt, J. F., & Buratowski, S. (2004). Transitions in RNA polymerase II elongation complexes at the 3' ends of genes. *The EMBO journal*, 23(2), 354-364.
72. Kim, M., Krogan, N. J., Vasiljeva, L., Rando, O. J., Nedeá, E., Greenblatt, J. F., & Buratowski, S. (2004). The yeast Rat1 exonuclease promotes transcription termination by RNA polymerase II. *Nature*, 432(7016), 517-522.
73. Kraemer, B., Crittenden, S., Gallegos, M., Moulder, G., Barstead, R., Kimble, J., & Wickens, M. (1999). NANOS-3 and FBF proteins physically interact to control the sperm–oocyte switch in *Caenorhabditis elegans*. *Current Biology*, 9(18), 1009-1018.
74. Kressler D, Hurt E, Baßler J. Driving ribosome assembly. *Biochim. Biophys. Acta.* 2010;1803:673–683.
75. Kuai, L., Fang, F., Butler, J.S. and Sherman, F. (2004) Polyadenylation of rRNA in *Saccharomyces cerevisiae*. *Proc. Natl. Acad. Sci. U.S.A.* 101, 8581–8586
76. Kuwabara PE and Labouesse M (2002) The sterol-sensing domain: Multiple families, a unique role? *Trends Genet* 18:193-201.
77. Lamitina T, Huang CG and Strange K (2006) Genome-wide RNAi screening identifies protein damage as a regulator of osmoprotective gene expression. *Proc Natl Acad Sci. U S A* 103:12173-12178.
78. Lehmann, R., & Nüsslein-Volhard, C. (1987). Involvement of the pumilio gene in the transport of an abdominal signal in the *Drosophila* embryo. *Nature*, 329(6135), 167-170.
79. Leung, M.C., Williams, P.L., Benedetto, A., Au, C., Helmcke, K.J., Aschner, M. and Meyer, J.N. (2008) *Caenorhabditis elegans*: an emerging model in biomedical and environmental toxicology. *Toxicol Sci*, 106, 5-28
80. Levy AD, Yang J and Kramer JM (1993) Molecular and genetic analyses of the *Caenorhabditis elegans* *dpy-2* and *dpy-10* collagen genes: A variety of molecular alterations affect organismal morphology. *Mol Biol Cell* 4:803-817.
81. Liao S, Chen X, Xu T, Jin Q, Xu Z, Xu D, Zhou X, Zhu C, Guang S and Feng X (2021) Antisense ribosomal siRNAs inhibit RNA polymerase I-directed transcription in *C. elegans* *Nucleic Acids Res* 49:9194-9210.
82. Luke, B., Panza, A., Redon, S., Iglesias, N., Li, Z. and Lingner, J. (2008) The Rat1p 5 to 3 exonuclease degrades telomeric repeat-containing RNA and promotes telomere elongation in *Saccharomyces cerevisiae*. *Mol. Cell* 32, 465–477.
83. Luo, W., Johnson, A. W., & Bentley, D. L. (2006). The role of Rat1 in coupling mRNA 3'-end processing to transcription termination: implications for a unified allosteric–torpedo model. *Genes & development*, 20(8), 954-965.

84. Luteijn MJ, van Bergeijk P, Kaaij LJ, Almeida MV, Roovers EF, Berezikov E and Ketting RF (2012) Extremely stable Piwi-induced gene silencing in *Caenorhabditis elegans* EMBO J 31:3422-3430.
85. Maine EM and Kimble J (1989) Identification of genes that interact with *glp-1*, a gene required for inductive cell interactions in *Caenorhabditis elegans* Development 106:133-143.
86. Meeuse, M. W., Hauser, Y. P., Morales Moya, L. J., Hendriks, G. J., Eglinger, J., Bogaarts, G., ... & Großhans, H. (2020). Developmental function and state transitions of a gene expression oscillator in *Caenorhabditis elegans*. Molecular systems biology, 16(7), e9498.
87. Mendenhall, A., Crane, M.M., Leiser, S., Sutphin, G., Tedesco, P.M., Kaeberlein, M., Johnson, T.E. and Brent, R. (2017) Environmental Canalization of Life Span and Gene Expression in *Caenorhabditis elegans*. J Gerontol A Biol Sci Med Sci, 72, 1033-1037.
88. Miki TS and Großhans H (2013) The multifunctional RNase XRN2. Biochem Soc Trans 41:825-830.
89. Miki TS, Carl SH and Großhans H (2017) Two distinct transcription termination modes dictated by promoters. Genes Dev 31:1870-1879.
90. Miki TS, Carl SH, Stadler MB and Großhans H (2016) XRN2 autoregulation and control of polycistronic gene expression in *Caenorhabditis elegans* PLoS Genet 12:e1006313.
91. Miki TS, Richter H, Rügger S and Großhans H (2014b) PAXT-1 promotes XRN2 activity by stabilizing it through a conserved domain. Mol Cell 53:351-360.
92. Miki TS, Rügger S, Gaidatzis D, Stadler MB and Großhans H (2014c) Engineering of a conditional allele reveals multiple roles of XRN2 in *Caenorhabditis elegans* development and substrate specificity in microRNA turnover. Nucleic Acids Res 42:4056-4067.
93. Miki, T.S., Richter, H., Rügger, S., and Großhans, H. (2014a). PAXT-1 promotes XRN2 activity by stabilizing it through a conserved domain. Mol. Cell, 53: 351–360.
94. Morgan, C. T., Lee, M. H., & Kimble, J. (2010). Chemical reprogramming of *Caenorhabditis elegans* germ cell fate. Nature chemical biology, 6(2), 102-104.,
95. Morgan, D. E., Crittenden, S. L., & Kimble, J. (2010). The *C. elegans* adult male germline: Stem cells and sexual dimorphism. Developmental biology, 346(2), 204-214.
96. Nagarajan VK, Jones CI, Newbury SF and Green PJ (2013) XRN 5'→3' exoribonucleases: Structure, mechanisms and functions. Biochim Biophys Acta 1829:590-603
97. Negishi T, Kitagawa S, Horii N, Tanaka Y, Haruta N, Sugimoto A, Sawa H, Hayashi KI, Harata M and Kanemaki MT (2022) The auxin-inducible degron 2 (AID2) system enables controlled protein knockdown during embryogenesis and development in *Caenorhabditis elegans* Genetics 220:iyab218.
98. Nishimura K, Fukagawa T, Takisawa H, Kakimoto T and Kanemaki M (2009) An auxin-based degron system for the rapid depletion of proteins in nonplant cells. Nat Methods 6:917-922.

99. Nishiwaki K and Miwa J (1998) Mutations in genes encoding extracellular matrix proteins suppress the emb-5 gastrulation defect in *Caenorhabditis elegans* Mol Gen Genet 259:2-12.
100. Nolde, M. J., Saka, N., Reinert, K. L., & Slack, F. J. (2007). The *Caenorhabditis elegans* pumilio homolog, puf-9, is required for the 3' UTR-mediated repression of the let-7 microRNA target gene, hbl-1. *Developmental biology*, 305(2), 551-563.
101. O'Neil, N. J., Bailey, M. L., & Hieter, P. (2017). Synthetic lethality and cancer. *Nature Reviews Genetics*, 18(10), 613-623.
102. O'Rourke SM, Dorfman MD, Carter JC and Bowerman B (2007) Dynein modifiers in *C. elegans*: Light chains suppress conditional heavy chain mutants. *PLoS Genet* 3:e128.
103. Petfalski, E., Dandekar, T., Henry, Y. and Tollervey, D. (1998) Processing of the precursors to small nucleolar RNAs and rRNAs requires common components. *Mol. Cell. Biol.* 18, 1181–1189
104. Poole, T.L. and Stevens, A. (1995) Comparison of features of the RNase activity of 5'-exonuclease-1 and 5'-exonuclease-2 of *Saccharomyces cerevisiae*. *Nucleic Acids Symp. Ser.* 33, 79–81
105. Porrua, O., Boudvillain, M., & Libri, D. (2016). Transcription termination: variations on common themes. *Trends in Genetics*, 32(8), 508-522.
106. Proudfoot NJ. Ending the message: poly(A) signals then and now. *Genes & Development.* 2011;25(17):1770–82.
107. Proudfoot, N. J. (2016). Transcriptional termination in mammals: Stopping the RNA polymerase II juggernaut. *Science*, 352(6291), aad9926.
108. Qu, L.H., Henras, A., Lu, Y.J., Zhou, H., Zhou, W.X., Zhu, Y.Q., Zhao, J., Henry, Y., Caizergues Ferrer, M. and Bachellerie, J.P. (1999) Seven novel methylation guide small nucleolar RNAs are processed from a common polycistronic transcript by Rat1p and RNase III in yeast. *Mol. Cell. Biol.* 19, 1144–1158.
109. Reilly, M. B., Cros, C., Varol, E., Yemini, E., & Hobert, O. (2020). Unique homeobox codes delineate all the neuron classes of *C. elegans*. *Nature*, 584(7822), 595-601.
110. Richard P, Manley JL. Transcription termination by nuclear RNA polymerases. *Genes & Development.* 2009;23(11):1247–69.
111. Richter, H., Katic, I., Gut, H., and Großhans, H. 2016. Structural basis and function of XRN2 binding by XTB domains. *Nat. Struct. Mol. Biol.*, 23: 164–171.
112. RNAfold web server. (n.d.). <http://rna.tbi.univie.ac.at/cgi-bin/RNAWebSuite/RNAfold.cgi>
113. Rosenberg, H. F. (2008). Eosinophil-derived neurotoxin/RNase 2: connecting the past, the present and the future. *Current pharmaceutical biotechnology*, 9(3), 135-140.
114. Saito, T. L., Hashimoto, S. I., Gu, S. G., Morton, J. J., Stadler, M., Blumenthal, T., ... & Morishita, S. (2013). The transcription start site landscape of *C. elegans*. *Genome research*, 23(8), 1348-1361.

115. Sakyiama J, Zimmer SL, Ciganda M, Williams N and Read LK (2013) Ribosome biogenesis requires a highly diverged XRN family 5'->3' exoribonuclease for rRNA processing in *Trypanosoma brucei* RNA 19:1419-1431.
116. Sebollela, A., Louzada, P. R., Sola-Penna, M., Sarone-Williams, V., Coelho-Sampaio, T., & Ferreira, S. T. (2004). Inhibition of yeast glutathione reductase by trehalose: possible implications in yeast survival and recovery from stress. The International Journal of Biochemistry & Cell Biology, 36(5), 900-908.
117. Shobuike, T., Sugano, S., Yamashita, T. and Ikeda, H. (1995) Characterization of cDNA encoding mouse homolog of fission yeast dhp1 + gene: structural and functional conservation. Nucleic. Acids Res. 23, 357–361
118. Singh, J. (2021). Harnessing the power of genetics: fast forward genetics in *Caenorhabditis elegans*. Molecular Genetics and Genomics, 296(1), 1-20.
119. Skourti-Stathaki K, Proudfoot Nicholas J, Gromak N. Human Senataxin Resolves RNA/DNA Hybrids Formed at Transcriptional Pause Sites to Promote Xrn2-Dependent Termination. Molecular Cell. 2011;42(6):794–805. pmid:21700224.
120. Solomon A, Bandhakavi S, Jabbar S, Shah R, Beitel GJ and Morimoto RI (2004) *Caenorhabditis elegans* OSR-1 regulates behavioral and physiological responses to hyperosmotic environments. Genetics 167:161-170.
121. Stevens, A. and Poole, T.L. (1995) 5'-exonuclease-2 of *Saccharomyces cerevisiae*: purification and features of ribonuclease activity with comparison to 5'-exonuclease-1. J. Biol. Chem. 270, 16063–16069
122. Straight AF, Shou W, Dowd GJ, Turck CW, Deshaies RJ, Johnson AD and Moazed D (1999) Net1, a Sir2-associated nucleolar protein required for rDNA silencing and nucleolar integrity. Cell 97:245-256.
123. Subramaniam, K., & Seydoux, G. (2003). Dedifferentiation of primary spermatocytes into germ cell tumors in *C. elegans* lacking the pumilio-like protein PUF-8. Current Biology, 13(2), 134-139.
124. Sugano, S., Shobuike, T., Takeda, T., Sugino, A. and Ikeda, H. (1994) Molecular analysis of the dhp1 + gene of *Schizosaccharomyces pombe*: an essential gene that has homology to the DST2 and RAT1 genes of *Saccharomyces cerevisiae*. Mol. Gen. Genet. 243, 1–8
125. Sun, D., Han, C., & Sheng, J. (2022). The role of human ribonuclease A family in health and diseases: A systematic review. Iscience, 105284.
126. Suzuki, H., & Tsukahara, T. (2014). A view of pre-mRNA splicing from RNase R resistant RNAs. International journal of molecular sciences, 15(6), 9331-9342.
127. Timmons L and Fire A (1998) Specific interference by ingested dsRNA. Nature 395:854.
128. Trinquier, A., Durand, S., Braun, F., & Condon, C. (2020). Regulation of RNA processing and degradation in bacteria. Biochimica et Biophysica Acta (BBA)-Gene Regulatory Mechanisms, 1863(5), 194505.
129. Vagenende V, Yap MG and Trout BL (2009) Mechanisms of protein stabilization and prevention of protein aggregation by glycerol. Biochemistry 48:11084-11096.

130. Venema J, Tollervey D. Ribosome synthesis in *Saccharomyces cerevisiae*, *Annu. Rev. Genet.*, 1999, vol. 33 (pg. 261-311).
131. Wagschal, A., Rousset, E., Basavarajaiah, P., Contreras, X., Harwig, A., Laurent Chabalier, S., Nakamura, M., Chen, X., Zhang, K., Meziane, O. et al. (2012) Microprocessor, Setx, Xrn2, and Rrp6 co-operate to induce premature termination of transcription by RNAPII. *Cell* 150, 1147–1157.
132. Wan G, Yan J, Fei Y, Pagano DJ and Kennedy S (2020) A Conserved NRDE-2/MTR-4 complex mediates nuclear RNAi in *Caenorhabditis elegans* *Genetics* 216:1071-1085.
133. Wang M and Pestov DG (2011) 5'-end surveillance by Xrn2 acts as a shared mechanism for mammalian pre-rRNA maturation and decay. *Nucleic Acids Res* 39:1811-1822.
134. Wang, A., & Bolen, D. W. (1997). A naturally occurring protective system in urea-rich cells: mechanism of osmolyte protection of proteins against urea denaturation. *Biochemistry*, 36(30), 9101-9108.
135. Wei, P.C., Lo, W.T., Su, M.I., Shew, J.Y. and Lee, W.H. (2012) Non-targeting siRNA induces NPGPx expression to cooperate with exoribonuclease XRN2 for releasing the stress. *Nucleic Acids Res.* 40, 323–332.
136. West S, Gromak N, Proudfoot NJ. Human 5'- 3' exonuclease Xrn2 promotes transcription termination at co-transcriptional cleavage sites. *Nature.* 2004;432(7016):522–5. pmid:15565158
137. West, S., Gromak, N., & Proudfoot, N. J. (2004). Human 5'→ 3' exonuclease Xrn2 promotes transcription termination at co-transcriptional cleavage sites. *Nature*, 432(7016), 522-525.
138. Wheeler JM and Thomas JH (2006) Identification of a novel gene family involved in osmotic stress response in *Caenorhabditis elegans* *Genetics* 174:1327-1336.
139. Wickens, M., Bernstein, D. S., Kimble, J., & Parker, R. (2002). A PUF family portrait: 3' UTR regulation as a way of life. *TRENDS in Genetics*, 18(3), 150-157.
140. Wolke, U., Jezuit, E. A., & Priess, J. R. (2007). Actin-dependent cytoplasmic streaming in *C. elegans* oogenesis.
141. WormBase : Nematode Information Resource. (n.d.). <https://wormbase.org/#012-34-5>
142. Wreden, C., Verrotti, A. C., Schisa, J. A., Lieberfarb, M. E., & Strickland, S. (1997). Nanos and pumilio establish embryonic polarity in *Drosophila* by promoting posterior deadenylation of hunchback mRNA. *Development*, 124(15), 3015-3023.
143. Xiang, S., Cooper-Morgan, A., Jiao, X., Kiledjian, M., Manley, J.L., and Tong, L. 2009. Structure and function of the 5'→3' exoribonuclease Rat1 and its activating partner Rai1. *Nature*, 458: 784–788.
144. Xu, Z., Zhao, J., Hong, M., Zeng, C., Guang, S., & Shi, Y. (2021). Structural recognition of the mRNA 3' UTR by PUF-8 restricts the lifespan of *C. elegans*. *Nucleic Acids Research*, 49(17), 10082-10097.

145. Zakrzewska Placzek, M., Souret, F.F., Sobczyk, G.J., Green, P.J. and Kufel, J. (2010) *Arabidopsis thaliana* XRN2 is required for primary cleavage in the pre-ribosomal RNA. *Nucleic Acids Res.* 38, 4487–4502.
146. Zamore, P. D., Williamson, J. R., & Lehmann, R. (1997). The Pumilio protein binds RNA through a conserved domain that defines a new class of RNA-binding proteins. *Rna*, 3(12), 1421.
147. Zhang L, Ward JD, Cheng Z and Dernburg AF (2015) The auxin-inducible degradation (AID) system enables versatile conditional protein depletion in *C. elegans* *Development* 142:4374-4384.
148. Zhang, H., Rigo, F., & Martinson, H. G. (2015). Poly (A) signal-dependent transcription termination occurs through a conformational change mechanism that does not require cleavage at the poly (A) site. *Molecular cell*, 59(3), 437-448.
149. Zhang, M., Yu, L., Xin, Y., Hu, P., Fu, Q., Yu, C. and Zhao, S. (1999) Cloning and mapping of the XRN2 gene to human chromosome 20p11.1–p11.2. *Genomics*. 59, 252–254
150. Zhang, Q., Ma, D., Wu, F., Standage-Beier, K., Chen, X., Wu, K., ... & Wang, X. (2021). Predictable control of RNA lifetime using engineered degradation-tuning RNAs. *Nature chemical biology*, 17(7), 828-836.
151. Zhou X, Feng X, Mao H, Li M, Xu F, Hu K and Guang S (2017) RdRP-synthesized antisense ribosomal siRNAs silence pre-rRNA via the nuclear RNAi pathway. *Nat Struct Mol Biol* 24:258-269.
152. Zugasti O, Rajan J and Kuwabara PE (2005) The function and expansion of the Patched- and Hedgehog-related homologs in *C. elegans* *Genome Res* 15:1402-1410.
153. Muñoz-López, M., & García-Pérez, J. L. (2010). DNA transposons: nature and applications in genomics. *Current genomics*, 11(2), 115-128.
154. Pfam. (n.d.). [pfam.xfam.org](https://pfam.xfam.org). Retrieved April 19, 2021, from <https://pfam.xfam.org/family/xtbd>